A UNIPOLAR INVERTER DRIVE FOR A CAGE INDUCTION MOTOR

by

PATRICK REGINALD PALMER

B.Sc.(Eng.), A.C.G.I., A.M.I.E.E.

Thesis submitted to the University of London
for the degree of Doctor of Philosophy
and for the Diploma of Imperial College

Department of Electrical Engineering
Imperial College of Science and Technology

September 1985

ABSTRACT

This thesis describes a novel pulse-width-modulated, voltage fed, unipolar inverter drive scheme for a squirrel-cage induction motor, which enables effective shoot through protection. Standard PWM techniques were employed. The proposed scheme was tested using standard two pole, totally enclosed, fan cooled, three phase induction motors, rated at 4 kW and 415 Vac. Simple alterations are required to the motor windings, and these were made by the manufacturer.

A review of inverter technology covers the principal categories of inverters, switching devices and detail circuitry. The modes of operation of unipolar schemes are discussed and their advantages and disadvantages identified.

A description of the experimental drive and its operating details follows, reference being made to measured current waveforms. Measured torque-speed and efficiency-speed graphs are presented and discussed.

For a more detailed examination of the performance a theoretical model of the entire inverter-induction motor scheme is developed. The model for the motor is based on a mutually coupled coils approach. The predictions confirm the explanation of the operation given previously. Theoretical comparisons are made between the proposed

unipolar drive and equivalent conventional inverter drives.

There is then an extensive study of the inverter under fault conditions, where it is shown that the behaviour of the inverter under fault conditions is predictable and controllable. Suitable methods of fault detection are described briefly.

The power rating of the motor under unipolar inverter feed at 5Ø Hz is investigated using experimental tests and theoretical calculations. From this a simple rule for derating a motor is suggested, and a table of standard frame sizes and their ratings, under both mains feed and unipolar inverter operation, is drawn up.

Finally, it is concluded that the unipolar inverter, cage induction motor drive is a viable alternative to existing types of drive, and offers high reliability and low maintenance.

ACKNOWLEDGEMENTS

I would like to thank my supervisor, Dr B.W.Williams, for his constant interest throughout this project. I would also like to express my gratitude to all my fellow students and academic or technical staff who have helped me in any way. Particular thanks are due to Paul and Dr S.Williamson. Finally, I wish to thank the Science and Engineering Research Council for their financial support and G.E.C. Small Machines for providing the motors required.

CONTENTS

LIST OF SYMBOLS

A	area
B	flux density
d	depth within stator slot
e	exponential
f	supply frequency in Hz, function to be integrated
h	time step length
I	current
I'	circulating current
$\underline{I}$	current vector $(I_1, I_2, I_3, \ldots)$
$\underline{I}'$	next current state
I_1	primary current, rated current
I_1'	inverter rated current
I_2	secondary current
I_{rd}	direct axis rotor current
I_{rq}	quadrature axis rotor current
I_{sd}	direct axis stator current
I_{sq}	quadrature axis stator current
j	square root of -1
L	self inductance
$[L]$	inductance matrix
L_r	rotor inductance (dq)
L_{rr}	rotor self inductance
L_s	stator inductance (dq)
L_{sm}	mutual inductance between stator phases
L_{sr}	stator to rotor mutual inductance (dq)
L_{ss}	stator self inductance
M	mutual inductance, mutual inductance between stator phase halves

M_{sr_a}	mutual inductance stator winding A to rotor
M_{sr_b}	mutual inductance stator winding B to rotor
M_{ss}	mutual inductance between stator phase halves
N	number of turns linked
p	differential operator
R	resistance
$[R]$	diagonal resistance matrix
R_1	stator resistance
R_1'	unipolar stator resistance
R_2	refered rotor resistance
R_r	rotor resistance
R_{rd}	direct axis rotor resistance
R_{rq}	quadrature axis rotor resistance
R_s	stator resistance
R_{sd}	direct axis stator resistance
R_{sq}	quadrature axis stator resistance
s	slip
T	torque
$[T]$	transformation matrix
t	time
T_1, T_2	modulation edges in time
TM	time of one cycle of the carrier frequency
V	voltage
$\underline{V}$	voltage vector $(V_1, V_2, V_3, ...)$
V_A	armature voltage
V_a, V_b, V_c	stator voltages, conventional inverter leg output voltages
V_{ab}	conventional inverter leg to leg output voltage
V_d	direct axis voltage
V_{dc}	main dc power rail

V_f	field voltage
V_q	quadrature voltage
V_{rd}	direct axis rotor voltage
V_{rq}	quadrature axis rotor voltage
V_{sd}	direct axis stator voltage
V_{sq}	quadrature axis stator voltage
V_l	ac voltage (rating tests)
w	stator slot width, integral of function f
X_1	stator leakage reactance
X_2	refered rotor leakage reactance
X_m	magnetizing reactance
η	efficiency
θ	angle stator to rotor
θ_r	angle of rotor to arbitrary reference frame
θ_s	angle of stator to arbitrary reference frame
π	pi
ϕ	power factor angle ($\cos(\phi)$)
Ψ	flux vector
ω	angular speed of rotation
ω_s	supply frequency in rads/second

1.Ø INTRODUCTION

Some ten years after the invention of the poly phase induction motor by Tesla, in 1886 (ref. 1), Ward Leonard wrote; "The control of the speed on an electric motor from a state of rest to a state of full speed is a problem of rapidly growing importance to the electrical engineer. The operation by means of electric motors of elevators, locomotives, printing presses, travelling cranes, turrets of men-of-war, pumps, ventilating fans, air compressors, horseless vehicles and many other electric motor applications, too numerous to mention in detail, all involve the desirability of operating an electric motor under perfect and economical control at any desired speed from rest to full speed". (ref. 2)

The paper was a discussion of whether to use controlled voltage or inserted resistance in the control of motors. It introduced the now well known Ward Leonard system, which is essentially a voltage control for the armature of a dc machine. The words he wrote, if archaic, are very relevant now. The emphasis is still exactly where he placed it; on "perfect and economical".

The controlled armature voltage dc motor variable speed drive still has the pre-eminence, although the reasons have changed. Indeed the dc motor with electronic control, which replaced the Ward Leonard drive, has almost entirely taken over from systems that were competitive

with the Ward Leonard system.

It is worthwile noting that there has not been any new fundamental method of speed control. Voltage control, inserted resistance and frequency changing were all investigated very early on, and some economical drives resulted. These include the Krammer drive, the Scerbius drive, the Schrage motor, amplidynes and ,most recently, the Pole Amplitude Modulation motor and the spherical motor (ref. 3,4). Whether they were economical or not depended upon the application, and this is true of electronic drives as well.

Of the drives mentioned, some are ac and some dc, and the ac versus dc debate makes quite a dramatic story, because of the characters and companies concerned. Lord Kelvin himself recommended dc for the power generation and transmission at Niagra Falls (ref. 8). The story of Tesla's arguments for ac has even been the subject of a television documentary (ref. 5). It is a story that has been picked up again because of the introduction of controlled rectifiers, which have been used in high voltage dc power transmission since the early nineteen fifties. Such schemes are being constructed more often and the renewed interest in variable speed drives, because of the introduction of electronics at useful power ratings, has meant that the debate continues.

The mercury arc rectifier was introduced in 1928 and the

principles of controlled rectification, inversion, cycloconverters and even forced commutation, using capacitors, were soon established. Some novel drives were also being considered (ref. 11).

The thyristor eventually replaced the mercury arc rectifier, and is still doing so in old equipment. The introduction of bipolar transistors, gate turn-off thyristors (GTO) and field effect transistors (FET) in useful and increasing ratings have brought the possibility of commutation by the control terminal, without complicated high power circuits. Their reducing cost has also renewed interest in ideas that had been abandoned earlier as too expensive or complicated. Perhaps the most notable of these is the switched reluctance (SR) motor, which has recently achieved an advanced state of development (ref. 10).

Other recent interest has been in the frequency control of synchronous (including permanent magnet) motors and induction motors using inverters. Induction motors, particularly, have an established reputation for simplicity, reliability and robustness. They have long been used with controlled voltage, series resistance, cycloconverters and controlled slip power drives, using resistors, Krammer and Scherbius drives, both electronic (static), with controlled rectifiers, and rotary, from low power to high power.

The early thyristor inverters, developed in the nineteen sixties, using forced commutation, produced a variable frequency, quasi-square wave voltage output and operated from variable voltage DC sources (to maintain the flux in the machine at the designed level). A well known example is the McMurray impulse commutated inverter (fig. 1.1). However such systems have a number of disadvantages. At low dc link voltages the commutation ability is reduced and therefore the torque of the machine at low speeds is reduced or the components are over rated at high speed operation. The voltage output has a large harmonic content, which seriously affects the motor and a variable DC source is required.

Using thyristor devices, which are more easily and quickly commutated, a sinewave voltage output of variable frequency and amplitude, with low harmonic content, can be synthesised from a fixed DC souce. This is done by modulation of a high frequency square wave and is known as pulse-width modulation (PWM).

Another of the reasons for the increased interest in variable speed drives is economy, as Ward Leonard wrote. Labour has become more expensive and computers and integrated electronics have become, relatively, much cheaper. This has lead to rapid factory automation and some electronic control of any motor is necessary for interfacing the motor to the computer. Process industries have also become more significant with the development of

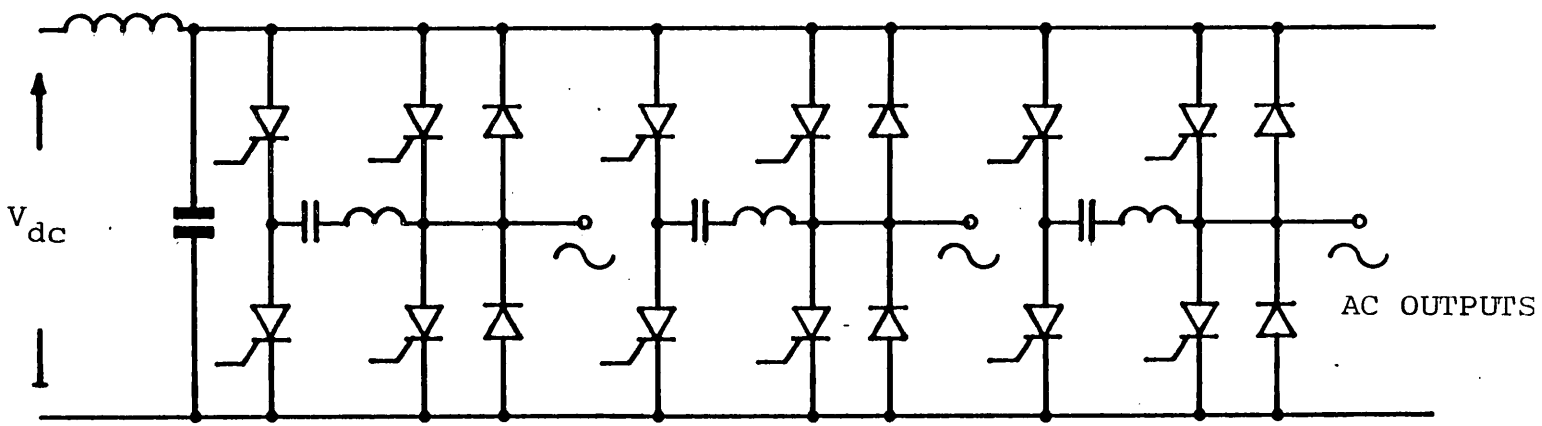

FIGURE 1.1 McMURRAY IMPULSE COMMUTATED THREE PHASE INVERTER

plastics and other oil based products, and extensive food processing. Energy efficiency, itself, became important suddenly in the nineteen seventies, with the oil crisis and greater public awareness. It has been widely argued that a variable speed drive is more efficient than a fixed speed drive on light load (refs. 6,7). This, in turn has caused great interest in the strategy used in PWM inverters.

However the DC motor drive has maintained and increased its popularity (ref 7), because it is a simple arrangement (see fig. 1.2) , with very reliable electronics. Either a controlled rectifier bridge or an uncontrolled bridge and a single force commutated chopper is used to supply the armature. Should the commutation or phase control fail, full volts are applied to the motor, which can withstand this condition until the isolating circuit breaker drops out. The brushes and commutator on the motor, which wear, have a regular maintainance period and can be renewed in advance of a failure.

One of the frequently refered to aims of installing an inverter and a cage induction motor is to increase reliability. It is hoped that the regular servicing required with dc drives may be dispensed with. However a disadvantage is that should a repair to an inverter drive be necessary, it would tend to require a highly skilled person. It may even be necessary to return it to the manufacturer. Thus one failure may be very expensive in

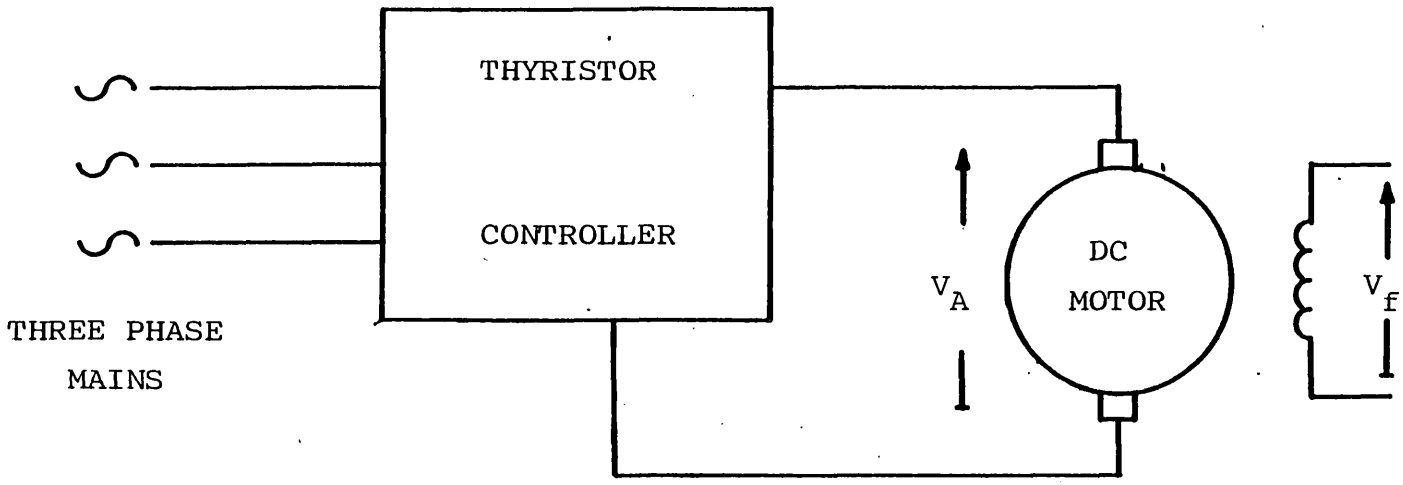

FIGURE 1.2 CONTROLLED ARMATURE VOLTAGE DC MOTOR DRIVE

lost production in some installations.

The six switch inverter bridge has a fault condition which may be disastrous as does the cycloconverter. The McMurray inverter and any forced commutated thyristor inverter may fail to commutate and the two devices in series across the dc rail will be on. A transistor or GTO bridge may fail because of interference on the logic signals. The resultant short circuit current will rise rapidly. Therefore it is usual to insert large amounts of inductance, to reduce the rate of rise of the fault current to a level at which there is time for the dc source to be turned off, before damage to the inverter bridge occurs. In the limit such an arrangement is the current source inverter, which has a phase controlled rectifying bridge and a large inductance in the DC link (see fig. 1.3).

The intention of the proposed Unipolar inverter is to return to a situation like that of the dc chopper drive, where the motor is in series with the switching elements and no extra inductance need be included. It is the possibility of utilizing a unipolar arrangement that makes the SR drive attractive (ref. 9).

The unipolar induction motor drive has been the subject of a number of patents (ref. 12). However they are limited in size because they use simple primitive electronics, and either rely on the near unity coupling of a bifilar

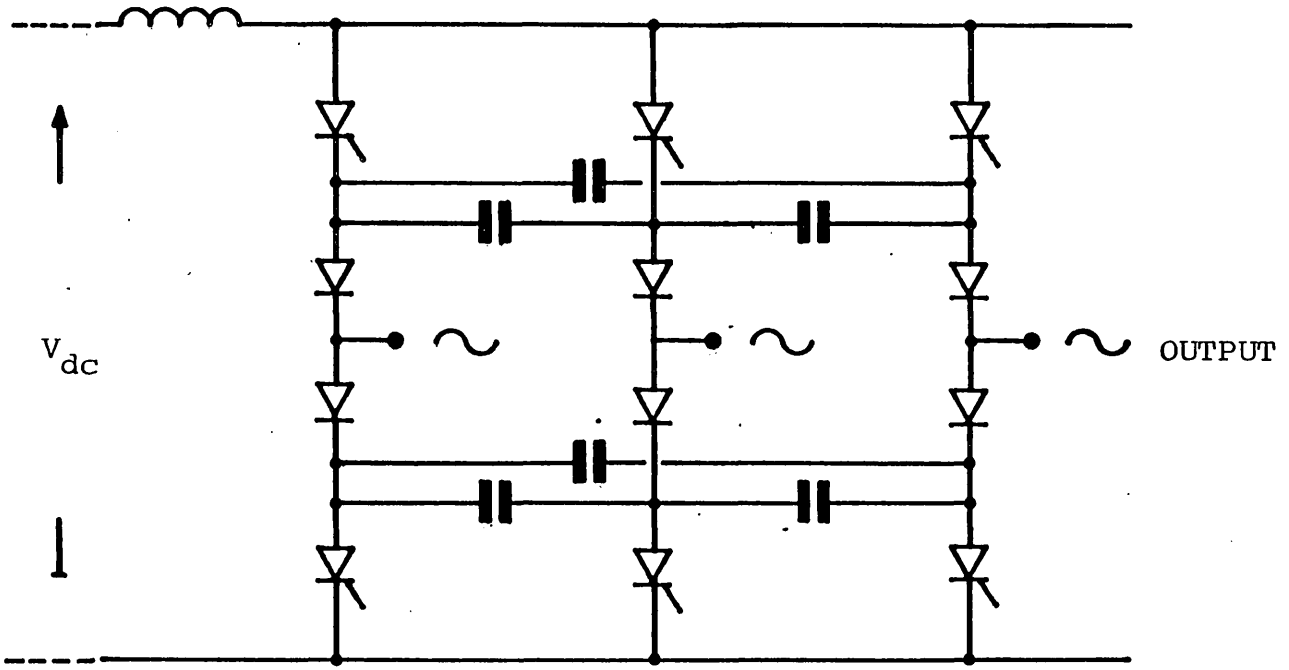

FIGURE 1.3 THREE PHASE CURRENT SOURCE INVERTER

winding, or on a high resistance in series with the winding, or on a third voltage rail. An example of one such drive is shown in figure 1.4. None discuss the possibility of larger drives or investigate the principles involved.

In this work reasonably large induction motors were used, at realistic voltages. The inverter bridges were half controlled asymmetrical half bridges, implemented with bipolar transistors (see fig. 1.5). Essentially six bridges are required for a three phase motor. The arrangement is general and can be sensibly applied to any size of motor. The PWM signals were obtained from the industry standard VLSI circuit made by Mullard.

The thesis starts with a more detailed study of the difficulties associated with conventional inverters. Then the complete unipolar drive proposed and the motors tested, are described and the method of operation is explained. This is followed by sample torque versus speed and efficiency versus speed curves leading on to discussion of the drive performance. To study the performance further and to run idealised experiments a mutually coupled coil model is developed and results are presented and discussed.

There is also an extensive study of the inverter under fault conditions, where it will be seen that the previous unipolar drives covered by patents scale up with reduced

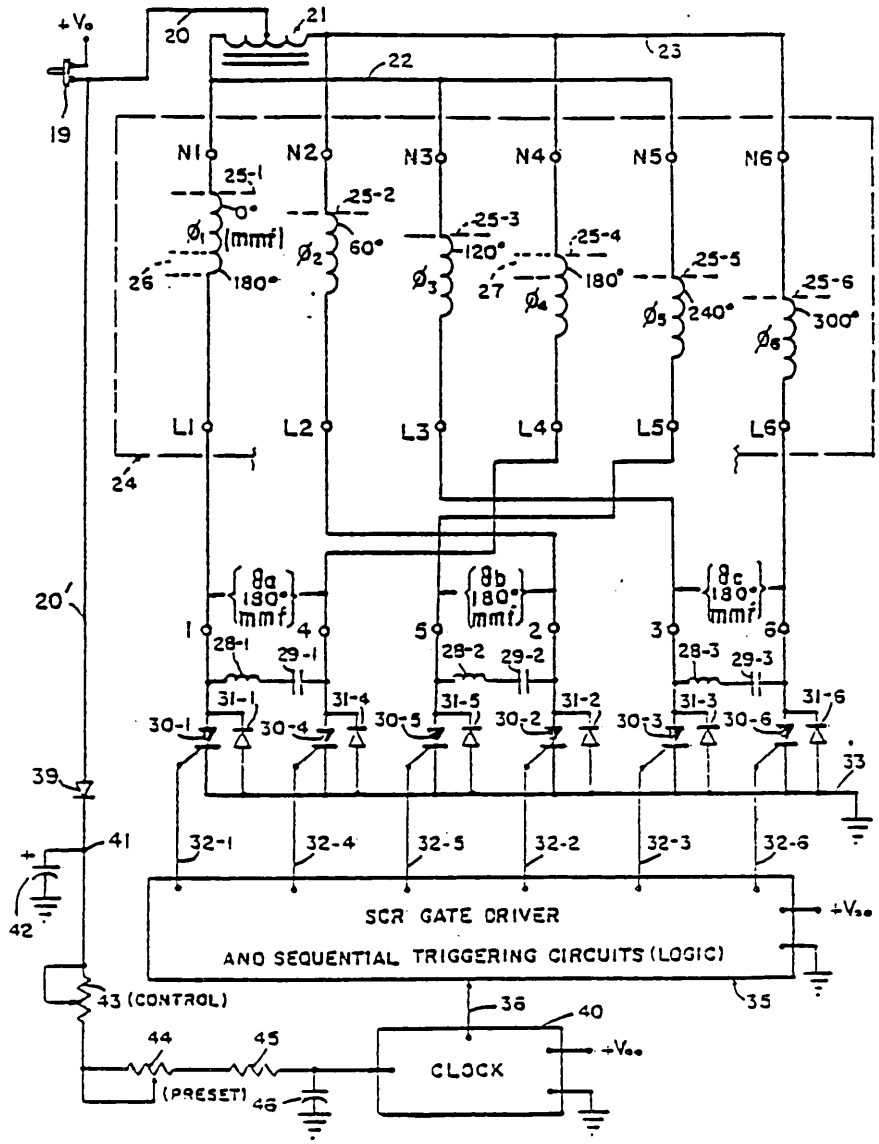

FIGURE 1.4 AN EXAMPLE OF A PATENTED UNIPOLAR DRIVE (PATENT No. 1385205)

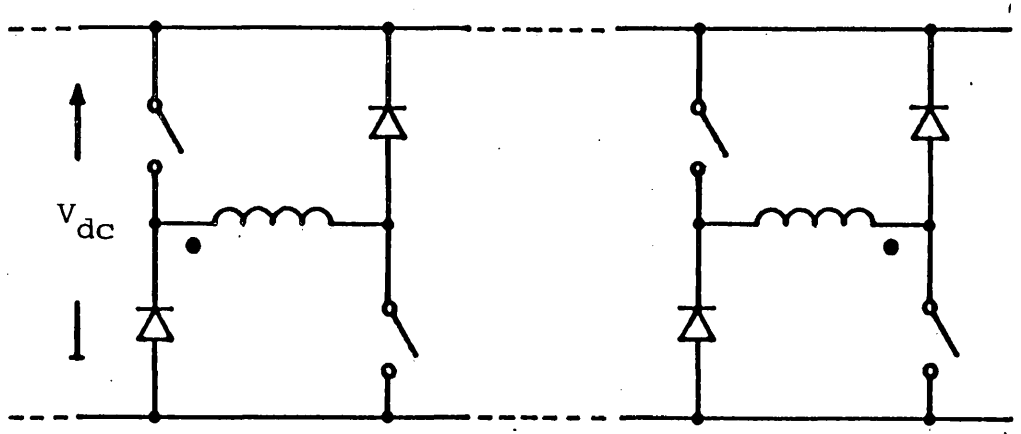

FIGURE 1.5 ASYMMETRICAL HALF BRIDGES CONNECTED TO COUPLED WINDINGS FOR REVERSIBLE FLUX

effectiveness. The work is completed with theoretical results obtained using a per-phase equivalent circuit and a discussion on the continuous rating of the unipolar inverter cage induction motor drive.

Finally conclusions are made and some suggestions given for further work covering a number of areas related to inverters in general and the unipolar inverter in particular.

2.Ø REVIEW OF INVERTER TECHNOLOGY

2.1 COMMON TYPES OF INVERTER

Most inverters above 3kW obtain their dc voltage rail from rectification of the three phase mains with a bridge as shown in figure 2.1. Should a variable dc link voltage be required, the diodes may be replaced by thyristors. In their most simple form such bridges can only allow forward conversion of power. To return power to the supply, another bridge in reverse must be switched in and the first switched out. Alternatively an inductance may be included in the link, which keeps the current flowing in the forward direction, whilst the link voltage is reversed. Both these techniques are used in dc converter drives, where the link voltage is reversed by change-over contactors.

The basic three phase inverter has a similar form to the rectifier. It requires six switching elements in three legs (see fig. 2.2). Incidentally a single phase inverter only requires two legs, but a two phase inverter would require three or four. Thus using three phases is the most economical method, in components, to give a poly phase system for inverters as well as for general ac use (see ref. 8 for discussion of three phase mains).

The bridge switches usually take the form of a forward conducting device with a diode in parallel, but in the

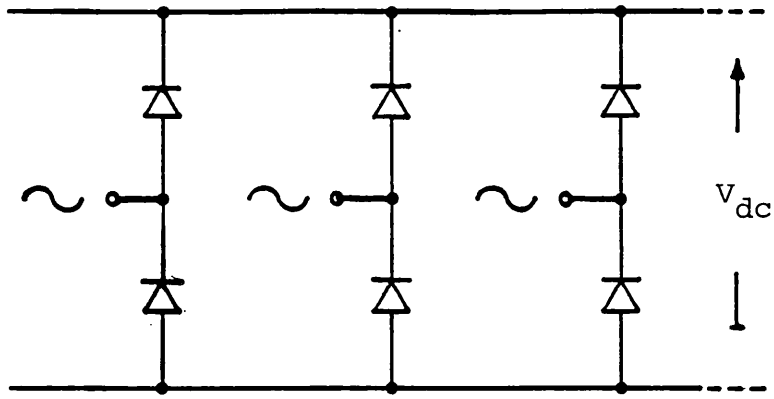

FIGURE 2.1 THREE PHASE RECTIFIER BRIDGE

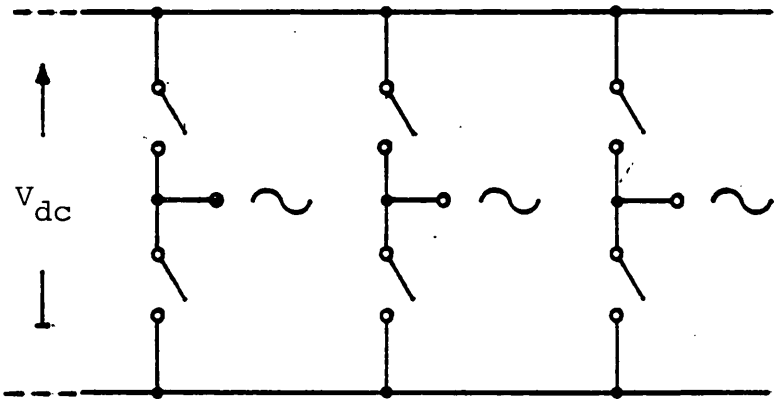

FIGURE 2.2 BASIC THREE PHASE INVERTER BRIDGE

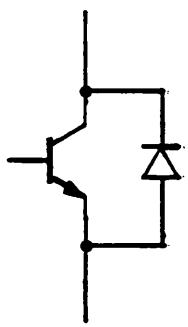

FIGURE 2.3 TRANSISTOR AND DIODE SWITCHING ELEMENT

opposite direction. (see fig. 2.3) The diode allows the inductive stored energy to be returned to the rail, when the complementary device in the leg is turned off.

However it can be seen immediately that such a system has a condition, where both switching devices may be on and the voltage rail is presented with a short circuit. This is known as simultaneous conduction or shoot-through. It is an effect well known to users of integrated logic circuits, which use a similar leg output. In motor inverters this condition will be catastrophic, because of the large short circuit current, and therefore must be controlled in some way.

Bridge inverters may be divided into two types by way of the voltage waveforms they produce. The most simple type is known as six step or quasi-square wave. The top and bottom devices are on alternatively for 180 degrees or 120 degrees of the cycle and the three legs switch with 120 degrees between them. This produces a voltage output with a significant harmonic content, which causes some extra losses in the machine resulting in machine derating (ref. 13).

The other type is the pulse width modulation inverters. The devices in a leg switch on alternatively at a frequency higher than the frequency of the motor. The high voltage and low voltage output periods for a leg are varied in a sinewave manner. This modulation is repeated

in the other two legs with a 120 degree displacement in the sinewave. The motor phase or line voltage is produced between the inverter legs. The motor voltage contains few harmonics and those around the modulation frequency are presented with a high impedance due to the leakage of the motor. Thus the current pulsations and torque ripple are small. Filter networks for high frequencies are also small. It is also possible to eliminate particularly troublesome harmonics with pwm (ref. 14).

Another aspect of variable frequency drives is that the motor voltage must remain proportional to the frequency in order to fully maintain the motor flux at the designed level. This is a direct result of the transformer equation:

$$V = N \frac{d}{dt} \Psi \qquad 2.1$$

In the six step inverter the voltage rail must be reduced with frequency to maintain this relationship. In pwm the modulation depth is changed to reduce the magnitude of the fundamental produced. Thus the rail can remain constant and a phase controlled rectifier bridge is unnecessary. Some quasi-square wave schemes use a single chopper to reduce the voltage, but it still represents increased complexity and cost.

2.2 SWITCHING DEVICES

The selection of the power electronic devices available is crucial to the method of implementing an inverter scheme. The first controlled power semiconductor device was the thyristor, which became available at useful ratings in 1960-61 (ref. 14). Methods of commutation developed for the mercury arc rectifier were directly applicable. The six step inverter was most popular, as few commutations per cycle were required. This was important because the turn off time of the thyristors was relatively slow for the higher voltage devices (ref. 15), and the losses associated with the subsequently large commutation circuits were high. Large commutation circuits were also needed because using a variable voltage rail meant that the commutation ability was variable. Some systems used a separate chopper to charge the commutation capacitor thus avoiding the problem.

In the nature of voltage fed induction motors, large transient loads cause a rapid increase in the current drawn. This can cause commutation failure, and subsequent shoot-through (ref. 16). This point was well known and thus the current fed inverter was developed from the time that the thyristor first appeared (ref. 17). A large inductance is included in the dc link with no capacitance to decouple it. It is basically a six step inverter. The link current is steered by the thyristors to the motor in phase sequence at the required frequency.

A commutation failure causes an increase in current at a rate set by the inductance and the link voltage. If the inductance is large enough the controlled rectifier or the chopper will have time to turn off before damage occurs. The current source inverter has a number of other advantages; the system may be auto-commutating, using 120 deg. conduction, where the on-coming thyristor commutates another, and also regenerative, because of the inductance in the link. Such inverters, when applied to synchronous motors can be motor line commutated and are known as brushless dc drives, because of the similarities in performance.

Developments in thyristors have brought fast recovery devices, suitable for pwm using forced commutation (ref. 18). However the possibility of the motor drawing too much current, resulting in commutation failure, is always present. It should be noted that it is possible to design fuses for thyristors and no damage to the equipment would result, although it would require maintenance.

The GTO, which has been used in inverters recently , is a type of thyristor, which may be turned off via the gate. It may be thought of in a number of ways, but for the present purpose it is best considered as a thyristor in which the holding current can be varied by the voltage on the gate (ref, 14). Its late development is because the technology of large scale integration was needed to make

it viable. A distributed network of parallel thyristors, known as islands, is created on the surface of the slice and reasonable performance can be obtained as the current is well spread out. However failure happens if an attempt is made to turn it off once the "controllable current" level has been exceeded.

The bipolar transistor has also been the subject of great interest of late. Similar physics apply to both the transistor and the thyristor and the problem of voltage ratings for transistors has been dealt with . The high voltage thyristor has a bevelled edge to reduce the field at the edge of the device. This can also be done to the transistor. Gaurd rings of glass are used by some to acheive the same effect (ref. 19). The current rating for a given silicon slice area has also improved with the use of LSI technology to give very long emitter-base junctions (upto 5m on a 5 mm die). Darlington configurations can be used for low base drive requirments.

However the safe operating area of the transistor (fig. 2.4) shows that the switching losses that can be tolerated are low and that the device is not rated to withstand the full voltage and current. In fact it can only withstand 2Ø percent of full current at the full voltage for 2Ø microseconds. This means that it is desirable to use a resistor-capacitor-diode (RCD) snubber as shown in figure 2.5. The full rating can then be used and the switching losses moved in part to the resistor,

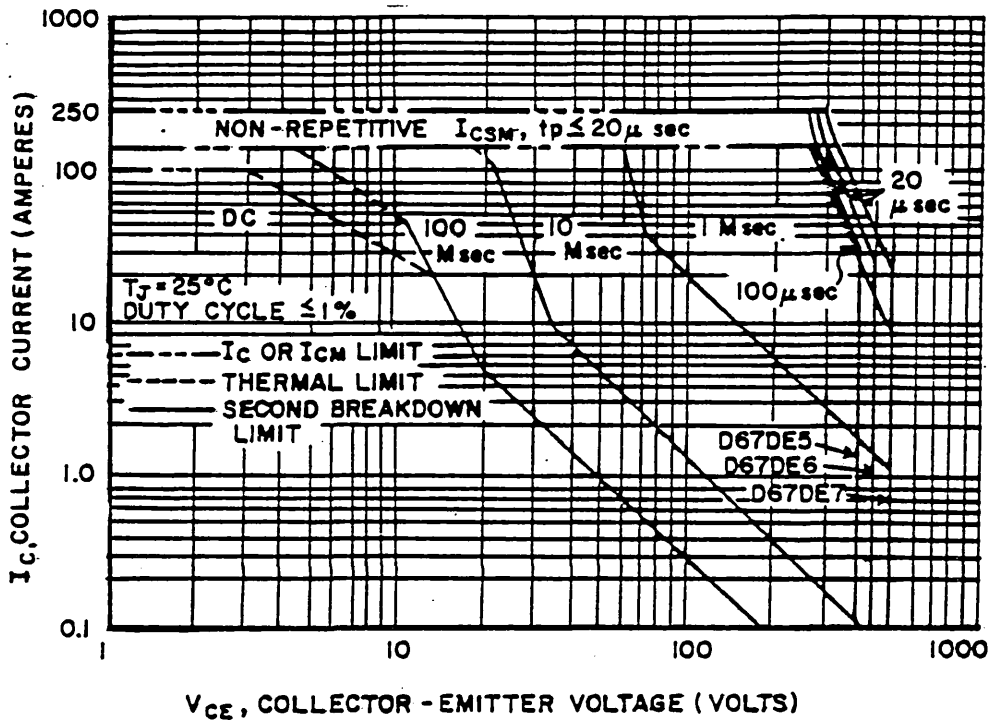

FIGURE 2.4 EXAMPLE SAFE OPERATING AREA FOR A TRANSISTOR (D67DE6)

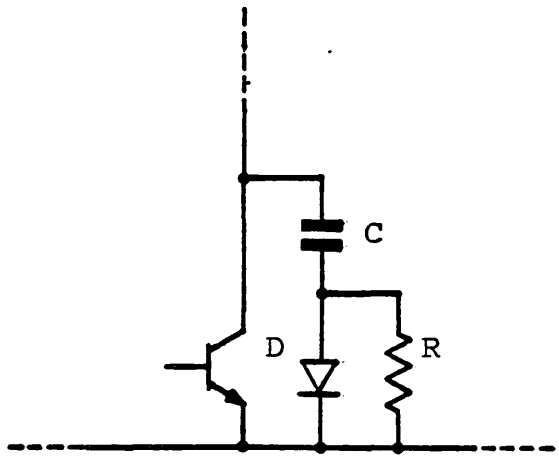

FIGURE 2.5 RCD TURN OFF SNUBBER FOR A TRANSISTOR

allowing very high switching frequencies. But it can be seen from figure 2.2 that, using the PWM stategy of alternate switching of the devices in each leg, the complementary snubber capacitor charges via the on-coming device in an uncontrolled manner.

Presently the trend is to use over rated transistors, without snubbers, at low switching frequencies. Another method with transistors is to include some inductance in the leg (see fig. 2.6) (ref. 2Ø). This has significant advantages in that snubbers may be used, with closer rated transistors and that some over-current detection may be applied, with the inductance giving it time to operate before the devices are damaged. Monitoring of the collector-emitter voltage or the emitter-base voltage can indicate an over-current condition (ref. 21). Other current sensing methods may also be applied successfully.

The power MOSFET transistor can be used without snubbers, due to it's very high speed switching, upto levels of about 3 kW. The utilisation of the slice area is poorer than that of the bipolar transistor and thyristor and that makes them expensive. However their simple drive requirements make them useful in small inverters and as bipolar drivers. Drain-source voltage monitoring may be used to detect over-current.

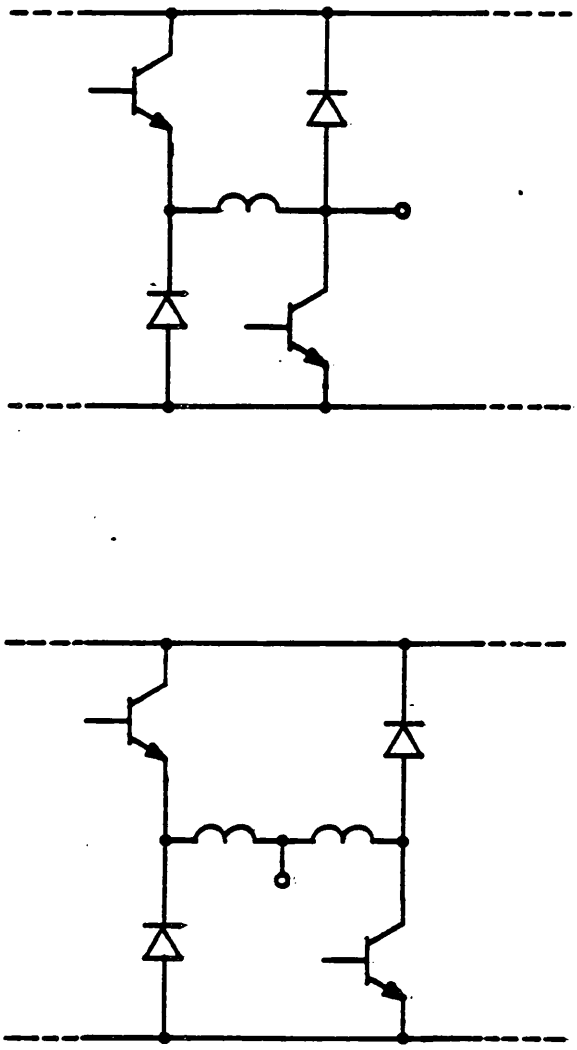

FIGURE 2.6 INVERTER LEGS INCLUDING INDUCTANCE

2.3 DRIVE CIRCUITS AND LOGIC INTERFACING

So far the devices used in inverters have only been considered from their relative ability to supply the waveforms to the motor. All of them require interfacing to the logic signals, which may be produced by simple circuitry ranging in complexity upto microprocessors. Thyristors can be turned on, or "fired", by light, but are usually given a small pulse of current. They usually have no off drive. Because of this the conditions of di/dt and dv/dt applied to the thyristor must be strictly controlled. The other devices mentioned commonly have some off drive and are more immune to dv/dt. Their distributed layout means that di/dt is not usually a problem.

Because the thyristor may be latched on, only a pulse of current into the gate is required. It must be long enough for the anode current to rise to the latching value. The upper device in an inverter leg needs a floating supply as the cathode is connected to the load and therefore changes voltage with the phase output. Such a drive is easily acheived for amplifying gate thyristors, and is one of their favourable characteristics. A small pulse transformer is usual, giving isolation and a sufficiently long pulse. It is common to use them on the lower devices as well to give complete isolation between the power side and the logic side.

As with thyristors, high voltage power bipolar transistors and GTOs are not made in the complementary form. This is because of the poor performance of the complementary devices, n and p type silicon being quite different in terms of their physical constants. Thus for these devices at the top of the leg it is also necessary to have some floating drive circuit. However they both require continuous base or gate current whilst on and ideally some voltage and current in reverse when off.

The obvious method is to use one transformer per device to give the voltage rails and to isolate the logic signals with optocouplers. However, using the standard three phase mains rectified to give the power rails, they will be near 600 V. If the switching speed of the devices is to be used (to reduce the losses in the devices), the 1000 V/uS rating for the best optocouplers may be exceeded and they may be unreliable. Other, more suitable, methods have been suggested including level shifting networks (ref. 22), a latching system using a pulse transformer as well (ref. 55) and fibre optics. The bottom devices are more straight forward to drive as they are at a fixed potential. FETs have lower drive requirements and complementary devices are also available at lower voltage ratings. N channel FETs may also be driven from pulse transformers and from level shifting networks.

However much care is taken in the design and construction of inverters, components may still fail. On some

components manufacturers are able to give percentage failure rates against time. Interference on the logic signals may also cause a shoot-through. This may be particularly important in industrial environments. Thus it is always necessary to build in some over-current sensing at the output stage and to include some inductance to limit the rate of rise of fault current.

2.4 THE UNIPOLAR INVERTER LEG

It has been shown that some significant inductance in the inverter drive is not only desirable but necessary. These inductances carry the full rated current and their losses can be troublesome. It may even be economical to fan cool them, as winding them with enough copper to reduce the losses to an acceptable level might be expensive. Reducing the size of the inductance in current source inverters has been the subject of some recent research (ref. 23).

The unipolar feed of motors has been used for some years in the control of small stepping motors, which are used in vast numbers in line printers. It takes the form shown in figure 2.7. This can be compared to the chopper drive for a dc motor in figure 2.8. In both cases the motor windings are in series with the switches and the current is unidirectional. The current can only rise at a rate set by the inductance, resistance and back emf of the motor. Any of the devices mentioned may be used for the switch. When the switching devices are turned off, the current continues around the diode path, due to the stored energy in the inductances of the motors. In a small motor the winding is very resistive and the current decays quickly. As motors increase in size, their resistance decreases. Thus the current takes a long time to decay around the diode free-wheel path. In certain applications a resistance may be included in the free-wheel path. In the dc motor case the free-wheeling period is only critical if

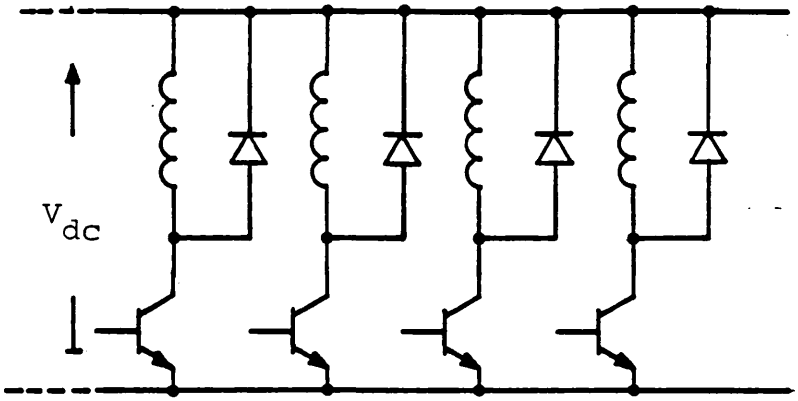

FIGURE 2.7 SMALL STEPPING MOTOR DRIVE (VR)

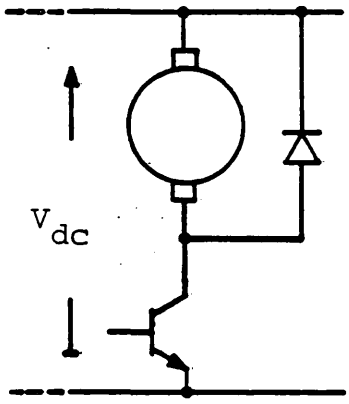

FIGURE 2.8 DC MOTOR AND CHOPPER DRIVE

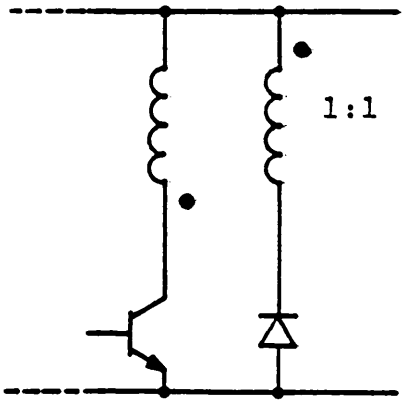

FIGURE 2.9 UNIPOLAR DRIVE WITH CATCH WINDING

the motor is required to stop or reverse quickly. This is because the equivalent of the phase changing in the stepper is accomplished by the commutator in the dc motor.

Another method in stepper and switched reluctance drives is to use bifilar wound coils (fig. 2.9), one of which is made of thin wire and is used for free-wheeling only. The inductive energy is then returned to the rail by this "catch" winding. It is a common technique in switched-mode power supplies. However the off device experiences voltages of almost twice that of the dc rail.

Coupled coils may be used in other motors to produce a reversible flux. Both coils have a switching device in series and a diode in antiparallel (fig. 2.10). Both this and the free-wheeling methods mentioned above have been used with bifilar wound induction motors and aspects of such drives are covered by several patents (ref. 12).

However the free-wheeling is very rapid as the energy is returned to the high voltage rail. In pwm schemes this is not convenient as it will necessitate a very high switching frequency to keep the current sinusoidal. Commercial pwm strategies rely on a combination of low voltage and high voltage free-wheel paths, depending on the point reached in the sinewave being reproduced.

This leads to the asymmetrical half bridge, figure 2.11. This is used successfully in sr motors upto 75 kW

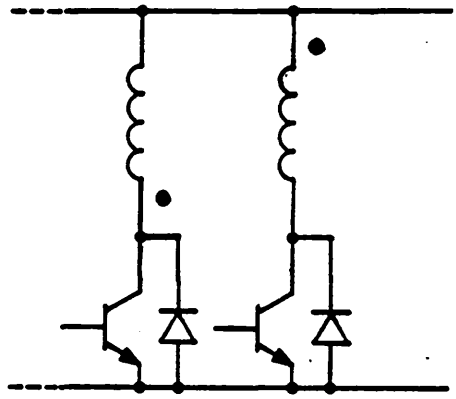

FIGURE 2.10 UNIPOLAR DRIVE WITH REVERSIBLE FLUX

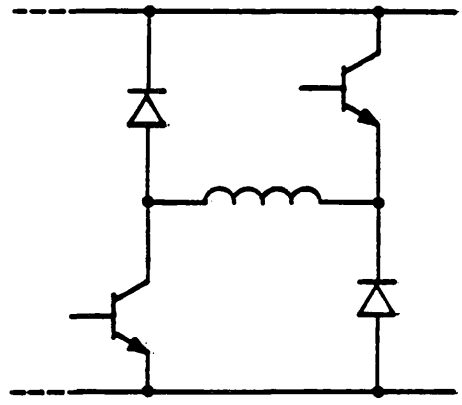

FIGURE 2.11 ASYMMETRICAL HALF BRIDGE

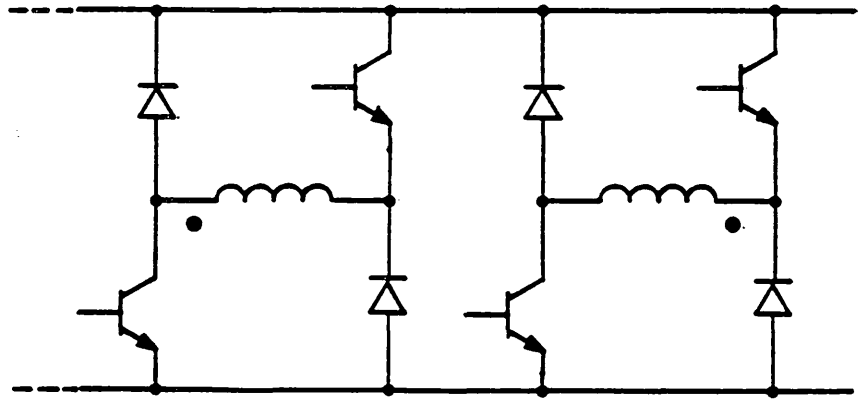

FIGURE 2.12 ASYMMETRICAL HALF BRIDGES APPLIED TO A UNIPOLAR DRIVE WITH REVERSIBLE FLUX

(ref. 13). The free-wheeling may be around a single diode path or through both diodes into the rail. Thus the devices need only to be rated at the rail voltage. This may be extended to bifilar induction motors merely by having another similar half bridge on the other half winding as shown in figure 2.12 (ref. 24). In fact as neither the winding resistance nor high coupling between phase halves is used for free-wheeling, they need not be coupled so closely, which is useful when considering fault conditions (cf. Sect. 6.3), and the system is not limited in size.

Snubbers may also be used on the switching devices as there is no direct path for them to charge. They charge and discharge only via the coupling of the two half windings (cf.Sect. 3.4). Thus high frequency switching may be used to obtain a very pure sinewave current.

The merits of the bifilar unipolar fed induction machine have been noted lately for their use in cycloconverter drives (ref. 25). These have not been discussed as they form a seperate type of drive for low speed use. However it is usual to include some inductance in the cycloconverter to prevent a short circuit between phase groups. This inductance may be dispensed with if unipolar feed is adopted as is the case with pwm drives.

3.Ø THE EXPERIMENTAL UNIPOLAR INVERTER

3.1 DESCRIPTION OF MOTORS

The topology of the inverter (Sect. 2.4) means that the motor is effectively connected in delta in that the full rail voltage may be applied to each coil independently. For safety under laboratory conditions and for reason of the then available bipolar transistors a lower voltage motor was desirable. Thus standard 415 V star connected induction motors were used. Two experimental motors were tested. Both were standard D112 frame size 4kW rated three phase squirrel cage motors. The motors were not special motors for inverters or high efficiency. The parameters of the motors are given in Appendix A. Their measurement is described in Section 5.6.

A totally enclosed fan cooled arrangement was chosen because it is considered to be the most desirable arrangement from the industrial view, being the most robust and free from environmental effects. However the frame size , thus cooled, can only dissipate approximately 8ØØW. Considerable derating on the continuous duty is necessary if it is used on an inverter of any description and particularly the unipolar inverter.

The first motor was a standard motor, which was, for reasons of packing factor, wound with two wires in bifilar. The only alteration required, and made by the

manufacturer, was to bring all twelve ends of the coils out to a terminal block. Tests on this motor indicated that a better design would be to have the coil pairs in the same slots but separated. This gives increased leakage between the phase halves and thus a higher impedance to a fault current (see Sect. 6.3).

The new motor was wound with one complete stator winding of half the amount of copper inside another, with insulation between. Fears that this might be detrimental to performance were unfounded. The inserted insulation was considered useful, because the full voltage rail appears betweem the similar ends of the coil pairs during some periods of the cycle. However it is not considered necessary now since no more than the voltage rail can appear on the adjacent windings for which their own insulation is adequate.

The motors were supplied with shaft extensions to facilitate 'swinging' the motor in pillow block bearings which allows shaft torque to be measured.

3.2 TRANSISTOR BRIDGES

Early work conducted with a thyristor bridge (ref. 26) soon led to the conclusion that it would be best to work with six half controlled asymmetrical half bridges connected to the motor as shown in figure 3.1, using the dot convention for each phase. This is very versatile and allows any waveform to be applied to the winding with current in one direction only. This means that twelve switching devices are required compared to six for a standard bridge. (However subsequent work has shown that a more commercially viable version can be easily effected with only six devices; the analysis and waveforms being no different from those presented later in Section 5.)

For reasons of the modulation depth and output voltage used for the tests (see Sect. 3.3) a voltage rail of 385V was required.

The transistors used were D67DE6, 450V, 100A Darlingtons (ref. 27). Whilst only 11A peak approximately is required to reach the motors rated output, a large margin was useful since failures due to mistakes made during testing were very much reduced, there being no over-current detection in the laboratory inverter. (Effective DOL starts were survived.) These transistors also allowed faults to be simulated as shown later (Sect. 6.2).

The bottom transistor drives (fig. 3.2) were fairly simple

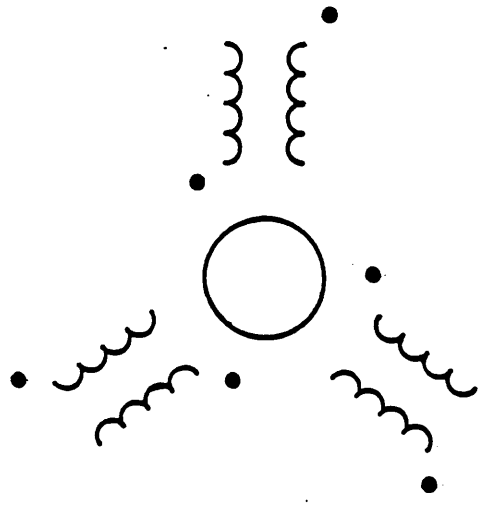

FIGURE 3.1 CONNECTION OF THE UNIPOLAR INDUCTION MOTOR STATOR WINDINGS

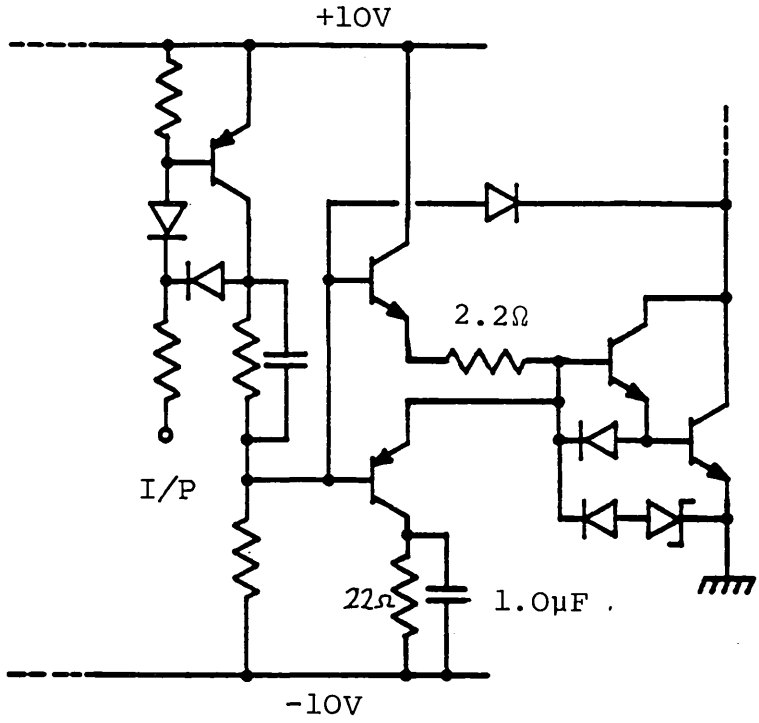

FIGURE 3.2 BOTTOM TRANSISTOR DRIVE CIRCUIT
(NEGLECTING RESISTORS INTERNAL TO THE DARLINGTON PAIR)

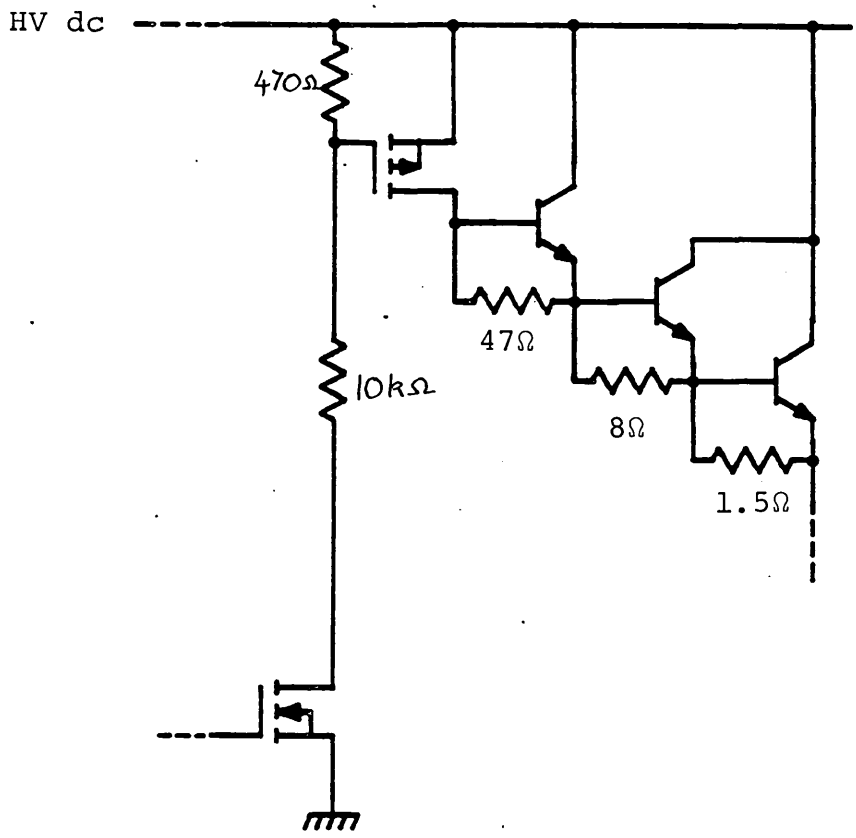

FIGURE 3.3 TOP TRANSISTOR DRIVE CIRCUIT
(INCLUDING RESISTORS INTERNAL TO THE DARLINGTON PAIR)

and gave sub microsecond switching times. The top transistors were turned on by a level shifting arrangement into a p channel - npn Darlington configuration (fig. 3.3). Turn off was by natural recovery, which was quite fast for these devices, as they were well out of saturation because of the Darlington arrangement.

RCD snubbers (see fig. 2.5,Sect. 2.2) of Ø.1uF on the top devices and Ø.22uF on the bottom devices were used. Those on the bottom were later dispensed with, as the bottom drive was much better, since it utilized base-emitter reverse bias at turn-off. Very fast freewheel diodes were used (ESM 243-4ØØ.)

The h.v. dc rails were obtained by rectification of the three phase mains via a large variac. Electrolytic capacitors were connected across this rail to reduce the effects of regulation at high peak currents. A small amount of high frequency decoupling was also used. During tests the variac did cause a little regulation at high loads. This was corrected for at each measurement point when necessary.

3.3 INVERTER MODULATION SIGNALS

The basic three phase PWM signals are produced by a Mullard VM5000 board. This is based on the HEF 4752V LSI circuit (ref. 28) and includes all the related circuitry. The data for the VM5000 may be found in Appendix B.

In its standard form the signals cause the transistors in a normal inverter leg to switch alternately, with a small change over delay. This produces Va, Vb and Vc respectively (fig. 3.4). The top switch, when on, causes a high output voltage and the bottom, when on, causes a low output voltage. In the standard inverter there are diodes in antiparallel with the transitors, so the voltage waveform stays the same irrespective of the load current. The current may redirect through a diode, should it want to, at the time that its antiparallel transistor would have been conducting.

For a delta connected load, the phase voltage is shown as Vab. This may be considered as a signed exclusive OR function; which is how it was manipulated for the configuration of six independant bridges used here. The HEF4572V uses a high frequency clock, FCT which is a multiple of the output frequency. There is also a synchronising pulse at the positive going zero transition of the red phase voltage. The FCT clock was divided down and then used to clock a three D type flip flop ring counter, which was synchronised to the inverter by the

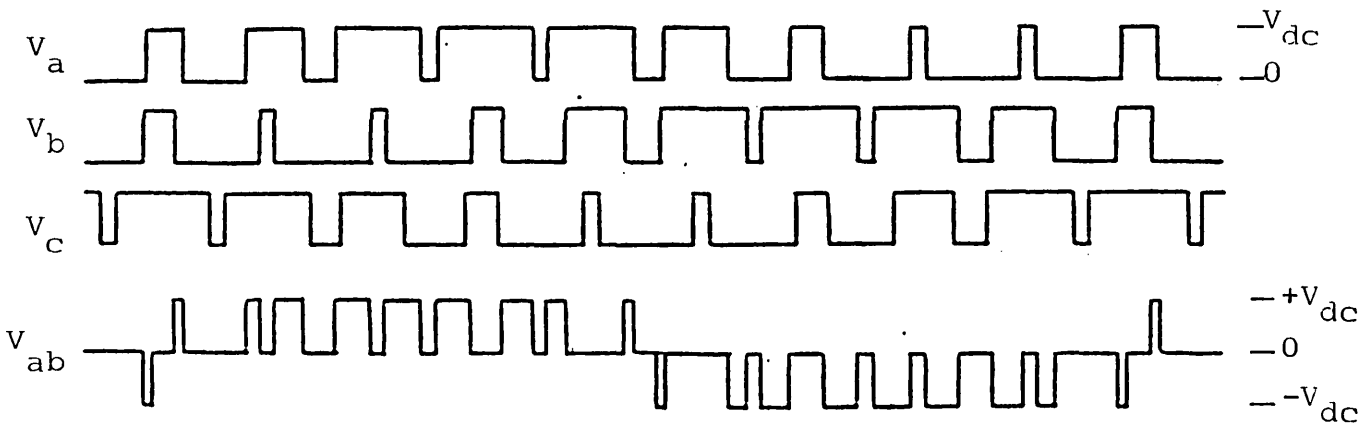

FIGURE 3.4 DERIVATION OF LOAD VOLTAGE FROM INVERTER LEG OUTPUTS

synchronising pulse that was available. This gave three square wave outputs at the same frequency as the fundamental and in phase with the motor's phase voltage. These square wave signals and their inverses were used to sign the phase voltages. To obtain the unsigned phase voltages, the 3 modulation waveforms were put through exclusive OR gates. Various combinations of the exclusive OR output and fundamental square wave were considered. The waveforms used for the tests were the square wave for one device in the bridge and all the modulation in the other device. This took the form of normal modulation from the exclusive OR for half the cycle then the modulation inverted for the negative half cycle. (see Appendix B)

The effect of this strategy results in modulation in the forward voltage and current sense whilst the fundamental frequency switching device is on. When it is off the free-wheel path is modulated from zero around a diode-transistor path to the full voltage via both diodes. When the bottom device is off, it is expected that the current will fall to zero, and the other phase half, with the complementary waveform, will start conducting current.

The same phase voltage waveforms may be produced in a variety of ways. This particular one was chosen because it reduces the stress on one device in each bridge, it only having to switch at a low frequency with a 50% duty cycle, which was useful given the simple bridge design.

The VM5ØØØ, in conjunction with other circuitry can be made to give voltage boosting at low frequency and overmodulation at high frequencies. However, because the fundamental output voltage is not specifically defined if it is used in overmodulation (the normal method), '1ØØ% modulation' (at 5ØHz) was used throughout. '1ØØ% modulation' can be accurately set by setting the VCT clock (voltage control) at twice the frequency of the FCT clock at the desired motor frequency. Thus taking 5ØHz that makes FVCT 2x5Øx336ØHz. During tests the VCT clock was set using a frequency meter. Then the output frequency for the motor is set at 5ØHz, or whatever is required, using the frequency meter connected to the FCT clock output.

At 1ØØ% modulation the output voltage is then Ø.624 times the rail voltage. Thus for a 24ØV motor a 385V rail was required. At frequencies less than 5ØHz the output voltage is in proportion to the frequency, as is commonly done to keep the motor flux constant.

3.4 DISCUSSION OF OPERATION

The details of the operation of the unipolar motor are best described with reference to the two coupled coils representing one phase of the motor-inverter.

There are four current states defined in all for the phase, although in terms of the bridge switching and symmetry these could be reduced to two. For the discussion, the main current is in the first half, and the four states are shown in figures 3.5,3.6,3.11 and 3.12

Case 1

The first case (fig. 3.5) shows forward voltage being applied to the phase half and its complement is in the state of its transistors being off and no current flowing. Following the dot convention, the induced voltage on the complementary coil is in the direction of the free-wheel diodes and, if the effects of the rotor induced EMFs are neglected, it will be less than the rail voltage. Thus current cannot flow. This state however is complicated by the presence of the snubber capacitors on the upper device. Should the snubber in the complement be uncharged as the inverter changes to this state (the usual case, similar to the conventional inverter leg), it will charge up by means of the transformer action. The rate of charging is controlled by the leakage reactance of the phase halves to each other, and their resistances, in a

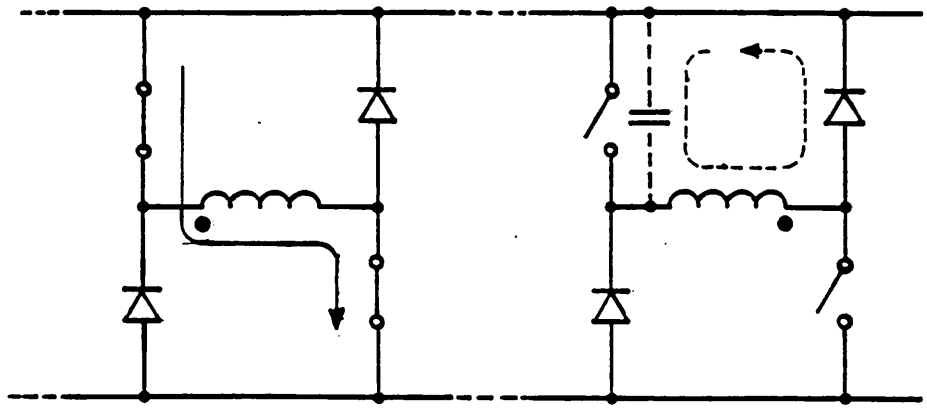

FIGURE 3.5 CASE 1

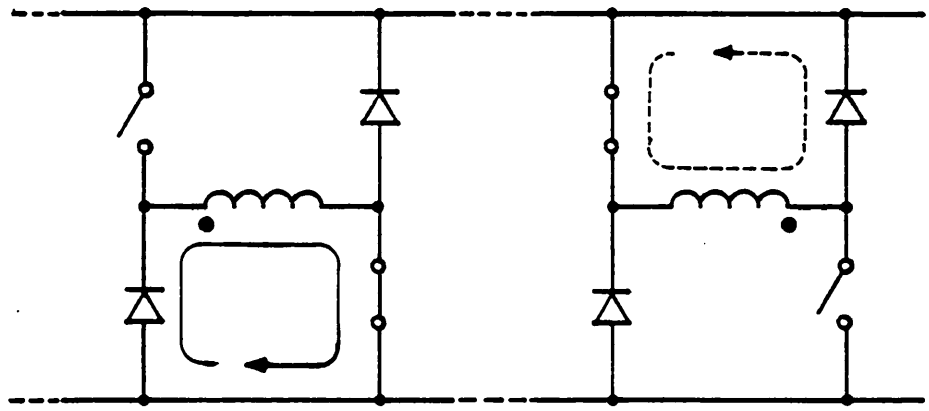

FIGURE 3.6 CASE 2

CONTINUOUS

→

CURRENT

DISCONTINUOUS

---→

CURRENT

similar fashion to faults discussed in Section 6.2. The charging currents are consequently in such directions to cancel each other out in terms of coupling to the rotor, and therefore do not affect it.

Case 2

The second case (fig. 3.6) shows both phase halves with one transistor on and one off. The main current is now presented with a single diode free-wheel path, which is approximately ØV (more accurately a few volts negative). Consequently, if the rotor is neglected ,again no current would flow in the complement because the induced voltage is in the wrong sense for its diode to operate (fig. 3.7). However,if the rotor is considered, a rotor induced EMF will appear in both coils. Current can flow in the complement if the rotor induced EMF is larger than the mutual coupling EMF. This will always be the case if the coils couple the rotor symmetrically and have leakage between each other and resistance.

Examination of the main current waveform, figure 3.8, reveals that the coil actually supplies its complementary currents which is impossible. Rather they share the rotor produced dØ/dt and this reduces the di/dt in the first coil and causes a di/dt in the second.

This effect may be compared to the well known circulating current effect in parallel windings (ref. 29). The two

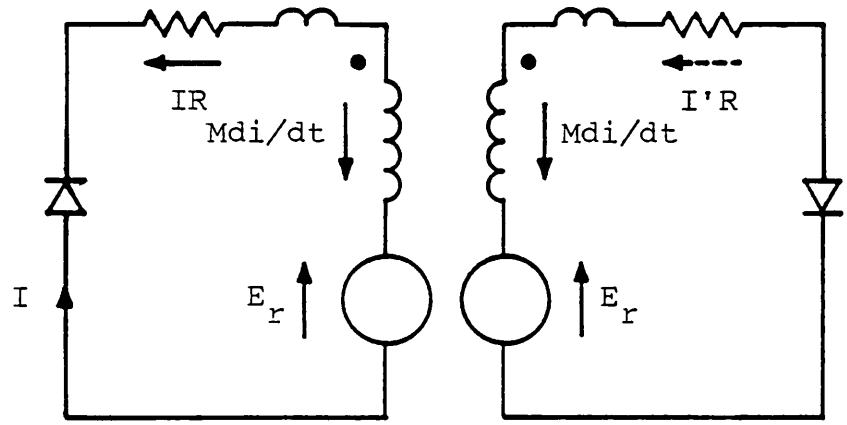

FIGURE 3.7 EQUIVALENT CIRCUIT FOR CASE 2
INCLUDING THE ROTOR

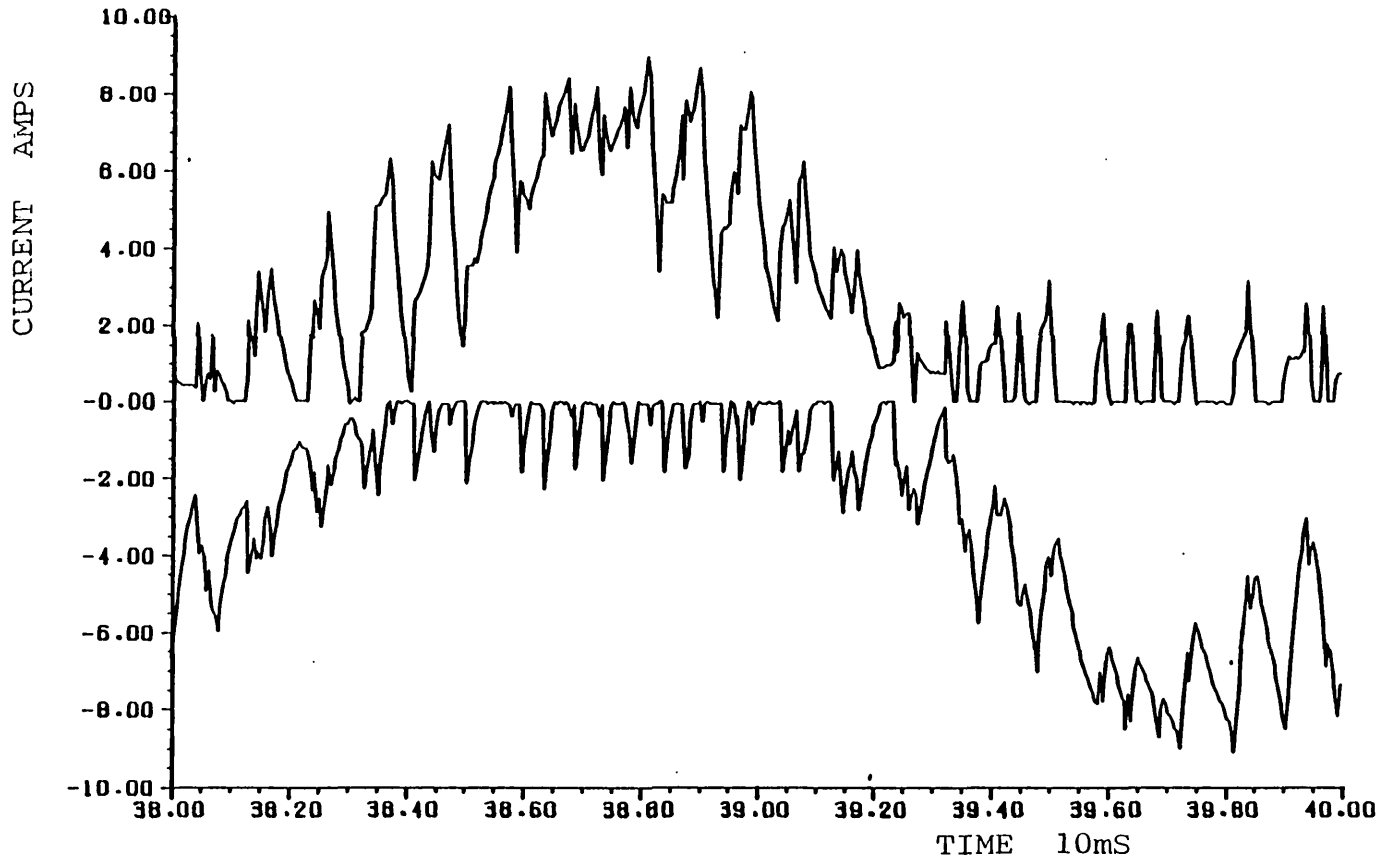

FIGURE 3.8 CURRENT WAVEFORMS FOR BOTH PHASE HALVES

half phase currents are in parallel and the currents induced destruct as far as the rotor coupling is concerned.

If the leakage between the phase halves is increased, the magnitude of these "circulating currents" is increased. This is apparent from figure 3.7. For the bifilar motor the mutual coupling inductances from the rotor to the phase halves are equal. However in the coil pair motor they are fractionally different (cf.Sect. 5.6). This has the effect of increasing the currents induced in the phase half that couples the rotor better during its OFF period and conversely reducing those in the other half during its OFF period. This asymmetry can be seen in fig. 3.8.

The circulating currents are quite large in the upper waveform. Figure 3.9 shows the voltage waveform that should be applied superimposed on the current waveform, which clearly identifies the spikes appearing during its off period as circulating currents, as the applied voltage is zero. The sharp spikes at the end of the circulating current period are snubber capacitor charging currents, as they appear when the rail voltage is reapplied.

The two effects appear separately in the lower waveform in figure 3.1Ø. The circulating currents are very small, and they have diminished before the rail voltage is reapplied and the snubber charged.

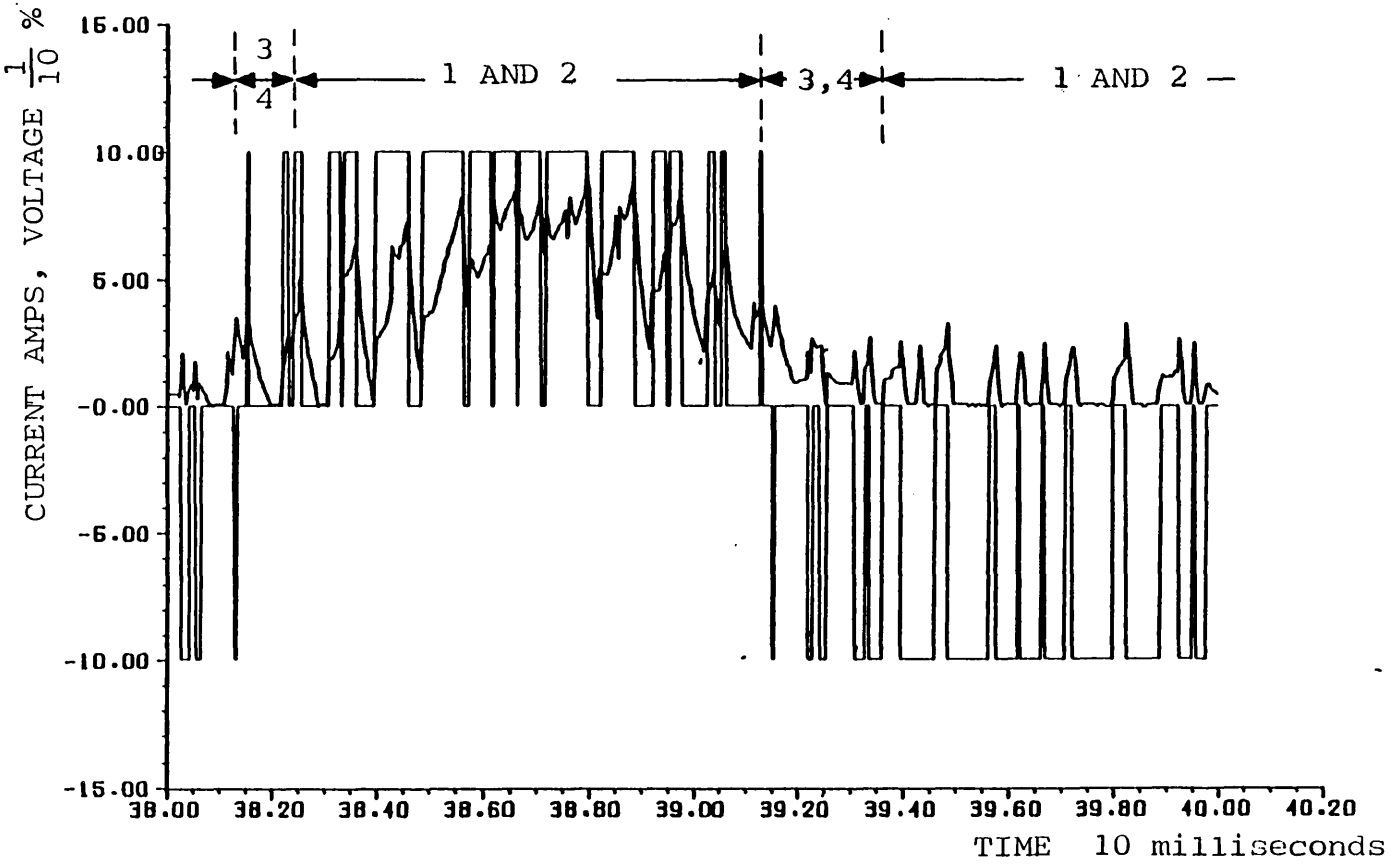

FIGURE 3.9 CURRENT WAVEFORM AND APPLIED VOLTAGE FOR ONE PHASE HALF (WITH INDICATION OF THE STATES)

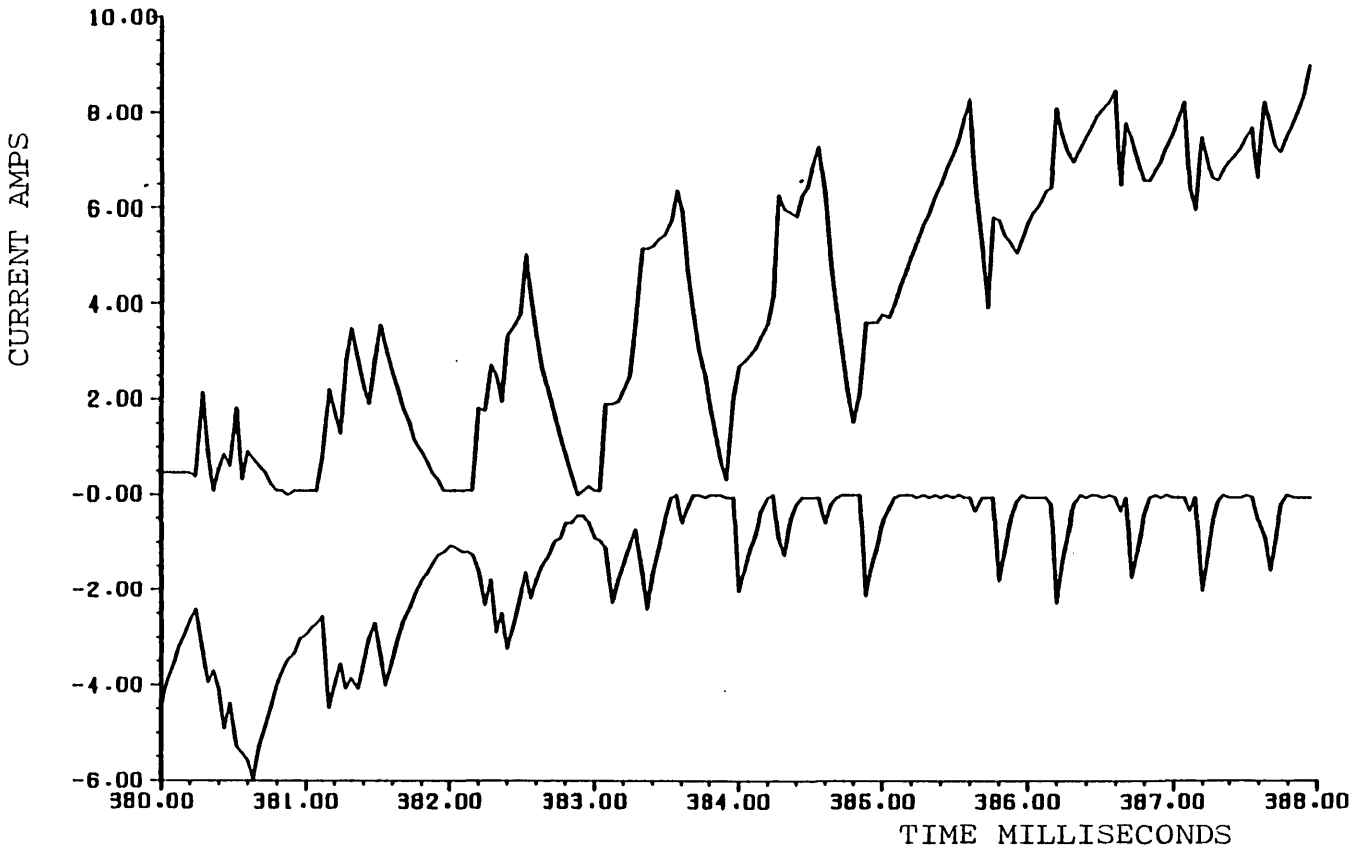

FIGURE 3.10 EXPANSION OF THE CURRENT WAVEFORM OF FIGURE 3.9

The first and second states are repeated whilst the voltage and the current are in the forward sense as marked on figure 3.9. The resulting mark-space ratio is changed, in the familiar pwm form, to give a sinewave current.

Case 3

The third state (fig. 3.11) is when the transistor switching at the fundamental frequency is turned off. The current remaining in the coil is now considered to be out of phase with the voltage. The current free-wheels through two diodes into the rail and thus the coil sees negative volts.

During this third state ,both the transistors are switched on in the complement and the new main current in the opposite direction begins to rise, although quite slowly. This is because the induced EMF caused by the current in the first coil free-wheeling is in such a direction as to oppose the applied voltage in the second.

Case 4

The fourth state (fig. 3.12) is when the currents in both halves are free-wheeling around a low voltage loop. The rotor induced EMF has the effect of boosting both of these currents.

The third and fourth states are repeated until the

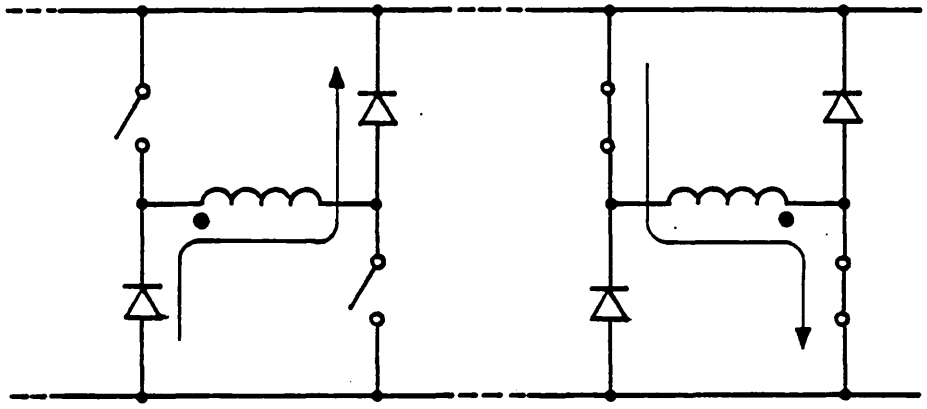

FIGURE 3.11 CASE 3

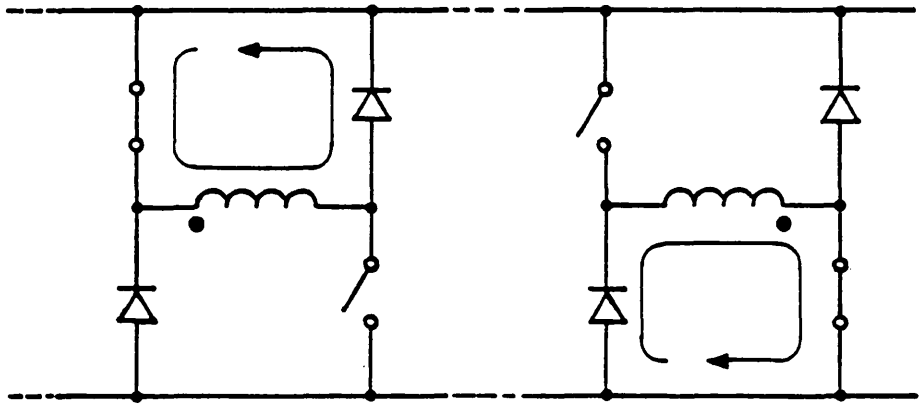

FIGURE 3.12 CASE 4

CONTINUOUS
CURRENT

original continuous current has fallen to zero, in a sinewave form, and then the first and second states operate on the complement.

It is important to note here that states 1 and 3 are similar, as are 2 and 4. The transistors are in the same state, but the current is in a different state. There remains in states 3 and 4 continuous current, which was acheived whilst PWM forward voltage was applied, which has not yet diminished to zero, although now out of phase. In states 1 and 2 the current is in phase.

The significance of states 3 and 4 is that this current is now regenerating. This regeneration is gentle because it is being modulated. Abrupt regeneration, which can be acheived by leaving both transistors off when the current is out of phase, was found to introduce torque pulsations, especially during braking (see Sect. 5.9).

The asymmetry in the current waveforms for the two phase halves (fig. 3.8) will not cause any problems in the form of Unbalanced Magnetic Pull (UMP). Each current in the unipolar motor may be reduced to its harmonic components (including a dc component) and may be considered (regarding UMP) in isolation of the other windings. As the six windings are individually symmetrical across the machine diameter, as is usual, there is no magnetic perturbation. Thus there is no UMP.

4.Ø RESULTS

4.1 LOAD AND MECHANICAL ARRANGEMENT

The mechanical arrangement was such that the motor shaft torque could be measured in the steady state. The induction motor was mounted in pillow block bearings on fabricated frames and a torque arm was bolted to its feet. The load was a 18ØØ rpm. 3 HP D.C. generator. They were coupled by 1" wide toothed pulleys and belt in a reduction ratio to match the rated speeds. The D.C. motor and the induction motor's mounting frames were securely fixed to a fabricated bed plate using adjustable cast iron cross members to allow for the belt tensioning.

The generator was loaded by an adjustable resistor bank and its field was controlled by a small variac with a rectifier and capacitor. This configuration facilitates loading of the motor in the stable portions of its torque-speed characteristic. As the motor is under inverter control these are the only parts of the characteristic of interest.

Torque was measured by a spring balance on the torque arm. A spirit level on the torque arm ensured that the spring balance was at right angles to it. Adjustment was made by a threaded screw on the spring balance mounting.

A strain gauge type load cell was tried, but the radio

frequency pickup was too great, the maximum output of the cell being only 15 mV. A commercial piezo-electric load cell with an amplifier is probably the solution, but none was available.

Transient torques, therefore, could not be measured. As the inverter current waveforms are very similar to those of a standard inverter (cf.Sect. 5.8), it was not considered necessary.

4.2 METERS AND METHODS

The D.C. link voltage was measured by a moving iron meter. The input power to the inverter was measured before the rectifier and after the variac. A digital power meter superseded the moving coil wattmeter and moving iron voltmeter and ammeter used during the early stages. A 5ØØ to Ø.5 current transformer with ten inserted turns and a 1Ø kHz bandwidth had to be used to reduce the current. A plug box was then used with the power meter for the two wattmeter method, and to allow measurement of the line voltages and current.

For some of the tests a Fluke 8Ø5ØA digital multimeter was used. It has a 1% accuracy throughout its ranges from 5% to 1ØØ% of full scale. This meter was also used for the resistance measurements for all the tests. It was checked against a 1 Ohm standard cell.

The motor speed was measured by means of a slotted disc on the shaft passing through a slotted optical sensor on the frame. The output of the sensor was shaped by a schmitt trigger circuit and its frequency measured by a meter. As there were sixty slots in the disc, the speed in rpm was displayed directly. The digital frequency meter was gated at a one second rate. A small, handheld, frequency meter was used for setting the various clock frequencies on the VM 5ØØØ. These were checked before and after each test as they drift a little with temperature.

4.3 TORQUE-SPEED CURVES AND DISCUSSION

For the torque speed curves to be consistent with the rating results in Sect 7.2 it was necessary to have the motor at its maximum rated temperature. Thus the motor was warmed up on a high load for some part of an hour, then stopped and the resistance of the stator winding was measured. The value required for an 80 degC. rise was 4.85 Ohms. This was not always quite achieved, but at the beginning of a test when the torque is low little error will result.

At higher torques the motor soon heats up and therefore the resistance at the end of each test was also measured. Because the standard rating for a motor allows for a 40 degC. ambient and the tests were taken at approximately 25 degC., another 15 degC. is allowable. Thus the results were reasonably meaningful.

However the very rapid rise in temperature that occurs near the breakdown torque did cause the torque speed curves to round off rather more quickly than predicted in Section 5.8. At low torques the motor tended to cool. For these reasons very brisk measurement of the torque, speed and input power is very important. The digital power meter was a little slow, because of its settling time. The DC motor with its resistive load also took a few seconds to stabilize to a constant load. The most suitable method is to have a shaft transducer measuring the torque and an

automatic measuring system for the other data. Then it is possible to measure the torque speed curve very quickly, before the temperature can change significantly. Such equipment was not available.

Four torque-speed and efficiency curves for the inverter, measured in the way explained are shown in figure 4.1. From 5Ø Hz down to 4Ø Hz the torque-speed characteristic moves in its entirety without changing shape. This is the effect hoped for with inverter control of induction motors (ref. 3Ø). The constant voltage upon frequency relationship is good over this range.

At 3Ø Hz, the breakdown torque is reduced, and the shape of the characteristic is changed. This trend is continued at 2Ø Hz. This is common in inverter drives. The current is approximately constant for the same torque, assuming the flux is the same. But this relationship is broken by the presence of the stator resistance, which causes voltage regulation and a drop in flux at the airgap. Thus the torque for a given current and the peak torque are reduced for the constant terminal voltage upon frequency relationship.

The efficiency characteristics of the unipolar inverter drive remain fairly constant from 5Ø Hz to 4Ø Hz. At 3ØHz the efficiency is still good, the peak having dropped about 1Ø percent. By 2Ø Hz the peak has dropped another 1Ø percent. This efficiency of course includes the inverter

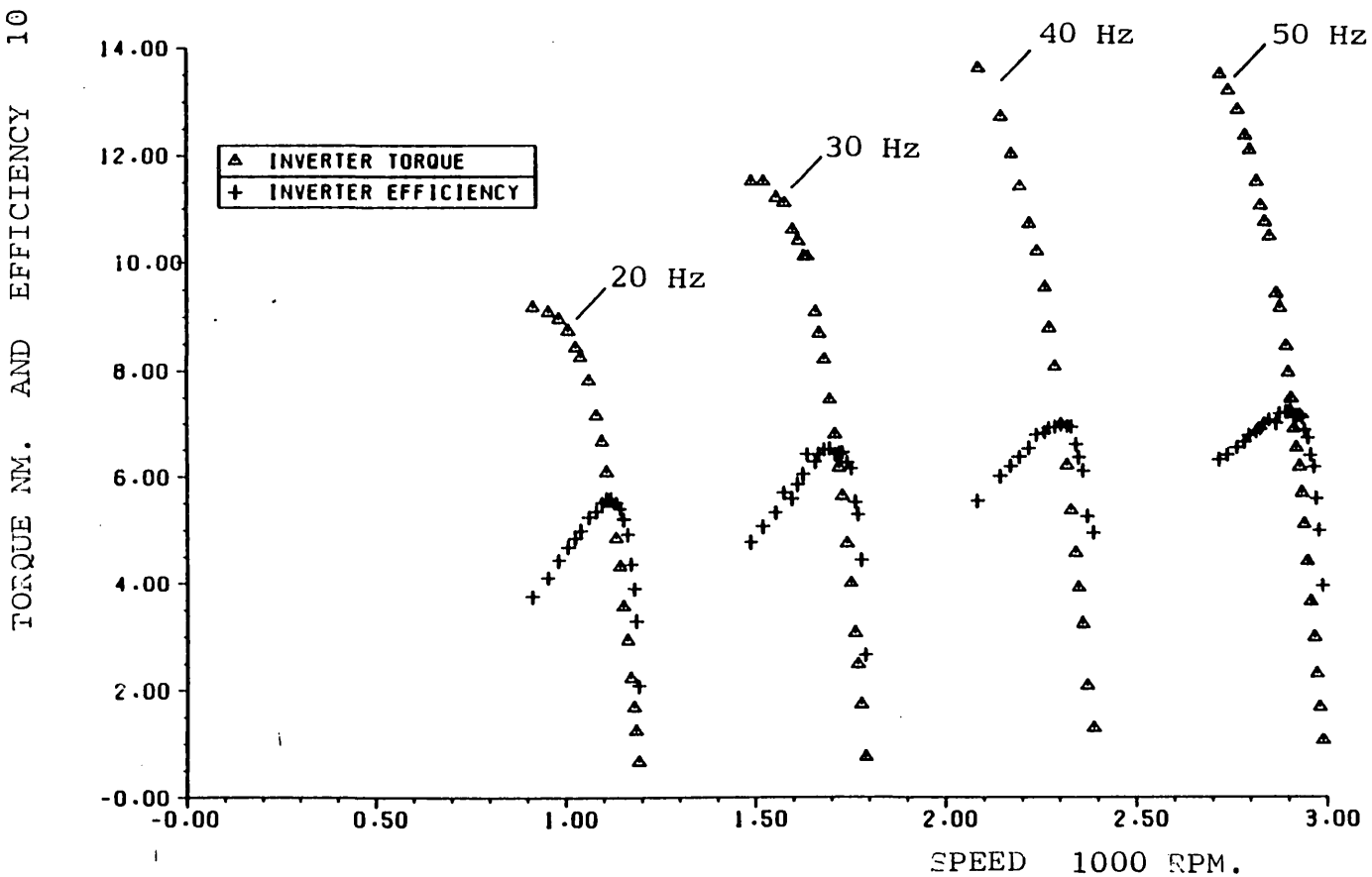

FIGURE 4.1 TORQUE AND EFFICIENCY VERSUS SPEED FOR THE EXPERIMENTAL DRIVE AT FOUR FREQUENCIES

losses, the snubber related losses being constant at about 65W . The other inverter losses account for approximately 1.8 percent throughout (cf.Sect 7.2). Assuming given current and constant torque, the stator losses will represent an increasing proportion of the output power as the frequency is reduced.

However the efficiency at 2Ø Hz is still reasonable. The losses at torques upto about 8.5 Nm. are allowable, if the cooling is the same as for 5Ø Hz. It is, therefore advisable to replace the fan on the shaft with a separately driven fan if the drive is to be used continuously at low frequencies and high torques.

The unipolar inverter drive is unusual in the respect that this loss in peak torque occurs at a higher frequency than is usual. To see the change in torque-speed curve due to the unipolar inverter feed compared to the normal AC operation the two curves are shown in figure 4.2. The torque is upto 2Ø percent reduced. The drop in efficiency is approximately 1Ø percent, although it should be noted that it is the total efficiency for the inverter drive which has been plotted and not that of the motor itself.

Most of this reduction in performance is due to the effectively doubled stator resistance. This can be seen from figure 4.3, where the torque-speed curve for a single three phase winding of the pair, fed with AC, has been included. It is noticeable that this curve does not

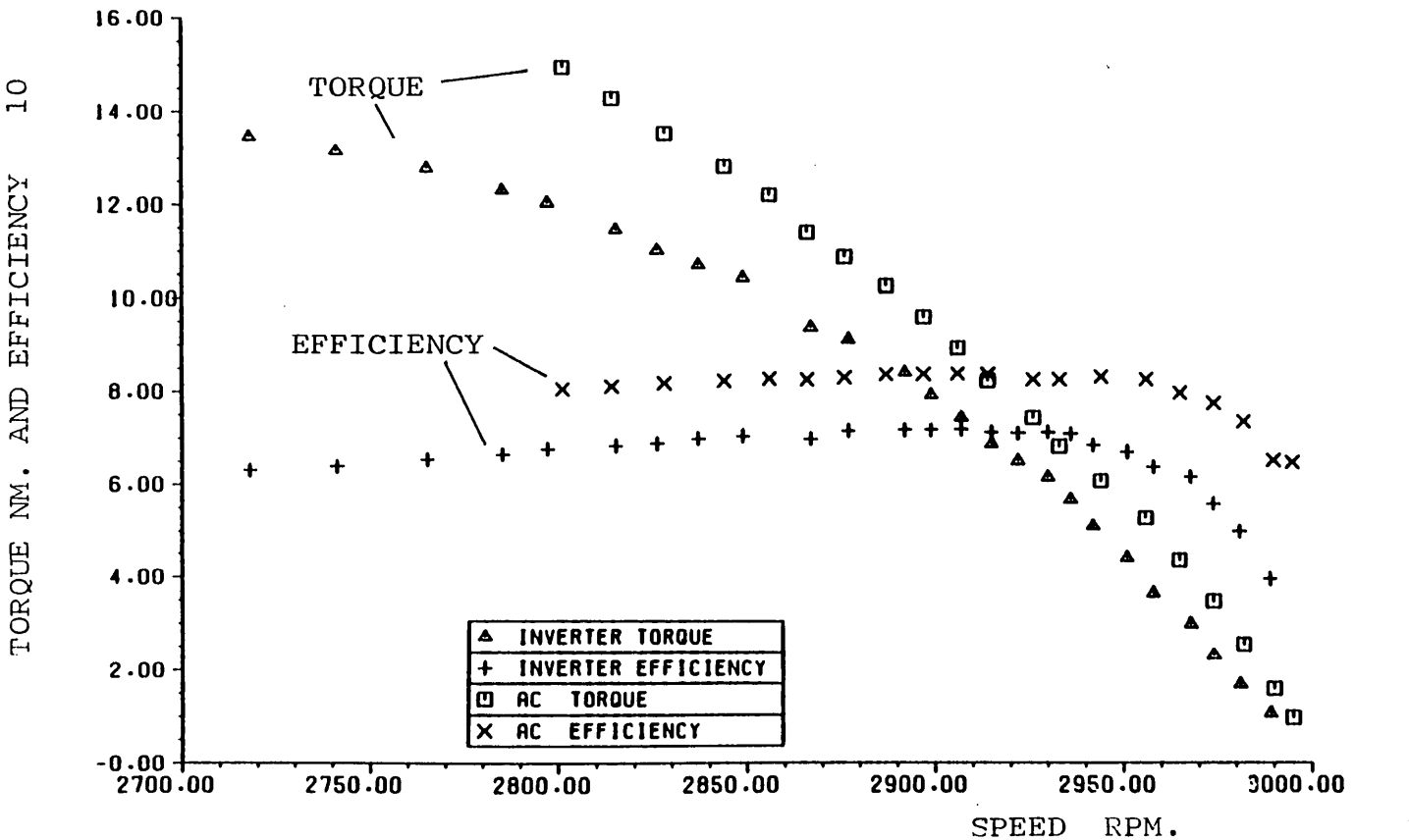

FIGURE 4.2 COMPARISON OF UNIPOLAR INVERTER DRIVE AND AC MAINS OPERATION

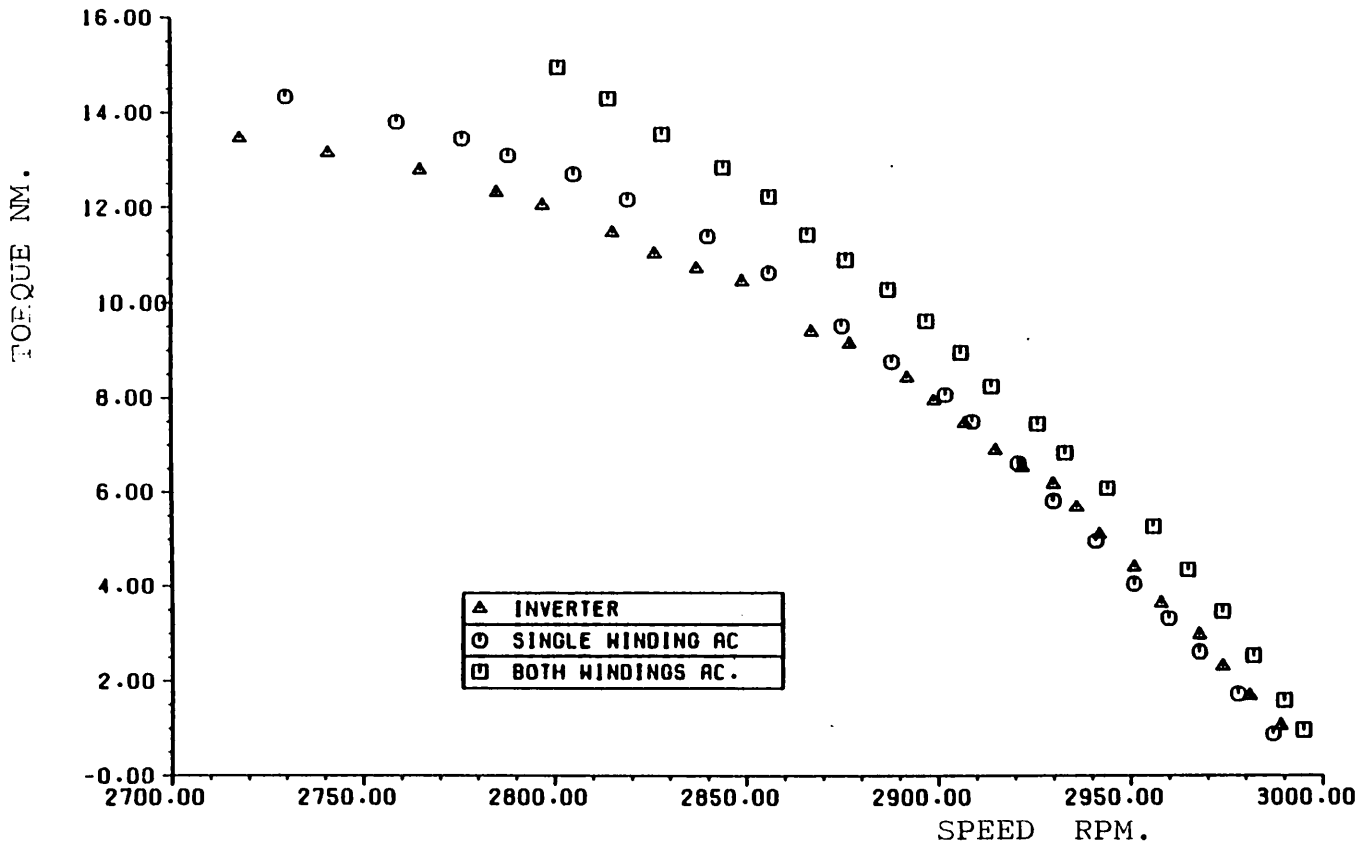

FIGURE 4.3 COMPARISON OF TORQUE SPEED CURVES

asymptote to 3ØØØ rpm. this is because of a dip in the supply frequency, and it is usual to correct for this. however it is quite clear that the loss in torque, due to the inverter waveforms, is not very great.

The most significant disadvantage, considering the torque-speed characteristic, is that the increased stator resistance reduces the peak torque. This is unfortunate, in so much that inverters are often expected to operate at high torques. Constant voltage boosting was tried, but led to excessive current being drawn at low loads. The motor, designed to be fairly saturated, became highly saturated. At 1Ø Amps, for example, the regulation due to the stator resistance is approximately 5Ø Volts. At 2Ø Hz the voltage predicted by the constant voltage upon frequency relationship is only 96 Volts. When the load falls off, the machine is heavily saturated. However this problem may be easily overcome by a control loop giving boosting proportional to the current (ref. 5Ø).

5.Ø INVERTER MODELLING

5.1 THE MUTUALLY COUPLED COIL MODEL

The current waveforms obtained from the inverter and discussed in Section 4.3, when summed for each phase coil pair look very similar to those produced by conventional inverter bridges. A comparison of measured results was considered to be difficult to make, because the differences are not very great and an induction motor is not linear. It is also difficult to get the same conditions, particularly the rotor temperature. The non-linearity, in the motor performance, due to saturation, might be increased, because the circulating currents may create local saturation.

The explanation of these effects also needs confirmation, as it is clear that they occur as a result of the flux in the other stator coils and the rotor. The simple two coil transformer approach is insufficient to model these effects.

Thus to reduce the number of unknown parameters and to conduct idealised experiments and comparisons it was necessary to model the whole motor and inverter.

A number of papers have been published, on such modelling, which have pointed out the difficulty presented by modelling discontinuous currents (refs. 31-33). For this

reason it was decided that the most generalized approach to machines, as developed in references 34 and 35, would be used.

The DQ model and per-phase harmonic equivalent circuits that have been of great use to others (refs. 34-42) were not considered helpful. The terminal constraints become confused by the transformations required and the topology of the circuit is not a direct function of time, unlike that of conventional inverters. The model presented follows the work of Sarker and Berg (ref. 43) and Nath and Berg (ref. 44). It was found later that all the advantages of the DQ method could be applied to the mutually coupled coil model, with none of the drawbacks mentioned. For this reason this approach is strongly recommended for normal motor-inverter modelling and such a conventional drive was also modelled for the purposes of comparison.

5.2 DERIVATION OF THE 8 COIL MODEL

The induction motor can be represented by a number of coils. The unipolar motor has six coils on the stator side. The cage may be considered to have the same number of coils as bars. However it is possible mathematically to reduce the number of coils representing the rotor to a smaller number. That it is a cage implies that it may be reduced to two coils with 90 degrees electrical orientation. A wound rotor with unbalanced conditions of supply or resistance is best represented by the same number of coils with which it is wound. The physical representation used is shown in figure 5.1.

It is now possible to form the matrix of inductances which relates the currents to the flux by the equation:

$$\underline{\Psi} = \left[L \right] \underline{I} \qquad 5.1$$

The diagonal terms of the matrix are the self inductances of each coil. The off diagonal terms are the mutual coupling inductances. The mutual coupling inductances from the rotor to the stator may be assummed to vary sinusoidally with rotor position angle theta. The same assumption leads to a zero term for the mutual coupling between the two rotor coils. The inductance matrix is given in figure 5.2.

The matrix is real and symmetric. Mathematically the

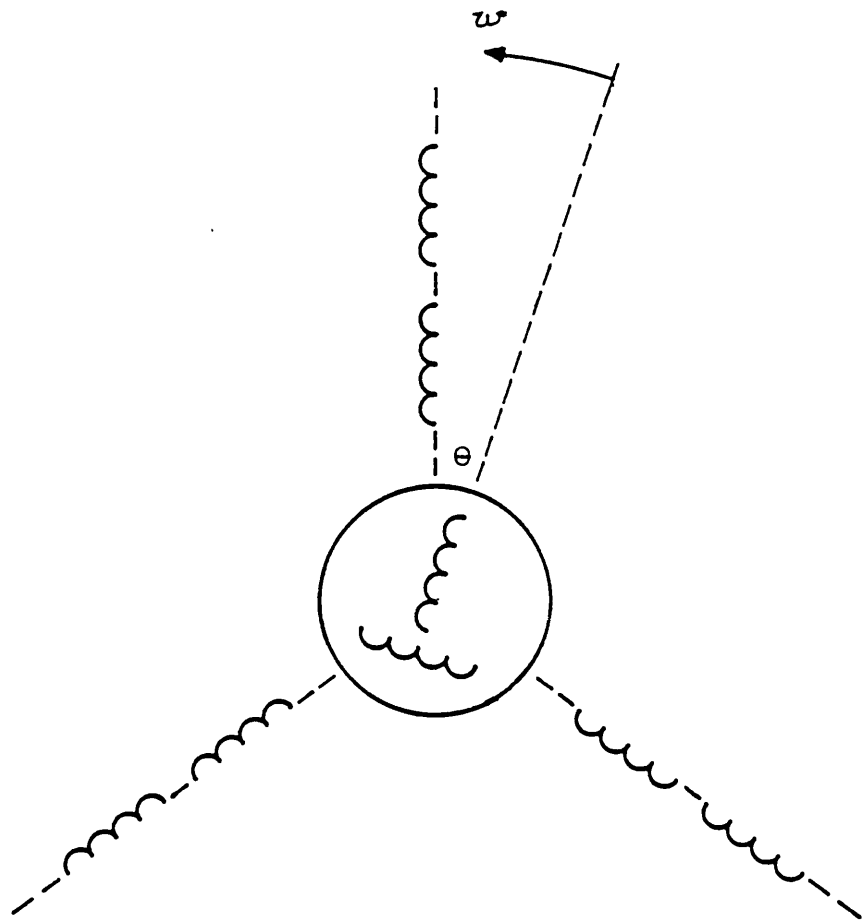

FIGURE 5.1 MUTUALLY COUPLED COILS USED TO REPRESENT THE MOTOR

$$[L] =$$

$$\begin{bmatrix}
L_{ss} & L_{sm} & L_{sm} & M_{ss} & L_{sm} & L_{sm} & M_{sr_a}\cos(\theta) & M_{sr_a}\cos(\theta+\frac{\pi}{2}) \\
 & L_{ss} & L_{sm} & L_{sm} & M_{ss} & L_{sm} & M_{sr_a}\cos(\theta-\frac{2\pi}{3}) & M_{sr_a}\cos(\theta-\frac{\pi}{6}) \\
 & & L_{ss} & L_{sm} & L_{sm} & M_{ss} & M_{sr_a}\cos(\theta+\frac{2\pi}{3}) & M_{sr_a}\cos(\theta+\frac{7\pi}{6}) \\
 & & & L_{ss} & L_{sm} & L_{sm} & M_{sr_b}\cos(\theta) & M_{sr_b}\cos(\theta+\frac{\pi}{2}) \\
 & & & & L_{ss} & L_{sm} & M_{sr_b}\cos(\theta-\frac{2\pi}{3}) & M_{sr_b}\cos(\theta-\frac{\pi}{6}) \\
 & & & & & L_{ss} & M_{sr_b}\cos(\theta+\frac{2\pi}{3}) & M_{sr_b}\cos(\theta+\frac{7\pi}{6}) \\
 & & & & & & L_{rr} & 0 \\
 & & & & & & & L_{rr}
\end{bmatrix}$$

FIGURE 5.2 INDUCTANCE MATRIX

$$[R] = \begin{bmatrix}
R_s & & & & & & & \\
 & R_s & & & & & & \\
 & & R_s & & & & & \\
 & & & R_s & & & & \\
 & & & & R_s & & & \\
 & & & & & R_s & & \\
 & & & & & & R_r & \\
 & & & & & & & R_r
\end{bmatrix}$$

Else Zero

FIGURE 5.3 RESISTANCE MATRIX

rotor may be resolved to one coil but the representation of the system then becomes complex.

The stator side could be reduced without introducing complex terms. The well known DQ method would reduce the stator coils to four. However doing so requires that the voltages applied have to be transformed (using the Park Transformation). Whilst the transformation is not difficult, in the unipolar inverter the topology of the circuit changes, depending on the current, and any number of the stator coils, from 3 to 6, may be conducting at one time.

On a digital computer working with an 8x8 matrix is equally as easy as working with 6x6, only slower.

The resistances are represented by the diagonal matrix in figure 5.3.

The equations relating the currents and fluxes to the terminal voltages are as follows:-

$$\underline{V} = p\,\underline{\Psi} + [R]\underline{I} \qquad 5.2$$

$$\underline{I} = \left[L \right]^{-1}\underline{\Psi} \qquad 5.3$$

Manipulation of these gives either of the following.

$$p\,\underline{\Psi} = \underline{V} - [R]\left[L \right]^{-1}\underline{\Psi} \qquad 5.4$$

$$\text{or} \quad p\,\underline{I} = \left[L\right]^{-1}\left[\underline{V} - \left[R\right]\underline{I}\right] + p\left[L\right]^{-1}.\left[L\right]\underline{I} \qquad 5.5$$

which may be time stepped for the solution.

Torque is given by

$$T = \frac{1}{2}\,\underline{I}^{t}\left[L_{\theta}\right]\underline{I} \qquad 5.6$$

where $\left[L_{\theta}\right] = \frac{d}{d\theta}\left[L\right]$

(the differential of the inductance matrix).

5.3 IMPLEMENTATION WITHOUT TRANSFORMATION OR MATRIX INVERSION

In the previous section it was mentioned that the mutual coupling terms for the stator to rotor, vary sinusoidally. Both the equations for the differentials require the inverse inductance matrix. Thus at each time step the inverse matrix must be recalculated. In a digital computer inverting matrices is very time consuming. Another method is to solve the simultaneous equations including L rather than inverting and multiplying. This is faster but still time consuming. This was the chief criticism of the method (cf. ref. 43 discussion). The solution offered by Robertson (ref. 45), was clumsy and lost generality, depending as it did on how the motor was connected.

An attraction of the DQ method is that the system may be frozen and the applied voltages modified by the corresponding angle (depending on the refence frame used).

for example

$$\begin{bmatrix} V_d \\ V_q \end{bmatrix} = \frac{2}{3} \begin{bmatrix} \cos\theta & \sin\theta \\ -\sin\theta & \cos\theta \end{bmatrix} \begin{bmatrix} 0 & \frac{3}{2} & \frac{3}{2} \\ 1 & -\frac{1}{2} & -\frac{1}{2} \end{bmatrix} \begin{bmatrix} V_a \\ V_b \\ V_c \end{bmatrix} \qquad 5.7$$

and the system equation becomes

$$p\underline{I} = \left[L_1\right]^{-1}\left[\underline{V} - [R]\underline{I} - [G]\underline{I}\right] \qquad 5.8$$

$$[G] = \begin{bmatrix} 0 & -L_s p\theta_s & 0 & -L_{sr} p\theta_s \\ L_s p\theta_s & 0 & L_{sr} p\theta_s & 0 \\ 0 & -L_{sr} p\theta_r & 0 & -L_r p\theta_r \\ L_{sr} p\theta_r & 0 & L_r p\theta_r & 0 \end{bmatrix} \quad [L_1] = \begin{bmatrix} L_s & 0 & L_{sr} & 0 \\ 0 & L_s & 0 & L_{sr} \\ L_{sr} & 0 & L_r & 0 \\ 0 & L_{sr} & 0 & L_r \end{bmatrix}$$

$$\underline{I} = \begin{bmatrix} I_{sd} & I_{sq} & I_{rd} & I_{rq} \end{bmatrix}^T \quad [R] = \begin{bmatrix} R_{sd}, R_{sq}, R_{rd}, R_{rq} \end{bmatrix} \text{ (Diagonal)}$$

$$\underline{V} = \begin{bmatrix} V_{sd} & V_{sq} & V_{rd} & V_{rq} \end{bmatrix}^T \qquad \text{Equations 5.9}$$

This is further removed from the inverter voltage waveforms, but the inductance matrix is only inverted once and the method is economical in computing time.

However close inspection of the inductance matrix of figure 5.2 and the equation 5.1,

$$\underline{\Psi} = [L]\,\underline{I}$$

leads to the conclusion that the cos(θ) and sin(θ) terms may be removed from the inductance matrix by trigonometrical identities. Thus L becomes

$$[L] = [T][L'][T]^{-1} \qquad 5.10$$

where $[L']$ has no terms in θ and $[L]^{-1}$ is given by

$$[L]^{-1} = [T]^{-1}[L']^{-1}[T] \qquad 5.11$$

$$[T] = \begin{bmatrix} 1 & & & & & & \\ & 1 & & & & & \\ & & 1 & & & \text{ELSE ZERO} & \\ & & & 1 & & & \\ & & & & 1 & & \\ & \text{ELSE ZERO} & & & & 1 & \\ & & & & & \cos(\theta) & -\sin(\theta) \\ & & & & & \sin(\theta) & \cos(\theta) \end{bmatrix}$$

Equation 5.12

As might be expected this is essentially the same as the transformation applied to the voltages in equation 5.7.

In the program the last two terms of the flux vector are transformed, then the stationary inductance matrix multiplies the new vector. The last two terms of the resulting vector are then transformed back to give the current vector. This is all done within one step and requires only eight extra multiplications over the number reqired for working with a stationary system. This represents very little cost in computer time. The solution, for the currents, is in the non-transformed quantities rather than the transformed quantities. In other words we are now working in observable terminal variables rather than in unreal quantities. This is very advantageous as the topology of the inverter depends on the currents.

The equation

$$p\underline{\Psi} = \underline{V} - [R]\underline{I} \qquad 5.13$$

was time stepped. This was because it is expected that fluxes cannot change rapidly where as currents can change almost instantaneously depending on the coupling and it was possible that this might happen in the inverter. Indeed some inverters rely on this mechanism (cf.Sect. 2.1).

The numerical integration used was a second order Runge-Kutta as developed by Heun (ref. 46).

$$w_{(i+1)} = w_i + \frac{h}{4} f(t_i, w_i) + \frac{3h}{4} f\left(t_i + \frac{2h}{3},\ w_i + \frac{2h}{3} f(t_i, w_i)\right) \qquad 5.14$$

The time step length h was determined from the system eigenvalues. These are found using the NAG routine, FO2AGF (ref. 47). The program writes out $[L]^{-1}\underline{R}$ from which the eigenvalues and eigenvectors are found. Because of the high coupling between the stator phase halves, a small timestep has to be used. The method used for modelling the inverter also adversely affected the time step.

5.4 INVERTER SIGNALS AND THE MODEL

The Mullard PWM chip HEF 4752V produces "double edged" modulation signals digitally. It uses two small look-up tables containing the "modulation numbers" (ref. 48). The time displacement of a given edge of the unmodulated square wave is determined by the modulation number for that edge multiplied by 8 cycles of the FCV clock, which determines the modulation depth.

There are only two tables although there are nine different strategies or 'gears'. The other seven are obtained from the first two by stepping through the relevant one at a lower rate. This is best seen from the diagram (fig. 5.4).

Because it is a digital method, it is simple to implement in FORTRAN. 1ØØ% modulation was used throughout and this means that pulses never quite disappear. Refering to figure 5.5, taking the midpoint of one positive block of the unmodulated square wave carrier as a reference, TSET, the edges to be modulated are then TSET+TM/4 and TSET+3TM/4. Three pointers, which are clocked when t exceeds TSET+TM, indicate the six modulation numbers required from a 21x2 array. With these, the two edges T1 and T2 for each phase may be found. The output voltage is then determined by comparing the real time to the times of T1 and T2 for the respective phase.

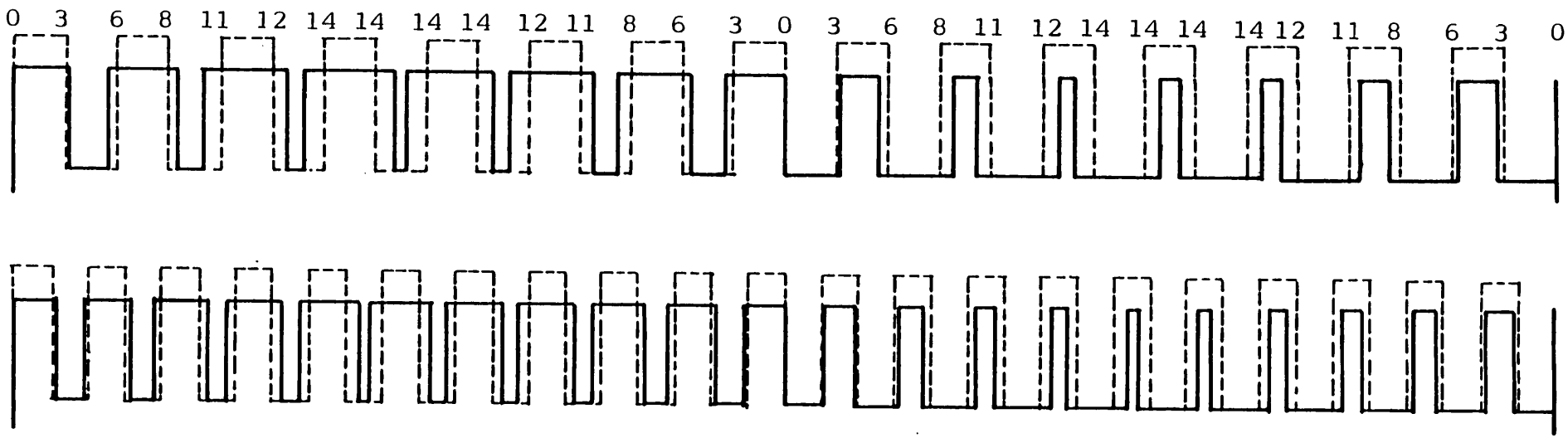

FIGURE 5.4 CONSTRUCTION OF THE MODULATED CARRIER USING MODULATION NUMBERS

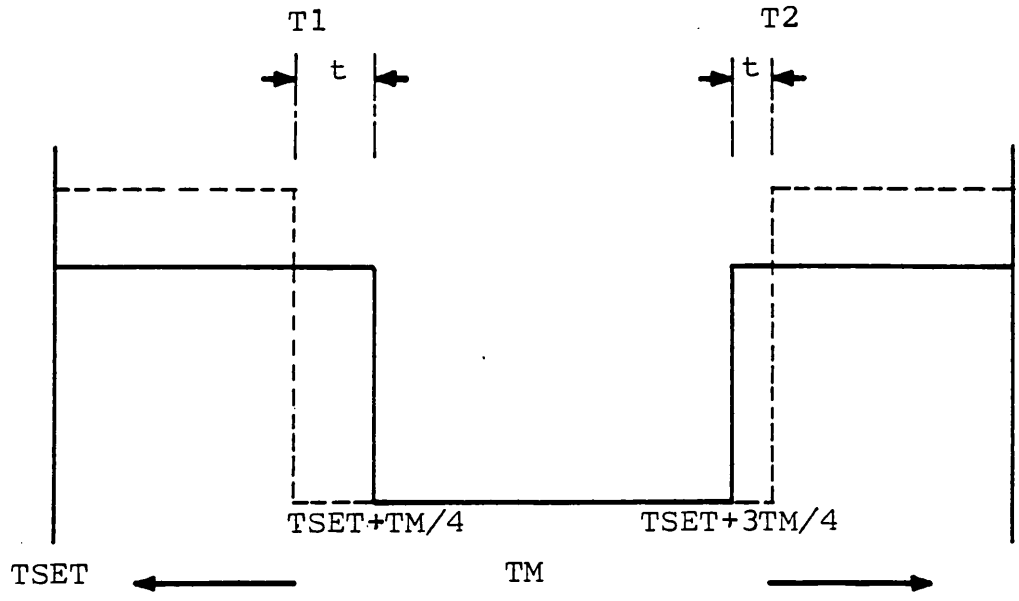

FIGURE 5.5 DETAIL OF METHOD FOR OBTAINING THE SWITCHING TIMES FOR THE MODEL

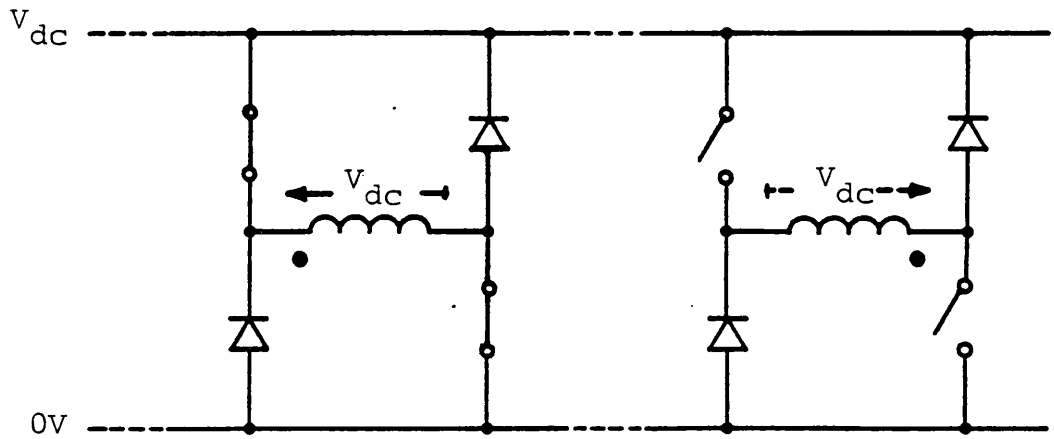

FIGURE 5.6 INDUCED VOLTAGE WHILST BOTH SWITCHES ARE OFF AND NO CURRENT IS REMAINING

The output voltage is that which is seen at the terminal of a conventional leg. The phase voltages for delta connection are the differences between the three terminal voltages.

In the unipolar inverter, during the time that there is forward current in a leg, the voltage applied is just this, either through the two transistors on, giving positive volts,only one transistor on giving essentially zero voltage free-wheeling, or both transistors off giving negative voltage free-wheeling. But what happens when there is no continuous forward current? The transistors are still switching in the same way but the voltage is undefined during the period that both transistors are off. The voltage that does appear on the winding, which has no current in it, is induced by the flux in the rest of the system. Since the mutual coupling between phase halves is high and the other half has both transistors on, it is practically the voltage rail in the negative sense (cf Sect 3.4). However there is no path for any current to flow, because of the direction of the diodes. (cf.fig.5.6)

Therefore it was decided that in the model the same voltage as determined above should be applied to each phase half, but diodes should be incorporated in series with each phase half in opposite directions.

The diodes were modelled by a short circuit in the forward

sense and by 4ØØØ Ohms in the reverse sense. This was achieved in the program by testing the sense of the current then altering the stator resistance in the calculations. 4ØØØ Ohms was chosen for several reasons. It allows a maximum reverse current of approximately Ø.1 Amps. This is approximately 1% of the peak forward current, although it never reaches it, because of the EMF induced by the complementary phase half, which reduces the nett voltage on the resistance. This then is the lowest resistance that is reasonable. The lowest value possible was used because a higher value has a greater penalty on the step length used as determined by the eigenvalues (cf Sect. 5.3). The step length used in general was 2uS, which gave a reasonable run time.

Circuit topology changes, employed by others (refs. 32,33) were not considered useful here. It would require extensive testing of the state of the currents and the voltages , because of the large number of topologies that the unipolar inverter can have. The connection matrix, as in reference 33, would be very large and difficult to implement.

The snubbers, which charge up via the transformer action between phase halves (cf Sect 3.4), were not modelled. The period for this charging is very breif and, as noted before, has no significant effect on the rotor. The distortion they cause to the voltages applied to the motor as the transistors turn off is very small, as it only takes a few microseconds (depending on the current) for them to charge.

5.5 THE MODEL FOR THE CONVENTIONAL INVERTER

As mentioned in Section 5.1, the unipolar motor becomes the standard motor when its phase halves are connected in parallel. This was done for the 415V mains rating test (Sect. 7.2).

In Section 5.4 it was said that the motor phase voltage waveforms are the same as those produced by a conventional, totem-pole output inverter. Thus it may be expected that a conventional three phase motor and inverter may be modelled merely by removing the "diodes" from the 8 coil model presented in Section 5.4. The equations for the voltage on each phase half, now with the same resistance are similar (see figs. 5.2,5.3), except for the mutual inductance terms for the stator to rotor.

In Section 5.6 it is found that the difference in mutual coupling inductance for the phase halves from stator to rotor was negligible. Taking them to be the same allows the 8 by 8 matrix to be reduced to 5 by 5 (fig. 5.7) and the resistance matrix also becomes 5 by 5, with the stator resistance suitably adjusted. The L_{sm} terms drop out, because the currents and rates of change of currents in the two phase halves are the same, if the M_{sr} terms are the same, and they have no effect. This serves to illustrate how flexible this approach to motor modelling is.

$$[L] =$$

$$\begin{bmatrix}
L_{ss} & L_{sm} & L_{sm} & M_{sr}\cos(\theta) & M_{sr}\cos(\theta - \frac{\pi}{2}) \\
 & L_{ss} & L_{sm} & M_{sr}\cos(\theta - \frac{2\pi}{3}) & M_{sr}\cos(\theta - \frac{\pi}{6}) \\
 & & L_{ss} & M_{sr}\cos(\theta + \frac{2\pi}{3}) & M_{sr}\cos(\theta + \frac{7\pi}{6}) \\
 & & & L_{rr} & 0 \\
 & & & & L_{rr}
\end{bmatrix}$$

FIGURE 5.7 INDUCTANCE MATRIX FOR THE CONVENTIONAL MOTOR MODEL

Working with a 5 equation system is more economical on computer time, and removal of the high resistances modelling the diodes and LMS terms increases the smallest eigenvalue. This allows a longer time step to be used. The step length is now only limited by the inverter switching frequency.

This model is to be used with the 8 by 8 model in the theoretical study (Section 5.8) to evaluate the performance of the unipolar inverter. For the comparisons the step length was reduced to 1 microsecond in an attempt to eliminate differences in the integration between the two models.

5.6 DETERMINATION OF MOTOR PARAMETERS

Some of the parameters used in the motor inductance and resistance matrices (cf.Sect.5.3) ,may be measured directly. The stator resistance was measured before and after each test (cf.Sect.4.2) and an average value was taken for the program.

To measure the stator self and mutual inductances a bar less rotor was made by etching, and ac tests conducted. Care was taken to use the same voltmeter for all the measurements to ensure that the mutual coupling term was a correct percentage of the self inductances.

These quantities were also measured using the dc inductance bridge test (ref.49, p21). The circuit for measuring self inductance is shown in figure 5.8.

The bridge is balanced and then the switch is opened. The equation for the voltage waveform of Vg is

$$V_g = - \frac{R_2}{R+R_2}.L.\frac{d}{dt}I_1 + \frac{R_2}{R+R_2}.M.\frac{d}{dt}I_2 + ...etc \qquad 5.15$$

The measured waveform is integrated,

$$\int_{\emptyset}^{\infty} V_g.dt = \frac{R_2}{R+R_2}.L.I_0 \qquad 5.16$$

where I_0 is the initial primary current,

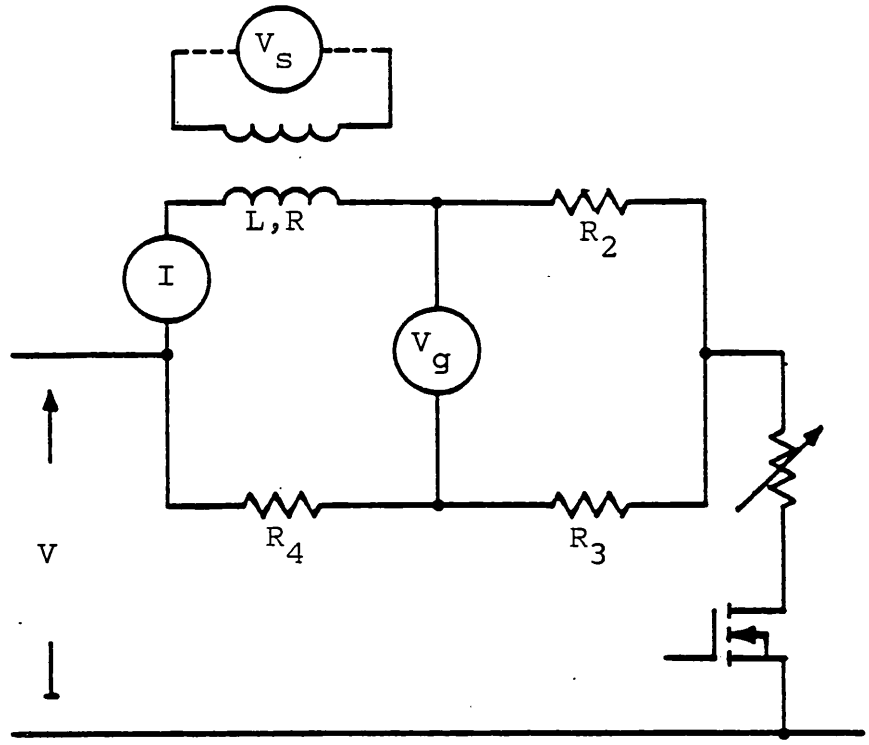

FIGURE 5.8 DC INDUCTANCE BRIDGE

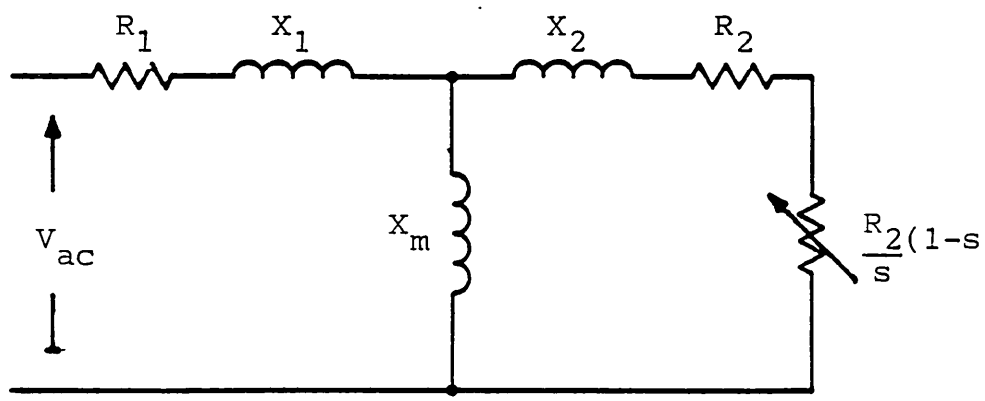

FIGURE 5.9 SINGLE PHASE EQUIVALENT CIRCUIT

and on integration the mutual terms drop out.

To integrate the voltage C.V.Jones (ref. 49) suggested a ballistic galvanometer. Such an item is fairly rare and so the digital storage oscilloscope was used and the data downloaded to a computer, which calculated the integral.

A mosfet driven by a signal generator was used in place of the switch to enable waveforms to be displayed repetitively. Values comparable to the ac tests were obtained, which implied that the eddy currents in the laminations were negligible.

The circuit for mutual inductance was the same as in figure 5.8, the voltage on the open coil being integrated:

$$\int_0^{\infty} V_s.dt = - M.I_0 \qquad 5.17$$

This method confirmed the ac test for phase to phase mutual coupling, but was of insufficient accuracy to determine the phase half to phase half coupling.

It is possible to determine the mutual coupling at a known level of saturation with the dc tests, but not the self inductance. In both tests it is preferable to reverse the supply between tests, to make sure the core is not successively magnetized due to hysteresis.

The changes in mutual coupling with increasing saturation in the ac tests, were found to be less than the difference between the different phases themselves, both of which were less than 2%. Thus it was decided that the results of the ac tests at 150V would be used. The 150V value was chosen, because it is the level of flux at which saturation is just beginning to occur. The differences in the measured values for the self inductances of the phase halves were less than one percent. For this reason, and because it simplifies the following mathematics, they were taken to be the same. This assumption is discussed in Section 6.3, where the leakage between phase halves is considered from the point of view of fault current control.

The other values for the model were obtained from the locked rotor test and the previously measured values. For the locked rotor test the phase halves were connected in parallel, and the motor was tested in the usual way.

The method is as follows;

Neglecting resistance,

$$L.\frac{d}{dt}I = V \qquad 5.18$$

Taking the first line of the inductance matrix,

$$\frac{d}{dt}\left[L_{ss}I_1+L_{sm}I_2+L_{sm}I_3+M_{sr}\cos(\theta)I_{rd}+M_{sr}\cos(\theta-\frac{\pi}{2})I_{rq}\right] = V_1 \qquad 5.19$$

using complex notation and substituting for I_2 and I_3, assuming I_1 is sinusoidal,

$$I_2 = I_1 e^{(j\frac{2\pi}{3})} \qquad 5.20$$

$$I_3 = I_1 e^{(-j\frac{2\pi}{3})} \qquad 5.21$$

$$\frac{d}{dt}\left[L_{ss}I_1 + L_{sm}I_1 e^{(j\frac{2}{3})} + L_{sm}I_1 e^{(-j\frac{2}{3})} + M_{sr}\cos(\theta)I_{rd} + M_{sr}\cos(\theta - \frac{\pi}{2})I_{rq}\right] = V_1 \qquad 5.22$$

Combining the rotor currents into I_r (complex) and simplifying,

$$\frac{d}{dt}\left[(L_{ss}+L_{sm})I_1 + M_{sr}I_r\right] = V_1 \qquad 5.23$$

At synchronism $I_r = 0$, thus

$$\omega_s(L_{ss} + L_{sm})I_1 = V_1 \qquad 5.24$$

Compared to the single phase equivalent circuit (fig. 5.9), at synchronism,

$$(X_1 + X_m)I_1 = V_1 \qquad 5.25$$

Therefore, $\omega_s(L_{ss} + L_{sm}) = X_1 + X_m$ 5.26

Considering the rotor, using the same approach, taking the fourth equation of the inductance matrix (locked rotor).

$$\omega_s\left[(M_{sr}+\frac{1}{2}M_{sr}e^{(j\frac{2\pi}{3})} + \frac{1}{2}M_{sr}e^{(-j\frac{2\pi}{3})})I_1 + L_{rr}I_r\right] = V_4 = 0 \qquad 5.27$$

Therefore $\frac{3}{2} M_{sr} I_1 + L_{rr} I_r = 0$

rearranging, $I_r = - \frac{3}{2} \frac{M_{sr}}{L_{rr}} I_1$ 5.28

Combining 5.23 and 5.28,

$$\omega_s \left[(L_{ss}+L_{sm}) - \frac{3}{2} \frac{M_{sr}^2}{L_{rr}} \right] I_1 = V_1 \qquad 5.29$$

Considering the single phase equivalent circuit again

$$X_1 I_1 + \frac{X_m X_2}{(X_m+X_2)} I_1 = V_1$$

rearranging,

$$X_1 I_1 + X_m I_1 - \frac{X_m^2}{(X_m+X_2)} I_1 = V_1 \qquad 5.30$$

Comparing 5.29 and 5.30,

$$\frac{3}{2} \frac{M_{sr}^2}{L_{rr}} = \frac{X_m^2}{(X_m+X_2)} \qquad 5.31$$

Taking $X_m = \omega_s M_{sr}$

$$\frac{3}{2} (X_m+X_2) = \omega_s L_{rr} \qquad 5.32$$

Thus it has been shown how the inductance matrix coefficients are related to the single phase equivalent circuit parameters.

The resistance of the rotor can be determined from the inductance relationships, because the time constant of the

rotor must remain the same.

$$\text{Hence: } \omega_s \frac{L_{rr}}{R_r} = \frac{(X_m + X_2)}{R_2} \qquad 5.33$$

Substituting for L_{rr} with eqation 5.32

$$R_r = \frac{3}{2} R_2 \qquad 5.34$$

For the bifilar motor the stator to rotor mutual coupling will be exactly the same for each phase half. However this is not so in the coil pair motor.

To measure the difference in these mutual coupling terms a single phase was excited, with the two phase halves connected in series and destructing. The equations governing this situation may be manipulated as follows;

$$V_1 = L_{ss}\frac{d}{dt}I_1 + L_{sm}\frac{d}{dt}I_2 - M_{sr}\frac{d}{dt}I_3 + R_sI_1$$

$$V_2 = L_{sm}\frac{d}{dt}I_1 + L_{ss}\frac{d}{dt}I_2 - M_{sr}\frac{d}{dt}I_3 + R_sI_2$$

$$V_3 = -M_{sr}\frac{d}{dt}I_1 - M_{sr}\frac{d}{dt}I_2 + L_{rr}\frac{d}{dt}I_3 + R_rI_3$$

because of the connections;

$$V=V_1-V_2, \quad I_1=I_2, \quad \frac{d}{dt}I_1 = \frac{d}{dt}I_2$$

hence,

$$V = (M_{sr_a} - M_{sr_b})\frac{d}{dt}I_3 \qquad 5.35$$

$$V_3 = 0 = -(M_{sr_a} + M_{sr_b})\frac{d}{dt}I_1 + (L_{rr}j\omega_s + R_r)I_3 \qquad 5.36$$

neglecting R_r, taking $M_{sr_a} + M_{sr_b} = 2M_{sr}$

$$V = 2(M_{sr_a} - M_{sr_b}) j\omega_s \frac{M_{sr}}{L_{rr}} I_1 \qquad 5.37$$

By these means a value of $(M_{sr_a} - M_{sr_b})$ was deduced. It was approximately 0.5mH, which is very small compared to M_{sr}, but was incorporated into the program anyway.

5.7 JUSTIFICATION OF THE 8 COIL MODEL

The measured current waveform in figure 5.1Ø (from fig. 3.8) was taken at a speed of 288Ø rpm and output power of 254Ø Watts. This is a fairly temperature stable operating point, which allows time for the current waveform to be data-logged. The stator resistance was 4.7 Ohms, measured before and after the test.

Puting this value of resistance into the mutually coupled coil program and setting the same speed produced the bold waveform, which is superimposed on the measured waveform in figure 5.1Ø. The waveforms agree quite well. The current spikes appearing on the predicted waveform during its OFF period appear precisely at the moment the voltage applied falls to zero. This is demonstrated in figure 5.11. This was the result expected in Section 3.4.

Returning to figure 5.1Ø; the capacitors in the snubbers were not modelled and therefore every second spike in the off period of the lower wave form is not predicted at all. For the same reason the steeple like spike at the right of each current spike in the OFF period of the upper waveform is also missed. The agreement around the change-over in voltage is not very good. There are long periods of zero voltage for both coils at that time (fig. 5.11) It may be that there is saturation affecting the terms of the inductance matrix and causing much higher circulating currents than predicted. It was mentioned in Section 4.4

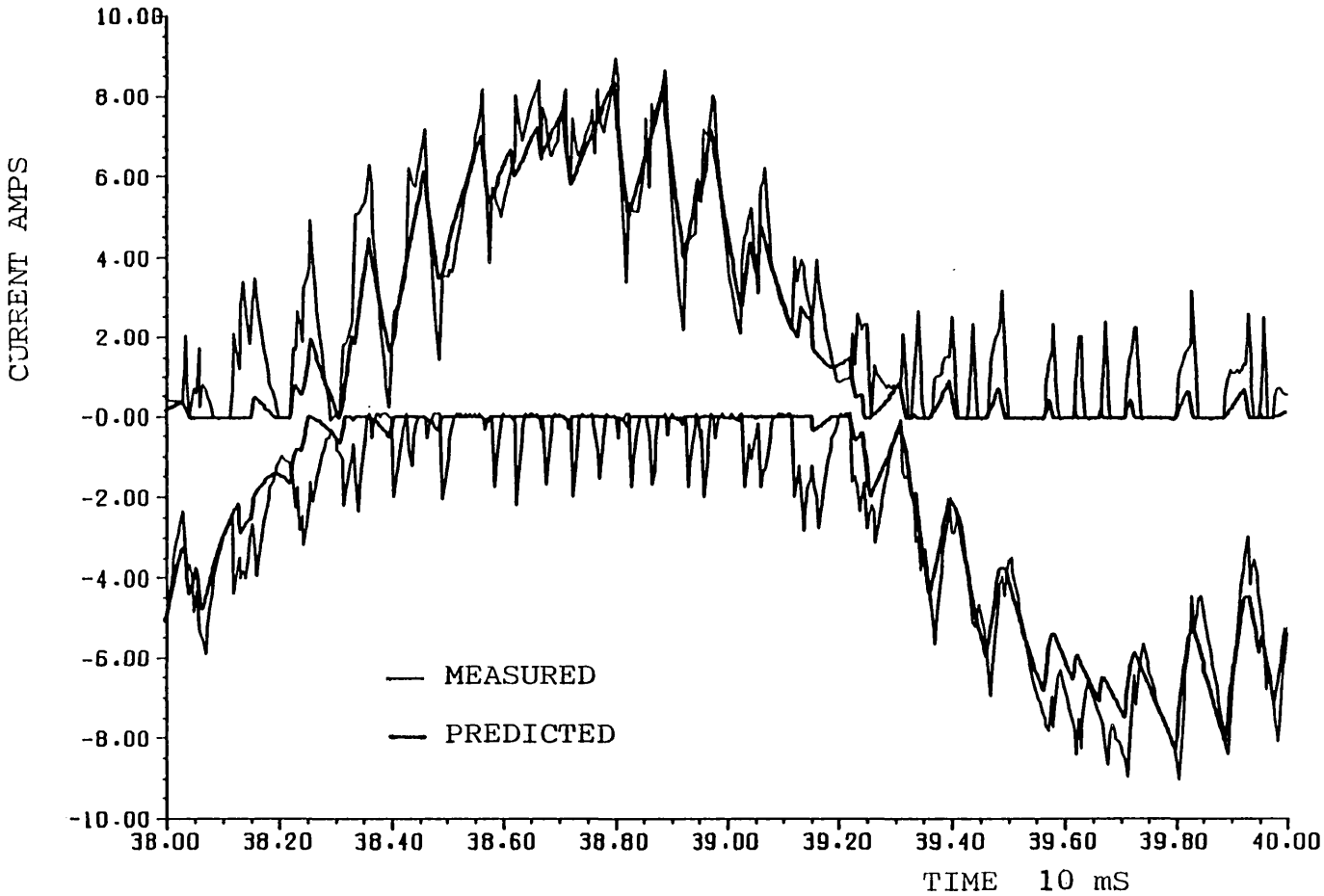

FIGURE 5.10 MEASURED AND PREDICTED CURRENTS FOR ONE PHASE

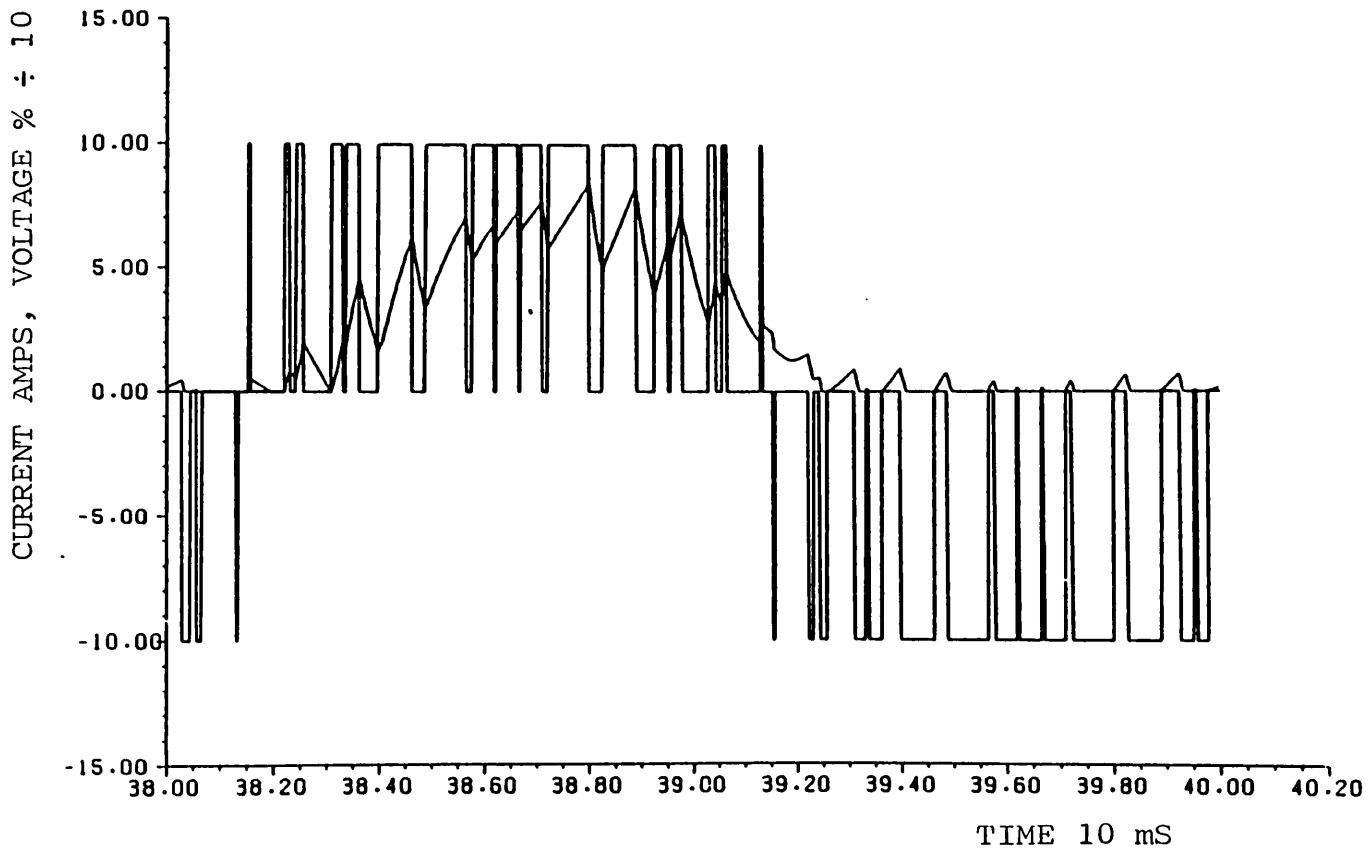

FIGURE 5.11 PREDICTED CURRENT AND APPLIED VOLTAGE

that an increase in the leakage between phase halves results in larger circulating currents.

To confirm that the spikes are indeed circulating currents, in the model the rotor was uncoupled from the stator and the stator phases also uncoupled. This leaves only the stator phase halves coupled. The current waveform that results (fig. 5.12) shows no spikes, which is the expected result, as the diodes are in the opposite direction to the induced voltage. The waveform is very smooth, because the phases are very inductive without the rotor dissipating mechanical work.

This waveform also confirms that the diodes are modelled quite effectively. The value of 4000 Ohms taken for the reverse blocking resistance was quite sufficient as the nett voltage applied to the diode is only ever small in the program due to the induced voltage from the other coil in the pair. In reality the diodes block the full voltage rail at some points such as when the snubbers charge. In Section 5.9 the strategy is such that the full voltage is applied throughout much of the OFF period, and a small error is introduced.

The agreement obtained in the summed currents (fig. 5.13) is rather better. The experimental result was obtained by threading the two wires for the two phase halves through the current probe in opposite directions. Care was taken to ensure that the positive current was the same phase

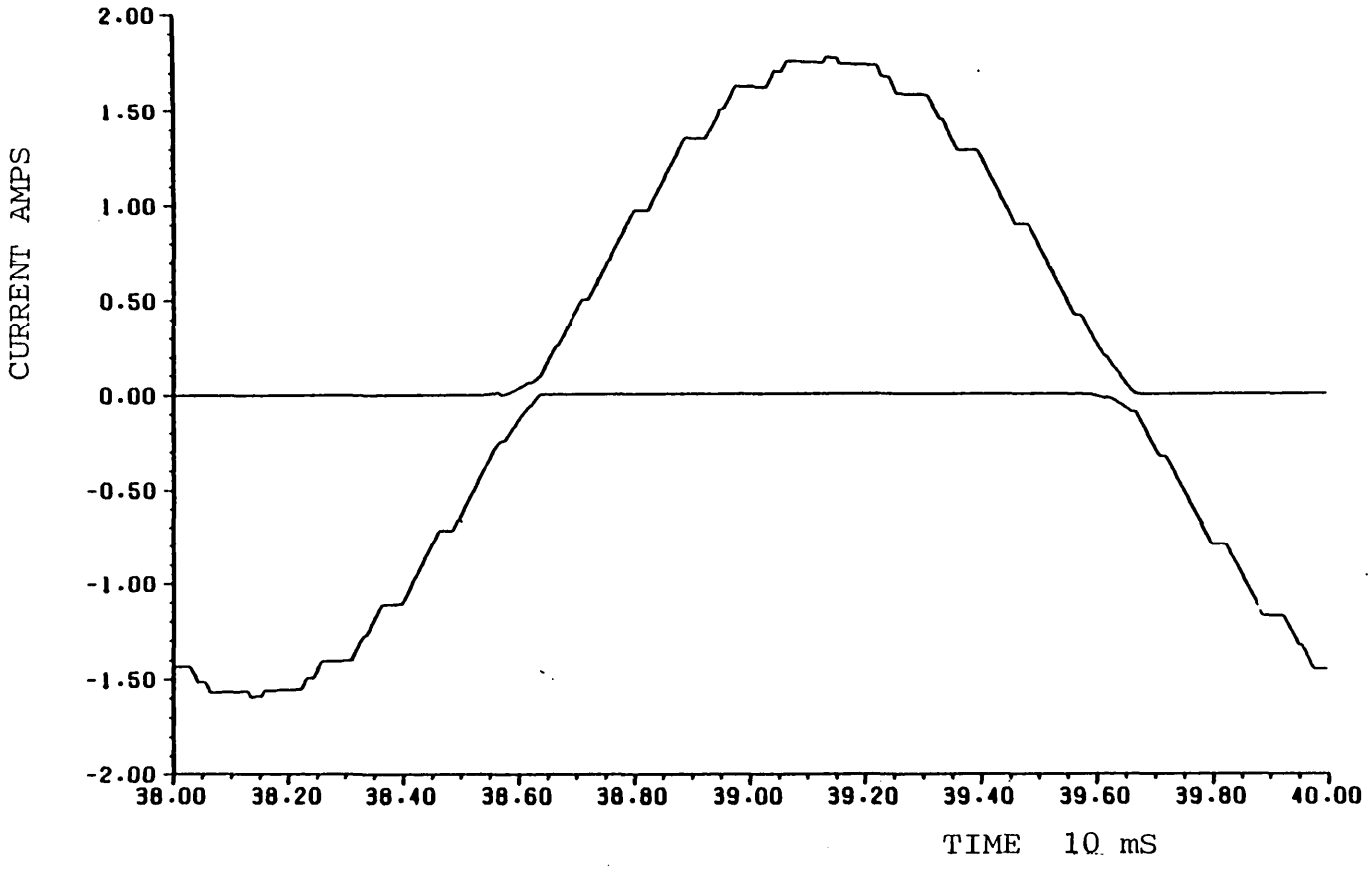

FIGURE 5.12 PREDICTED CURRENTS FOR ONE PHASE WITH AN OPEN CIRCUIT ROTOR

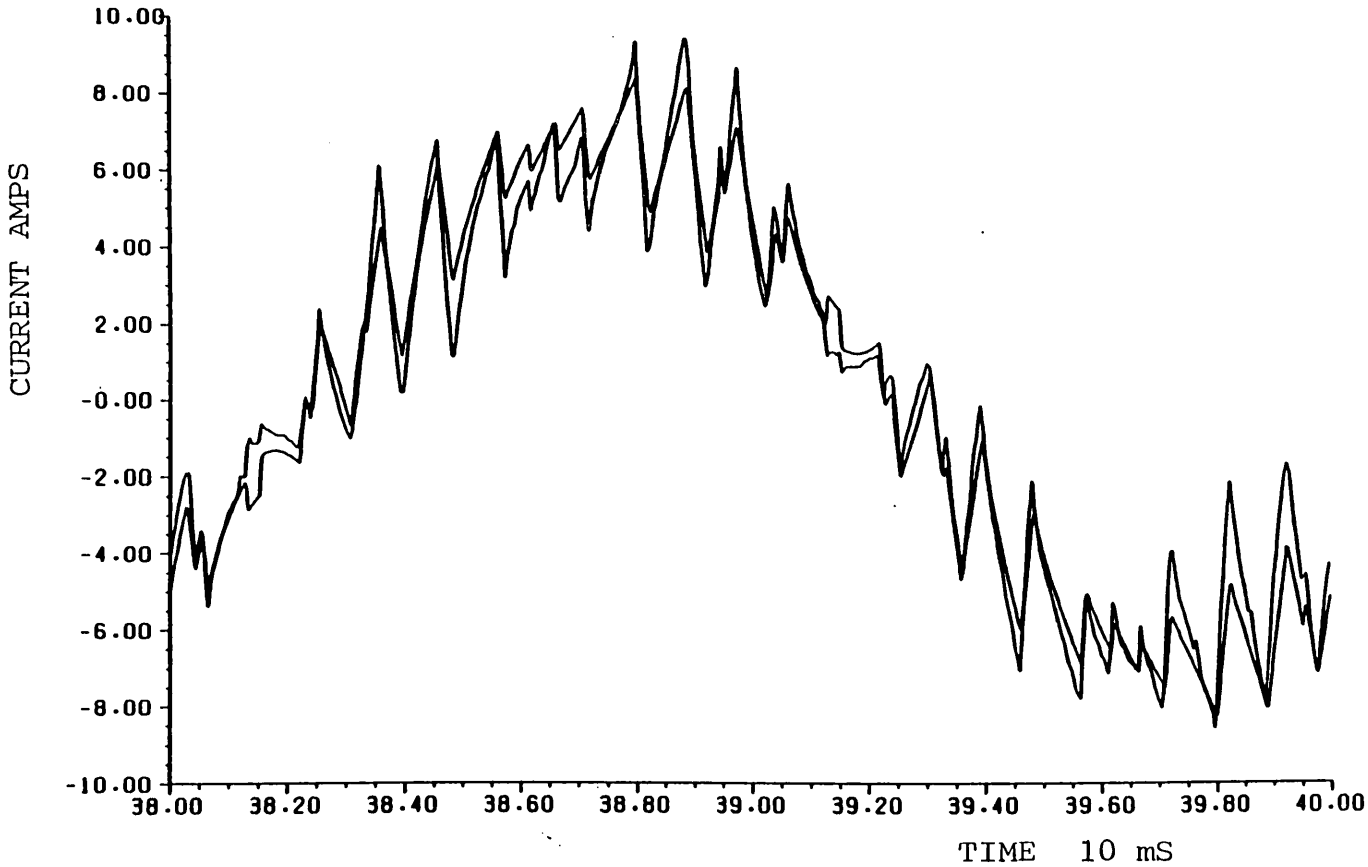

FIGURE 5.13 SUMMED CURRENTS, MEASURED AND PREDICTED

half as the positive current in figure 5.10. The speed was again 2880 rpm and the stator resistance 4.7 Ohms. The output power was 2430 Watts, which is less than before (2540W). This is because the rotor was not the same temperature. The rotor temperature is one of the variables that makes meaningful comparisons from experiments difficult.

Figure 5.14 shows three cycles of current. The difference in each cycle is quite noticeable and is due to the slotting. When displayed continuously, the current waveform has a ripple superimposed on it. It is possible to synchronise the ripple, which is related to the slip frequency by the number of rotor bars, by altering the load.

The calculated output power is higher than that measured here, but as noted above, it is very rotor temperature sensitive. The value of rotor resistance in the program is fixed. Whilst it is too low here, later it will be seen that the correspondence in the torque speed curves is quite good, the measured output being higher than both the measured outputs mentioned here.

The warm up for the values data-logged was done fairly rapidly and the motor left running whilst the data-logging was completed. Whilst this operating point is reasonably temperature stable, it does takes a long time to reach equilibrium. The results in Section 4.3 were taken quickly

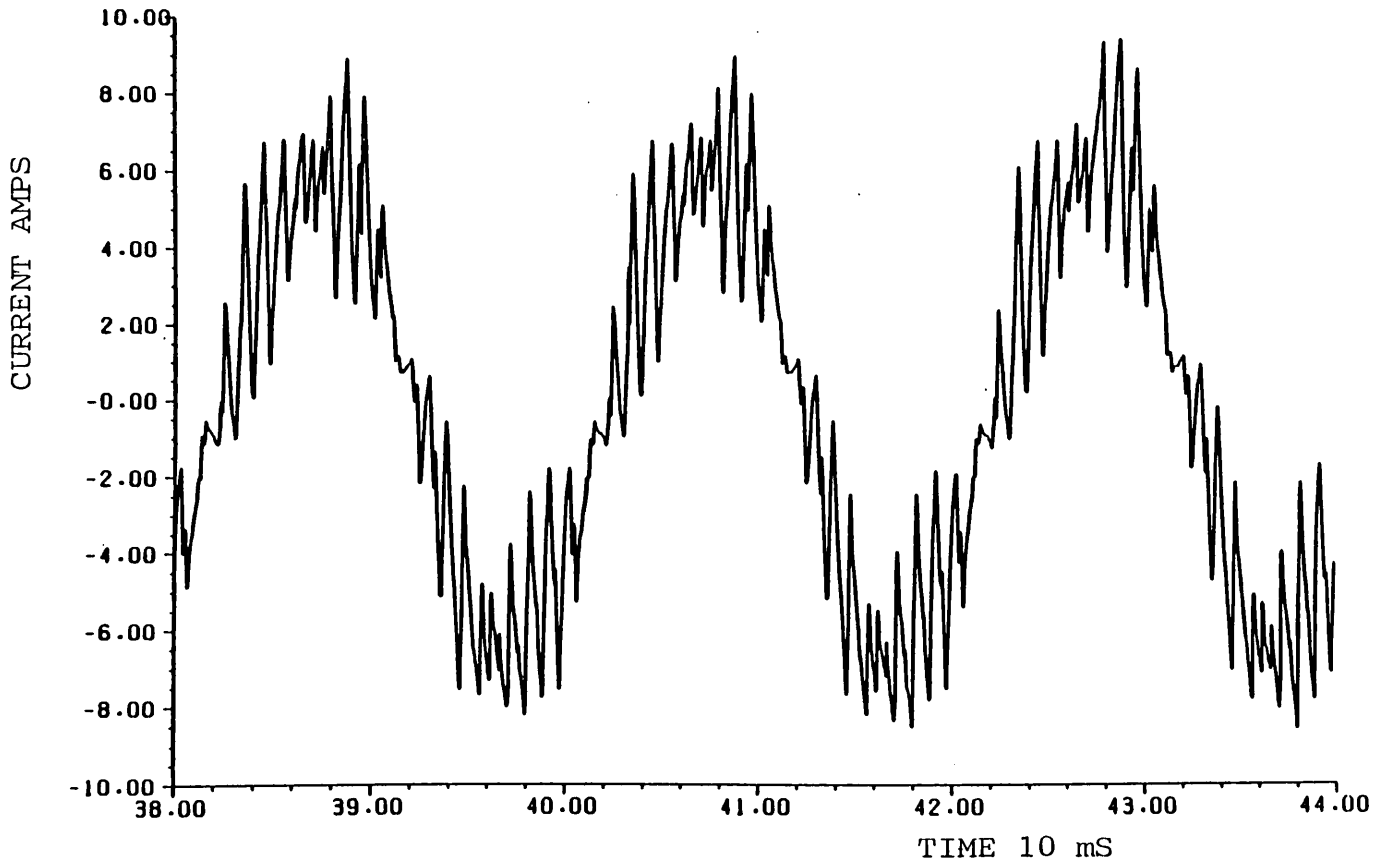

FIGURE 5.14 MEASURED CURRENT (THREE CYCLES)

after the motor has warmed up gently. Even then above this speed of 2880 rpm the motor heated up quite rapidly.

Because the model is idealized, there is no term for the iron loss. At the currents shown, the predicted waveform is smoother than the measured. This can be accounted for by the fixed values of leakage used. At high currents the closed rotor slot bridges are well saturated as are the semiclosed stator slots. The magnetising current would also be increased as the effective air gap lengthens. The fixed value of rotor resistance is a reasonable assumption, because of the rotor slot bridges, which mean that the currents at different depths see similar leakages and deep bar effect will not be too apparent at low slip. However at high slip and current these approximations can be expected to introduce increasing error, particularly for the non-fundamental harmonics of the applied voltages.

However the waveforms presented here show that the model performs in a similar way to the experimental motor and inverter, and is a suitable representation of them. The intention was that it should be idealized and in doing so there is some loss in accuracy over the measured results. The major mechanisms of the operation are included, and remembering the assumptions made, the model can be used for comparisons.

5.8 THEORETICAL COMPARISON OF UNIPOLAR AND CONVENTIONAL INVERTERS

The conventional inverter model was described in Section 5.5. It is based on the same assumptions as the novel inverter model. The question to be answered is whether the unipolar inverter waveforms have an effect on the available output power because of their form as well as the poor usage of the stator copper. It is also of interest to see what can be done to improve the output. The amount of torque ripple will also be considered.

To these ends the conventional inverter model (5 coil) was run, with the same values as the novel inverter model (8 coil), including the stator resistance (which would be halved in the conventional inverter).

The results are in table 5.1

rpm	T Nm.	Cu loss W.	Pin W.	Pout W.	
288Ø	9.48	477.4	3338.4	286Ø.4	8 Coil
288Ø	9.49	471.Ø	3333.5	2862.6	5 "
296Ø	3.61	98.5	1218.2	1119.5	8 "
296Ø	3.62	88.4	1211.3	1122.9	5 "

Table 5.1

Comparison of inverters using the same stator resistance

These results show very little difference. As expected the unipolar inverter has resistive losses over and above

those caused by the increased stator resistance. These are due to the "circulating currents", which is why the control of real circulating currents in machines is very important. However, in this novel arrangement the increase in these losses is negligible near the rating (less than 1.5%, which is Ø.2% on overall efficiency). At lower output power they become more significant, but are not very important , because the total loss is reduced.

The output power is reduced a little. The power dissipated by the "circulating currents" is supplied via the stator resistance and leakage and thus the airgap suffers more supply regulation.

It was found that the differences sought were very small. Thus care was taken to use similar step lengths in both programs (approximately 1 microsecond), to ensure the errors in the integrations and in the averaging of the powers and torques were similar. The consistency of the results can be seen in the fact that the power in equals the copper loss plus the power out to the first decimal place. The error is therefore an order of magnitude less than the difference. No account was made of the change in stored energy. The currents are so similar after one cycle of the supply in steady-state conditions that it was not considered necessary to calculate it although it probably accounts partly for the slight error in the power balance.

In figure 5.15 the summed current waveform for the 8 coil model is superimposed on the current waveform for the 5 coil model and their torques are also superimposed. The differences are negligible.

This implies that the performance is almost exactly the same as that of a conventional inverter, except for the increase in stator resistance. The peculiarities of the current waveform affect the rotor very little, as expected. Consequently the torque shows no ill effects.

Thus it becomes reasonable to model the novel inverter drive with the conventional inverter drive model, with increased stator resistance. It is also of advantage to do so, because a much larger time step can be used as suggested in Section 5.5. The torque speed curve thus calculated is shown superimposed on the measured curve in figure 5.16. The agreement is close, although at speeds less than 2880 rpm the measured torque is lower than the calculated. This was discussed earlier (Sect. 5.7) and is mainly due to the rotor heating, amongst the other effects mentioned.

The calculated torque speed curve, for half the value of stator resistance, is shown, with the calculated curve of figure 5.16, in figure 5.17. The effects of stator resistance on the torque speed curve are quite significant. The stator resistance can be considered as

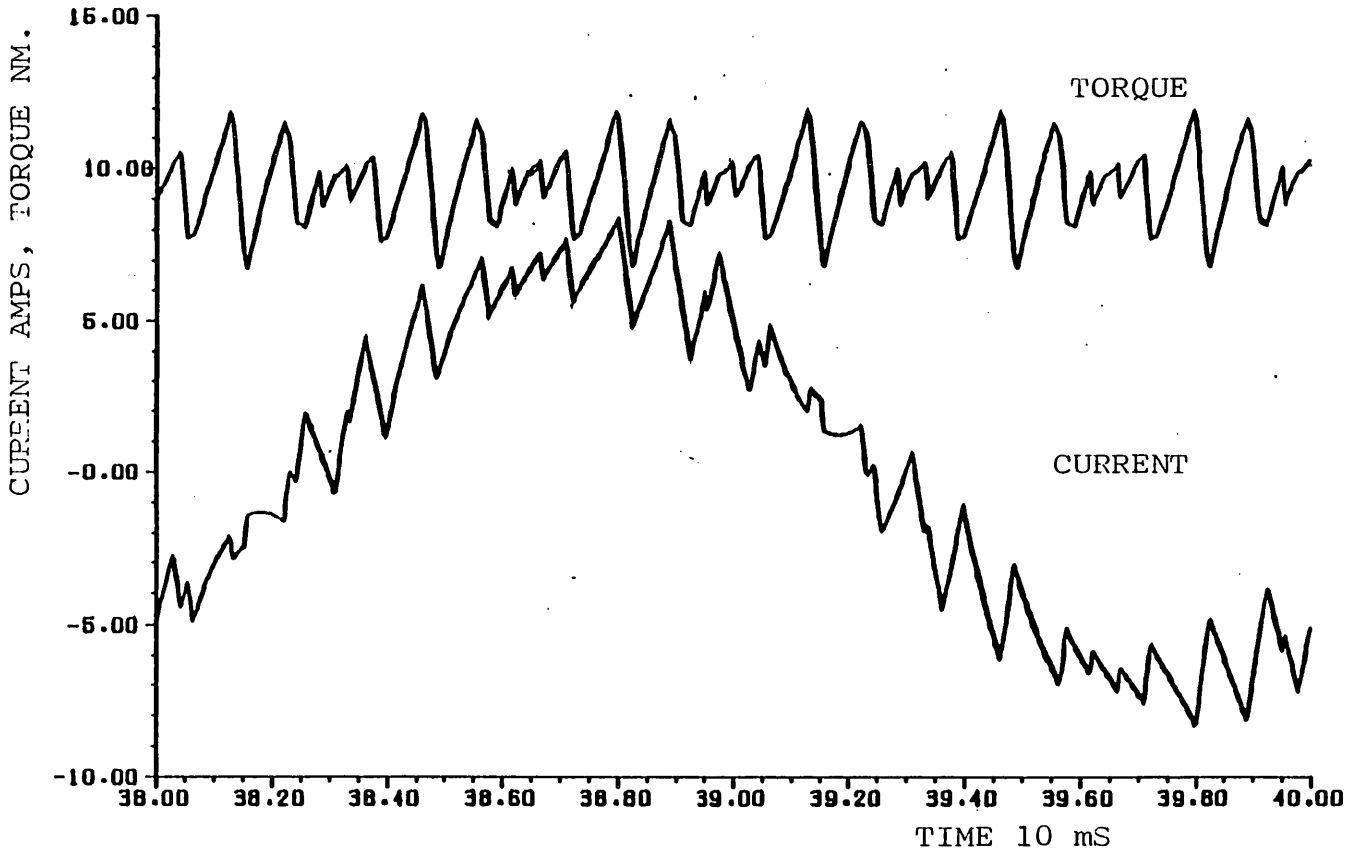

FIGURE 5.15 PREDICTED CURRENTS AND TORQUES FOR CONVENTIONAL AND UNIPOLAR INVERTERS

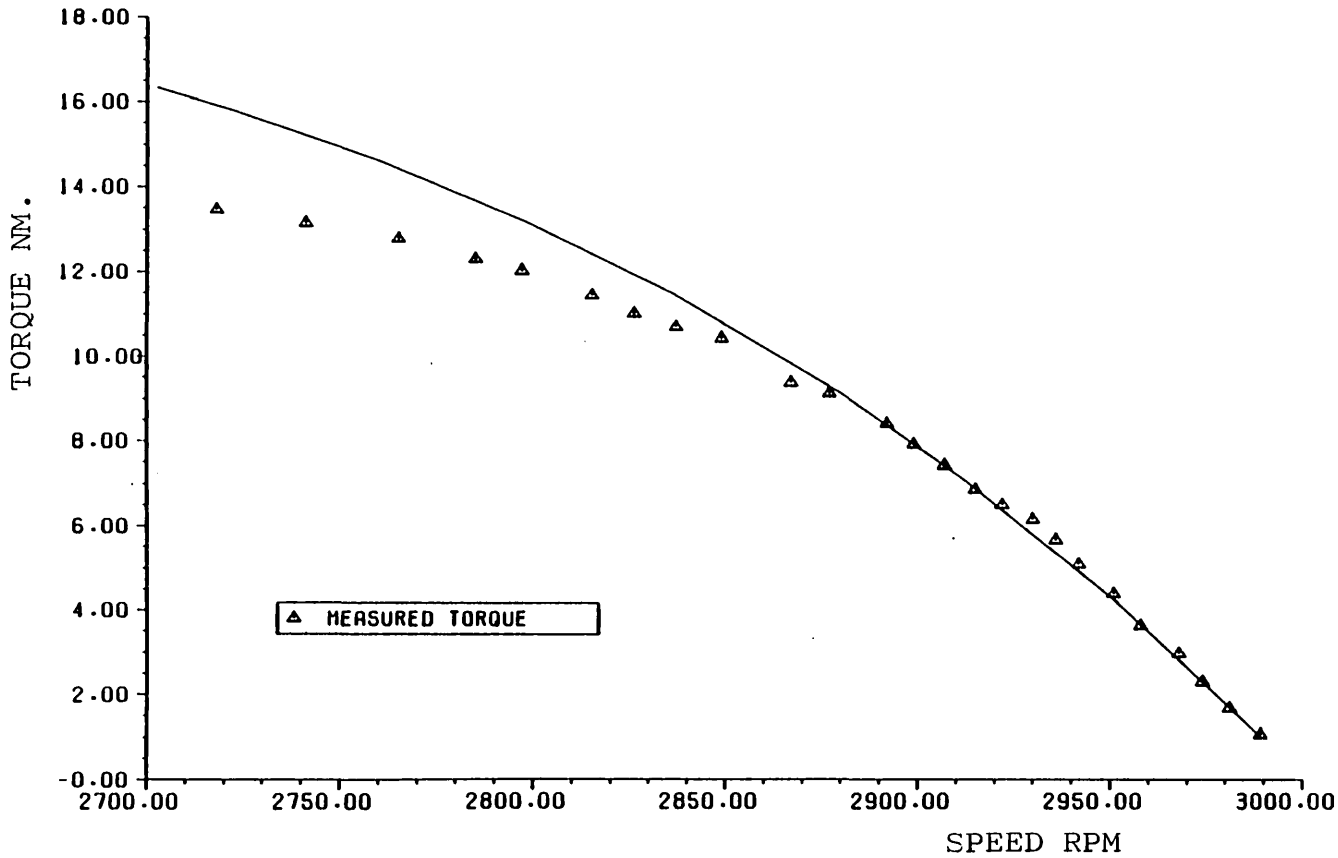

FIGURE 5.16 MEASURED AND PREDICTED TORQUE-SPEED CURVES FOR THE UNIPOLAR INVERTER

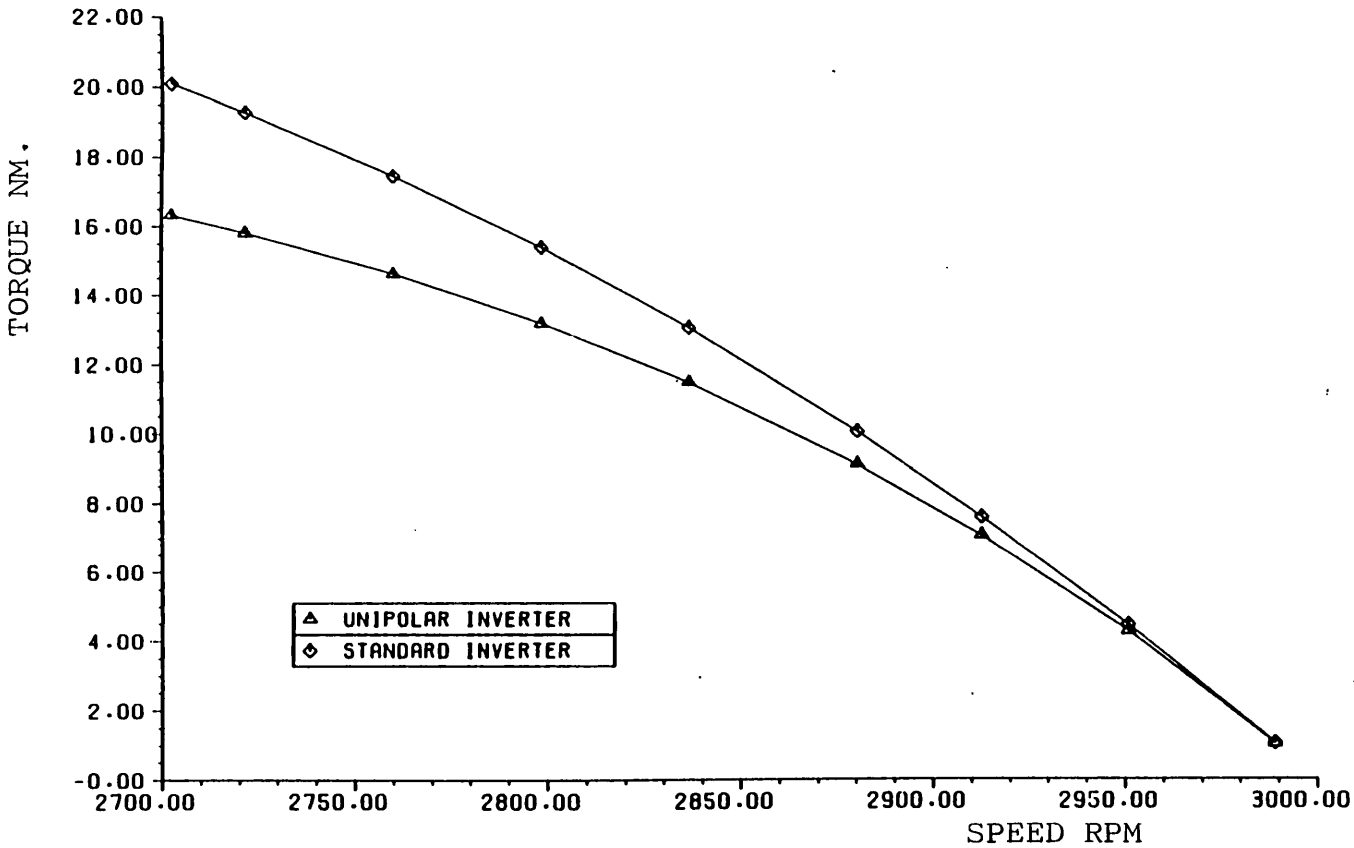

FIGURE 5.17 PREDICTED TORQUE-SPEED CURVES FOR THE UNIPOLAR INVERTER AND A STANDARD, CONVENTIONAL INVERTER

an impedance in series with the supply, causing voltage regulation. Thus the peak of the torque-speed curve is greatly reduced, but at low slip there is little difference. This is important, especially as inverter drives are commonly required to operate near their peak torque, for short periods. Therefore not only is the continuous output reduced but so too is the dynamic output.

So far only comparisons with inverter feed have been discussed. To put the loss in performance into perspective it is important to see how much loss in dynamic output and rating is caused by inverter feed compared to ac sinusoidal feed.

The torque-speed curves for the unipolar inverter with its stator resistance, the conventional inverter with half that value of stator resistance and the curves for sinusoidal supply for both motors are shown in figure 5.18. From this it can be seen that the predicted loss in performance, due to the harmonic content of the voltage waveforms, is small. The measured curves for the same conditions are shown in figure 4.3, Sect.4.3. The conventional inverter torque speed curve is not included, since one was not readily available and the difficulties in making comparisons from measurements makes it not worth-while.

Furthermore the torque speed curve is not really a good

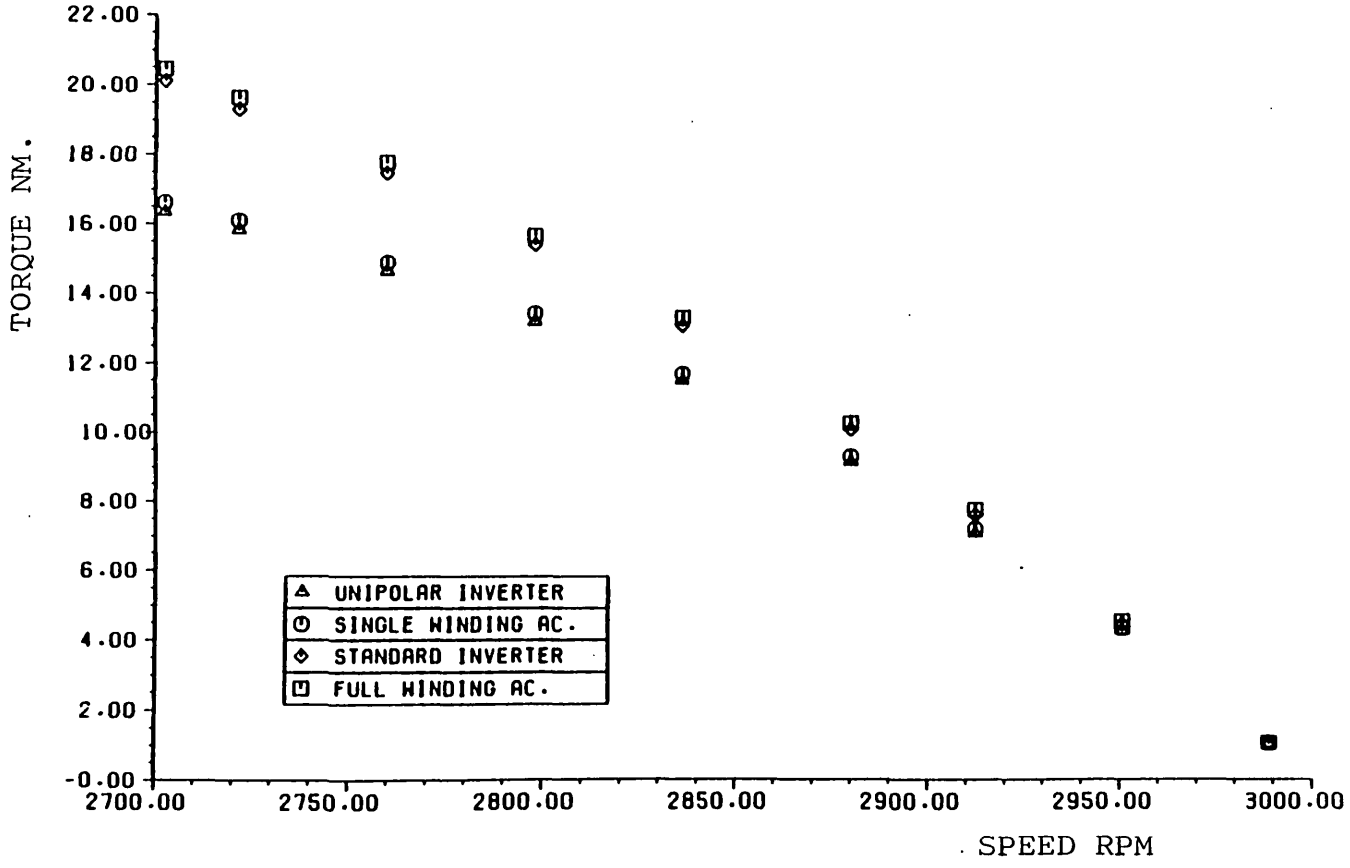

FIGURE 5.18 PREDICTED TORQUE-SPEED CURVES FOR BOTH TYPES OF INVERTER AND AC MAINS FEED (WITH BOTH STATOR RESISTANCES)

measure. Inverters allow for the rms voltage to be increased to lift the torque speed curve (ref. 50). This point is important when considering the dynamic performance of the drive. The losses are of more significance, particularly the copper loss. The graph in figure 5.19 presents the efficiencies (copper losses only) for inverter feed and sinewave feed. It can be seen that the efficiency of the inverter at low load is lower than for sinusoidal feed, because of the harmonic waveforms affecting the rotor. But this is relatively unimportant as the losses are below the maximum allowable.

At higher outputs the efficiencies become less than 0.5 percent different. (This is the same for both stator resistances). Other work (ref. 51) has shown that the strategy for the inverter voltage modulation is quite important for motor efficiency. Here it seems that it is relatively unimportant. This suggests that the parameters of the motor are also important in these considerations. However here the rotor resistance is taken to be constant as discussed in Section 5.7, which will affect these results a little.

This particular motor, being two pole, features a magnetic circuit with a high goodness factor (ref. 52). This implies low magnetizing current, and high power factor (cf.Sect. 5.6). Motors with four poles and more are quite different. These considerations are rarely mentioned with regard to inverters.

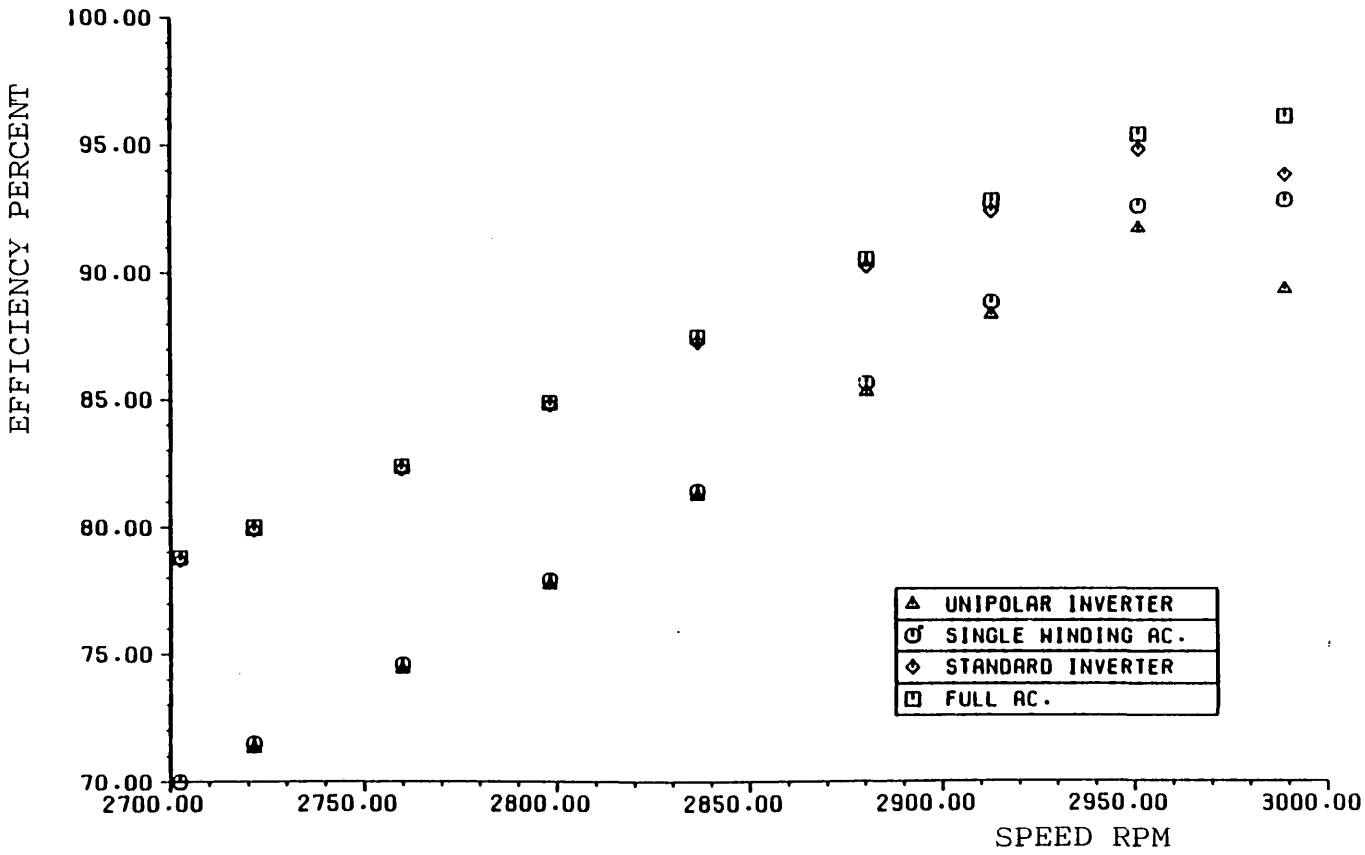

FIGURE 5.19 COMPUTED EFFICIENCIES BASED ON COPPER LOSSES

A very high switching frequency is allowable with the unipolar inverter, using snubbers on the transistors. Thus a sinewave with very little harmonic content can be achieved. It was hoped that this would regain some of the loss in efficiency caused by the increased stator loss. With this motor the gain would appear to be small, but with other motors the gain would be considerably higher as can be seen from reference 51. A high switching frequency may cause skin effect in the stator (ref. 53), which would necessitate the use of a filter. Whilst at such a high frequency the filter would be small, it represents more complexity.

Only the results for 5Ø Hz operation have been discussed here. The experimental results (Sect.4.3) show that the efficiency drops with frequency, but so too does the output power. If the machine is cooled equally over the frequency range, by a separate fan perhaps, overheating is not likely at torques less than the rated continuous torque at 5Ø Hz. In this case it is about 8 Nm. (The figures for input power in Section 7.2 include the fixed inverter losses due to the snubbers.) Thus the discussion, of 5Ø Hz performance is also valid at lower frequencies.

5.9 THEORETICAL STUDY OF SIMPLIFIED WAVEFORMS

Whilst the circulating currents do not seem to contribute much to the losses, it is worth considering how they might be eliminated. The snubber capacitor charging currents contribute to the losses also (see Sect. 4.3) and both can be dealt with by leaving the switches open in the bridge that is not conducting. Then there is no path for the snubbers to discharge through. The circulating currents, which occurred because both phase halves were presenting low voltage free-wheeling paths to the rotor flux (see Sect. 3.4), also no longer appear.

In effect the unipolar current is forced to be in phase with the voltage applied. At the end of the conducting half cycle the current free-wheels into the high voltage dc rail and therefore decays rapidly. In the previous strategy this free-wheel path is modulated, in such a way as to apply a fundamental sinewave of reverse volts. Such simplified waveforms were successfully implemented on the experimental inverter merely by using some additional logic circuitry, and did eliminate the circulating currents and the snubber charging currents. However, for the comparisons and discussion, results from the 8 coil model of Section 5.2 will be used.

Taking the speed of 288Ø rpm again, the voltage and current waveforms for one phase half are shown in figure 5.2Ø and may be compared to figure 5.11, Section 5.7.

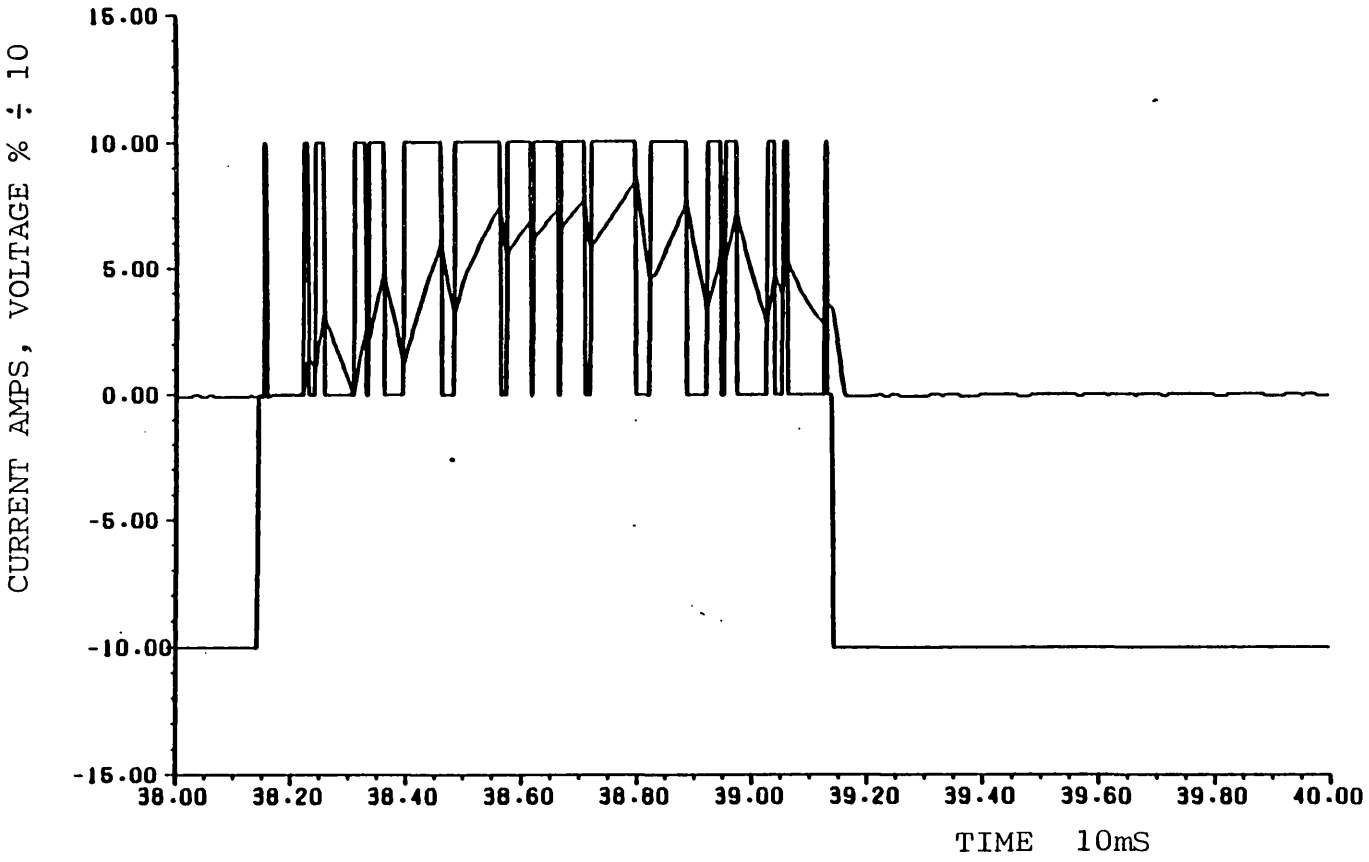

FIGURE 5.20 APPLIED VOLTAGE AND PREDICTED CURRENT WITH THE SIMPLIFIED STRATEGY

The circulating currents have gone. The current is pulled down rapidly at the end of the conducting half cycle. The summed currents for a phase, and the torque waveforms, are shown superimposed on those for the conventional waveform fed unipolar inverter in figure 5.21. There are only small differences, and these are greatest at the changeover point from one phase half to its complementary phase half.

However, experimentally it was soon found that the motor behaved badly under regeneration. Whilst motoring, the power factor, particularly for this motor, was very high and forcing the current to be in phase with the voltage made very little difference to its form. But, when the motor was regenerating, the current moved out of phase with the voltage, to return energy to the dc rail. Thus there is a conflict. As it can only free-wheel into the dc rail at this time, the regeneration is abrupt (see fig. 5.22). This causes a large change in torque. In the earlier case the energy is recovered in a sinusoidal manner and regeneration is as smooth as motoring (see fig. 5.23). The torque waveforms for both cases under regeneration are shown superimposed in figure 5.24.

Sample results for both strategies are given in table 5.2

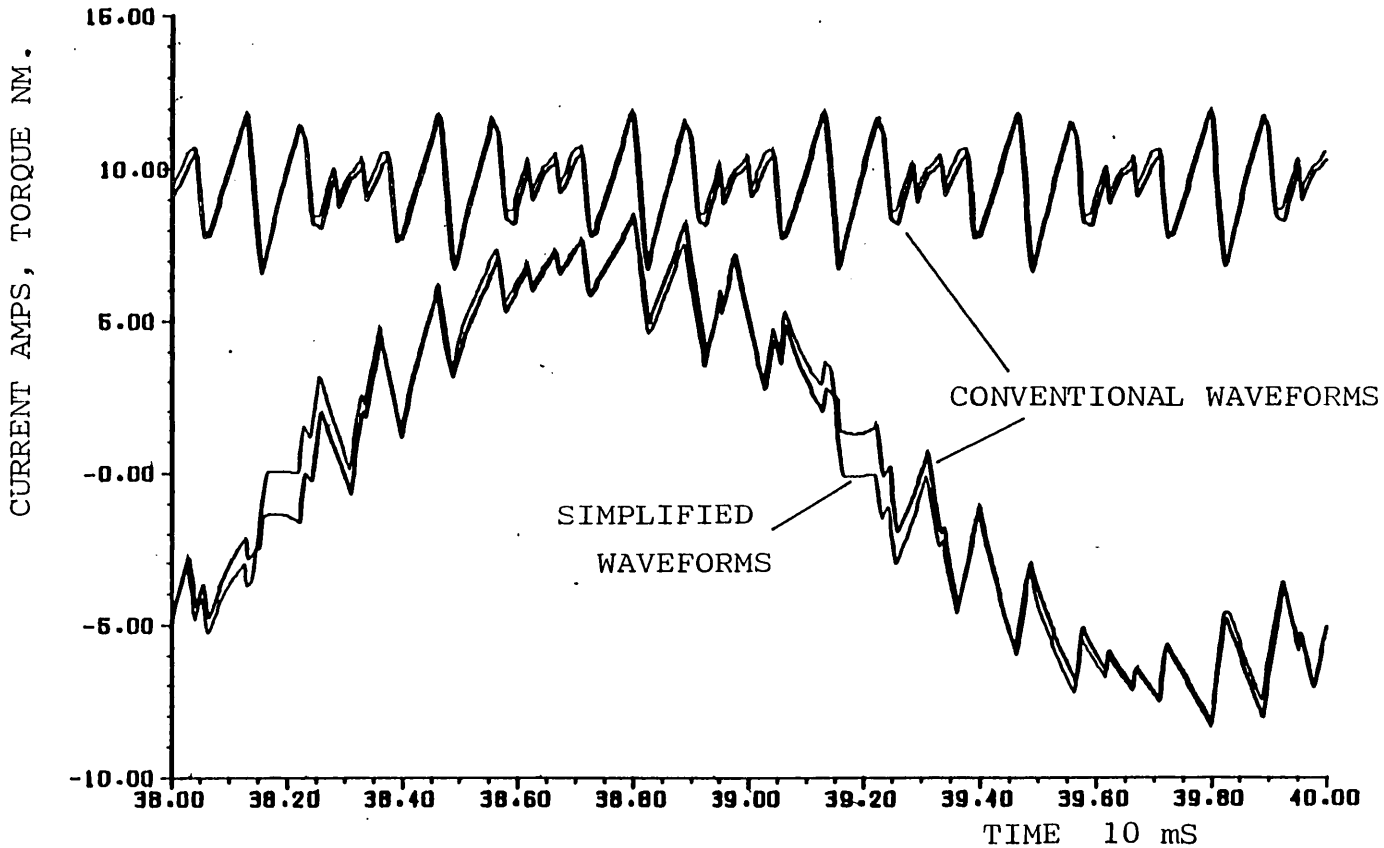

FIGURE 5.21 PREDICTED TORQUES AND CURRENTS WITH BOTH STRATEGIES

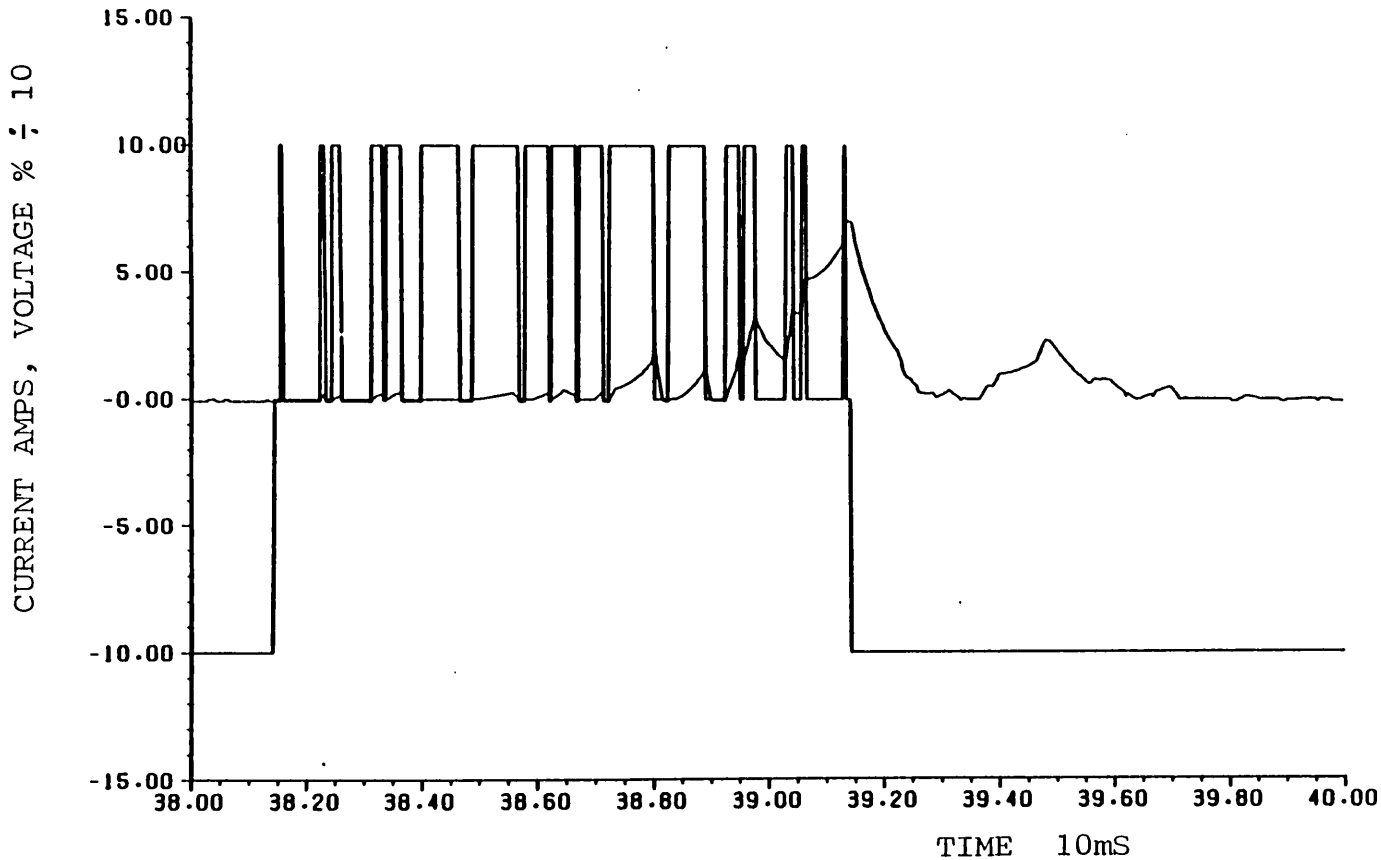

FIGURE 5.22 APPLIED VOLTAGE AND PREDICTED CURRENT WITH THE SIMPLIFIED STRATEGY (315 RADS/S)

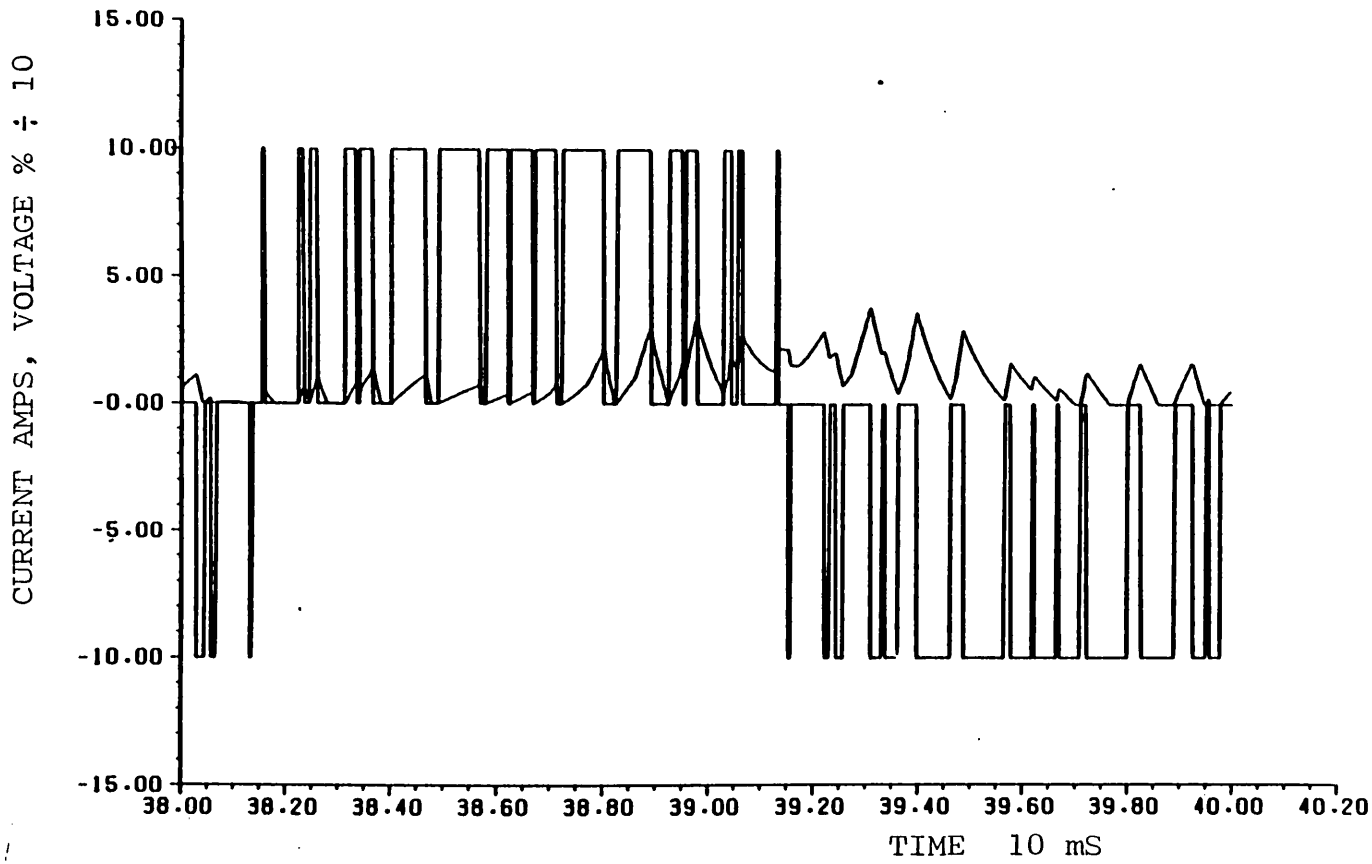

FIGURE 5.23 APPLIED VOLTAGE AND PREDICTED CURRENT WITH THE CONVENTIONAL STRATEGY (315 RADS/S)

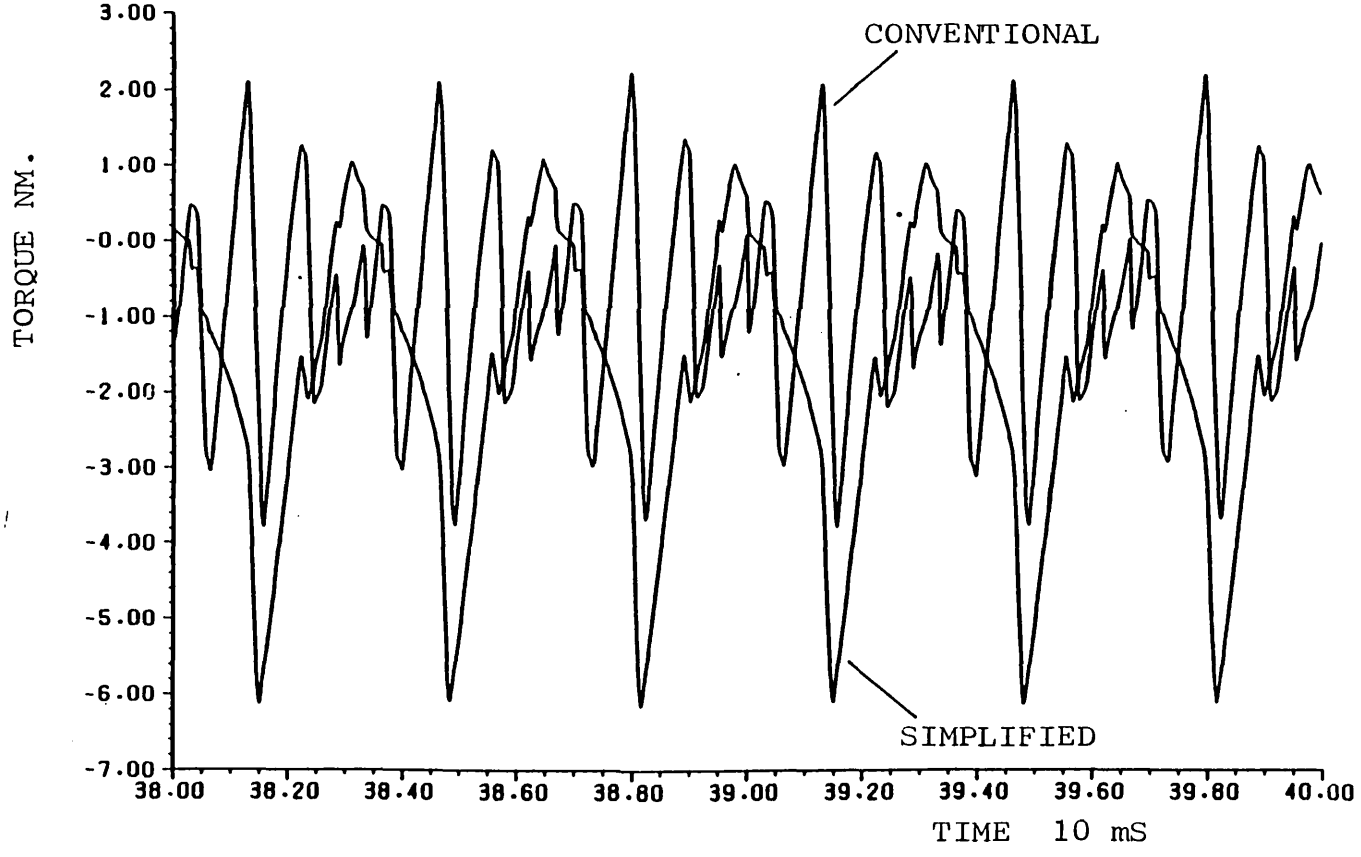

FIGURE 5.24 PREDICTED TORQUE WAVEFORMS FOR BOTH STRATEGIES

(315 RADS/S)

rpm	T Nm.	Cu loss W.	Pin W.	Pout W.	
2880	9.48	477.4	3338.4	2860.4	usual
2880	9.63	478.8	3427.9	2903.0	simple
2960	3.61	98.5	1218.2	1119.5	usual
2960	3.81	87.8	1308.8	1180.2	simple
3008	-3.18	178.1	-824.1	-1003.1	usual
3008	-6.74	325.0	-1601.8	-2121.7	simple

Table 5.2 Comparison of strategies

In the case of the simplified waveforms, the powers and the losses do not add up. This is because the 4000 Ohm resistors modelling the diodes are now subjected to the full dc rail voltage for some of the time that the phase half is off, and they carry a small current and dissipate some power. This extra power consumed comes directly from the dc rail and therefore does not significantly affect the motor efficiency, which can be obtained from the power out and the losses. The desired gain in efficiency has been achieved. It would be greater still given that snubbers (not modelled here) are usual, and they would no longer charge via the mutual coupling as described in Section 3.4.

In most voltage fed inverters, regeneration is only allowable at a slow rate, because power cannot be returned to the supply. In some a resistor across the dc rail is used to dissipate the energy should the dc voltage rail rise too high. However the rate of energy recovery in the case of the simplified waveforms is very

rapid and at a high torque given the speed. This can cause problems of oscillation depending on the components used and the mechanical system. The same may be true of the conventional inverter (ref. 54) and the conventionally fed unipolar inverter except that the ripple torque is much less.

The gain in efficiency is not very great and the cost in terms of ripple torques may be quite high. Should efficiency be of prime interest a conventional inverter using inserted inductances with very low resistance is the most suitable solution, as the problem of the increased stator loss is also removed. If the unipolar inverter is used with a high switching frequency, to reduce the torque ripple, the simplified waveforms would again be undesirible.

6.Ø FAULTS

6.1 POSSIBLE FAULTS

In a conventional inverter the only catastrophic fault possible is simultaneous conduction of two devices in one leg. This is commonly caused by incorrect signals due to interference, faulty logic curcuits, or the logic supply dipping and generating glitches. It is supposed that the power electronic design is correct. However, it is possible in GTO and thyristor inverters to get into a condition in which the current in the conducting device is too great. In such a case the current cannot be successfully commutated. Simultaneous conduction results when the other device in the leg turns on. The devices would be protected by fuses. Whilst replacing fuses is inexpensive, the downtime that results may be very expensive and the advantage of fusing lost.

The unipolar inverter has two fault conditions, one of which is very unlikely unless something is seriously wrong. The first may be compared to simultaneous conduction. Consider figure 6.1; When a is ON , b is OFF and when b is ON ,a is OFF. These are resectively cases 1 and 2 or 3 and 4 in Section 3.4. It is similar to the conventional swithing strategy. Should a come ON, and b fail to turn OFF, the phase half A (with both switches on) is now confronted by phase half B effectively short circuited by device b. The induced voltage is in the

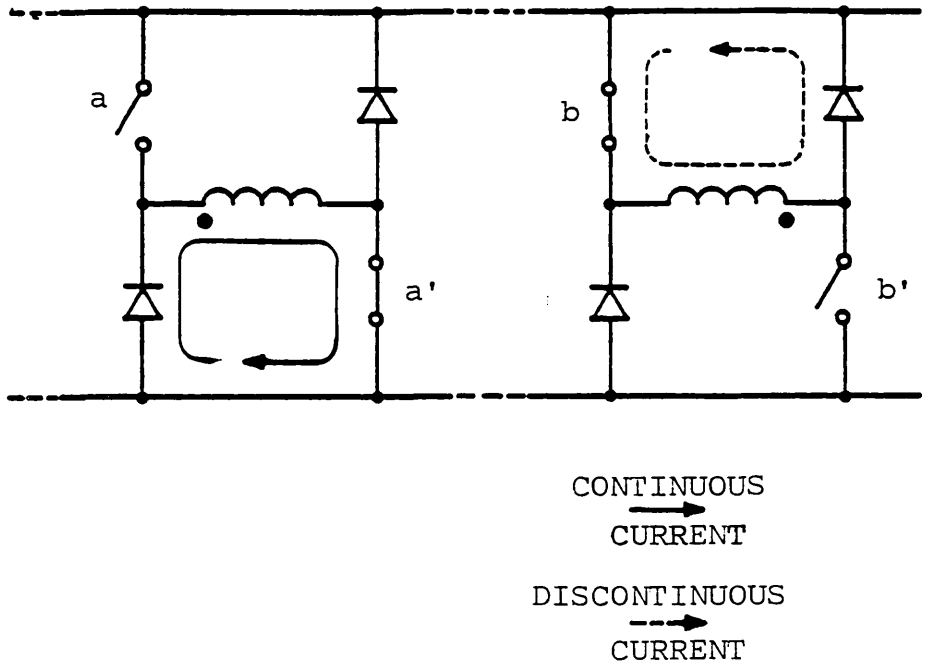

FIGURE 6.1 EXAMPLE SWITCHING STATE

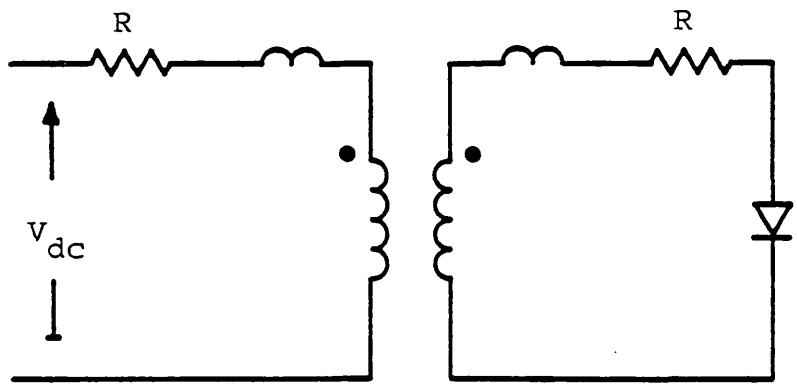

FIGURE 6.2 EQUIVALENT CIRCUIT FOR THE FIRST TYPE OF FAULT

positive sense for the diode. This allows a fault current to flow, the two phase halves being well coupled.

Inspection of the situation leads to the equivalent circuit as shown in figure 6.2.

The rate of rise of fault current is initially limited by the leakage inductances and the two phase resistances in series. The solution may be found from the equations:

$$V = L \frac{d}{dt} I_1 + M \frac{d}{dt} I_2 + R I_1 \qquad 6.1$$

$$0 = M \frac{d}{dt} I_1 + L \frac{d}{dt} I_2 + R I_2 \qquad 6.2$$

The solution for I_1 is:

$$I_1 = \frac{V}{R} \left(1 - \frac{1}{2} e^{\left(\frac{-Rt}{L-M}\right)} - \frac{1}{2} e^{\left(\frac{-Rt}{L+M}\right)}\right) \qquad 6.3$$

The second possible fault condition occurs when a', a, b', and b all conduct together. This may be compared to two legs in a conventional inverter both suffering simultaneous conduction. This is less likely. The earlier condition is likely to arise more often, because the complementary devices are switching alternately and it is not usual to switch the legs simultaneously. If this second condition does arise it probably means that there is a serious fault in the system.

The solution for the two phase halves both conducting is obtained from the following equations, with reference to the equivalent circuit:-

$$V = L \frac{dI_1}{dt} + M \frac{dI_2}{dt} + R I_1 \qquad 6.4$$

$$-V = M \frac{dI_1}{dt} + L \frac{dI_2}{dt} + R I_2 \qquad 6.5$$

The symmetry of the problem leads to the conclusion that

$$\frac{dI_1}{dt} = -\frac{dI_2}{dt}$$

and the solution for both currents is

$$I = \frac{V}{R} \left(1 - e^{\left(\frac{-Rt}{L-M}\right)} \right) \qquad 6.6$$

The initial rate of rise of the fault current is still determined by the leakage and resistance.

These are the results expected from the transformer equivalent circuit, but they are a simplification in that no other phases or the rotor circuits are considered. This simplified approach led to the conclusion early on that a coil pair motor would offer a lower rate of rise of fault current compared to the bifilar motor. Since the snubber capacitors also charge up by means of the coupling inductance of the phase halves (cf.Sect 3.4), the increase in leakage is welcome in that the magnitudes of the charging currents are also reduced.

6.2 FAULT SIMULATION

Whilst faults would occur during normal operation, it is overcomplicated to try and introduce a fault to the system and see what happens. The experimental inverter is capable of withstanding fault conditions, as such large transistors were used (cf.Sect. 3.2). However, a satisfactory test is to use one phase of the motor only. The first fault may be simulated by applying a step input voltage to one phase half and a short circuit to the other. Thus the rotor at least is included in the system.

The step input voltage was applied using one of the inverter transistors. A reduced voltage rail of 1ØØV was used throughout to reduce the stress on the system. Even so it was found that the voltage rail used for the inverter was not stiff enough to supply the fault current without drooping (it was via a variac). Therefore a 3ØA power supply and 18,6ØØuF capacitance were used to provide a stiff rail.

A signal generator provided the signal to the transistor. A repetition rate of about 1 second was used, with a variable on period. The results for both motors are shown in figure 6.3 and are expanded in figure 6.4.

There is an outstanding reduction in the rate of rise of the fault current achieved merely by replacing the bifilar coils in a phase by two separate, but parallel, coils. It

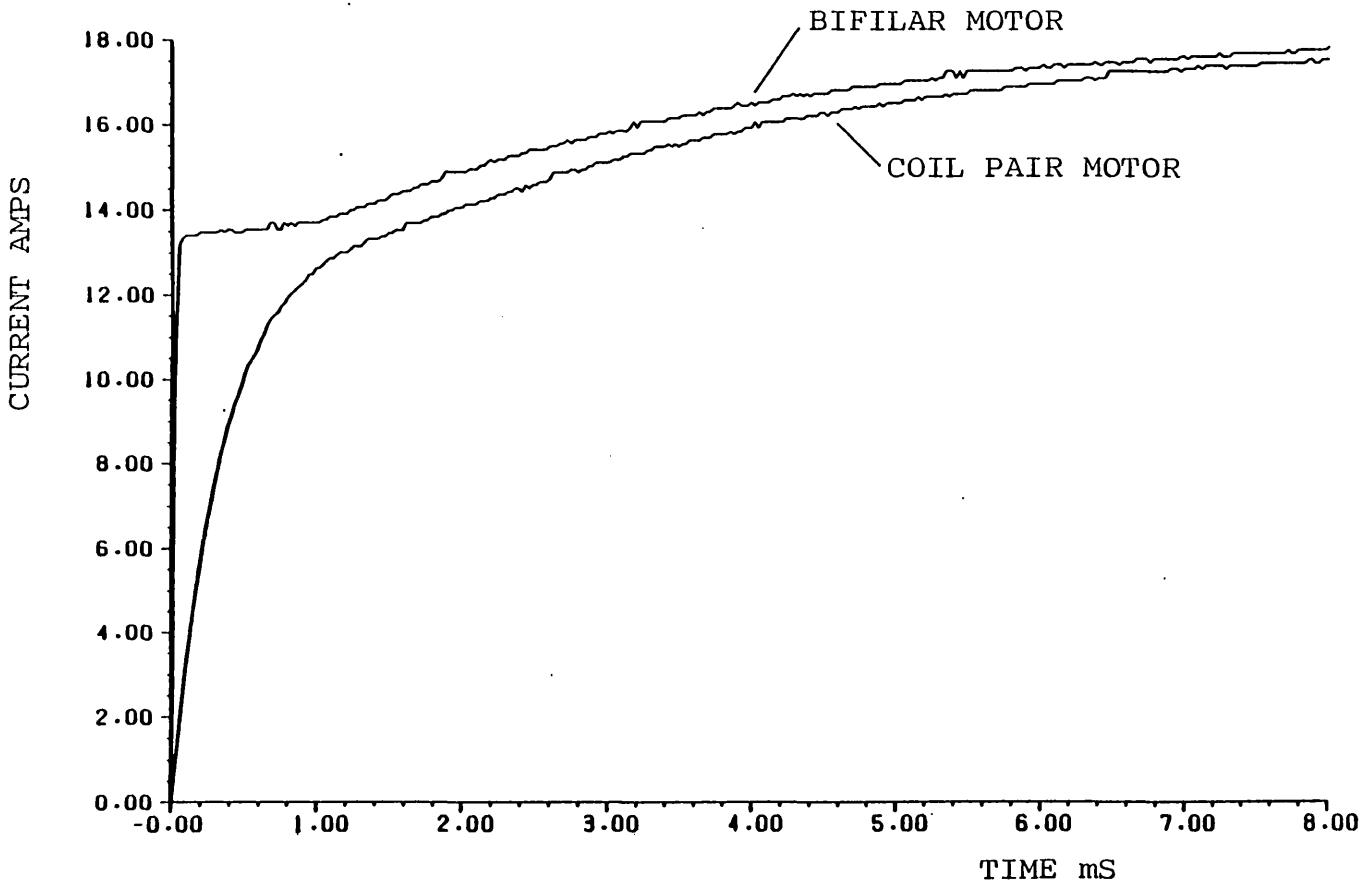

FIGURE 6.3 FIRST FAULT TYPE SIMULATED WITH EACH MOTOR

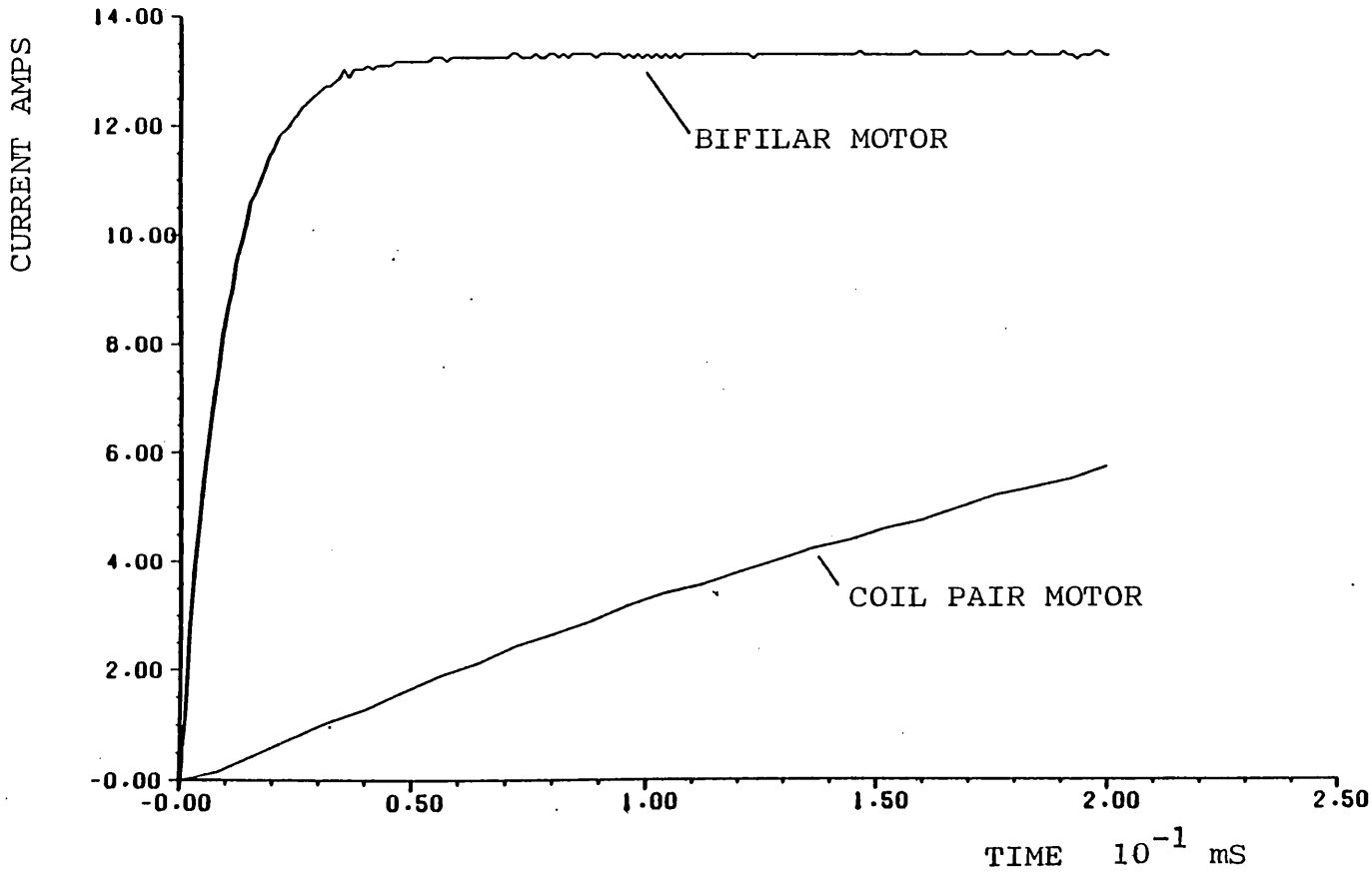

FIGURE 6.4 EXPANSION OF FIGURE 6.3

is also interesting to note that the iron does not saturate after 8 mS at 1ØØV and it was found that it still did not even after 1ØØ mS. This suggests that the motor has a large volt-seconds rating. Saturation would tend to increase the leakage in the coil pair case and reduce the self inductance, once it was saturated. In a transistor inverter this would allow even more time for the over-current detection circuit to function.

The second type of fault was simulated in a similar way. The two phase halves were connected in parallel, with their mmfs in opposition. The current for one phase half is shown in figure 6.5 along with that of the first type of fault. The current in the other phase half appeared identical to the one shown here.

Measuring from figure 6.5, for the coil pair motor, the initial rate of rise of fault current is Ø.Ø35 amps per microsecond (at 1ØØ V). That for the second fault is Ø.Ø76 amps per microsecond. The dc voltage rail that would be used for the motor is 34Ø V , which is the 24Ø V mains rectified. (385 V was used for the tests as explained in Section 3.3) This would lead to a rate of rise of fault current, for the first fault, of 0.120 amps per microsecond. Similarly the rate of rise of fault current for the second fault would be 0.26 amps per microsecond.

Any bipolar device rated at about 15 amps (a suitable size for this motor), can be turned off easily before damage

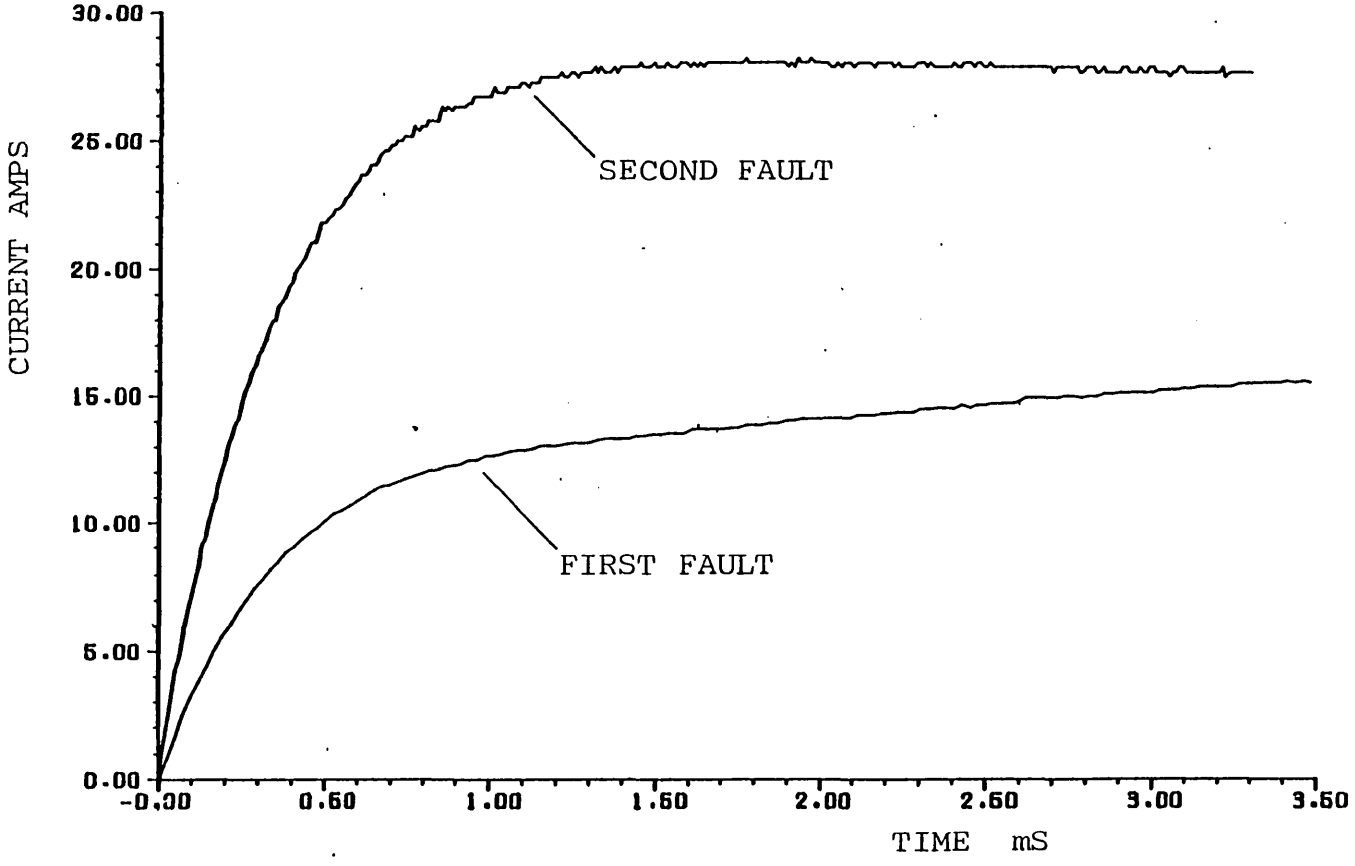

FIGURE 6.5 SIMULATED FAULT CURRENTS FOR BOTH CONDITIONS (AT 100V)

occurs, because the rate of rise of fault current is so low. Thus the devices may be very closely rated. The inductance that would have to be inserted in the conventional leg to give equivalent performance is approximately 1.3 milliHenries, rated to carry the full load current.

Most inverters above three kilowatts will use a dc link voltage of 590 V, derived from the three phase mains. In the unipolar motor, the winding will have more turns in proportion to the voltage and, as the magnetic circuit remains the same, the leakage between phase halves will increase in proportion to the self inductance. Thus the rate of change of current under a fault will be reduced further.

The inserted inductance, for the conventional inverter leg, must be scaled in the ratio of the voltages, for the same rate of rise of fault current. The inductance required becomes approximately 2.5 mH. It must be rated for the full load current and either be air cored or have enough iron to ensure that it does not saturate before the fault is cleared. This means that the inserted inductors (three or six being required) will occupy significant volume and may necessitate forced cooling in a separate enclosure. For the unipolar motor the cost is in the volume of the motor, because of the additional losses (cf. Sect. 7.2), but the motor is already fan cooled, and the inverter itself may be very compact.

6.3 ESTIMATION OF LEAKAGE REACTANCE BETWEEN COIL PAIRS

It has been shown that the leakage reactance between phase halves limits the dI/dt of fault currents and snubber charging currents. The value of this leakage for the coil pair motor was found to be very suitable. The rate of rise of fault current was well within controllable levels. The snubber charging currents were reduced to a low level (cf.Sect. 3.4). The resulting 'circulating currents' were found to be sufficiently small that they could be neglected (cf.Sect. 5.8).

Increasing this value of leakage may cause excessive losses due to the circulating currents (Sect. 3.4). Thus some method of determining the leakage between coil pairs must be found for use in the design of subsequent unipolar motors.

The elements of classical motor leakages have been separated in various ways (refs. 1,29,57). As would be expected, the leakage between coil pairs is related to these leakages. It will be shown how this leakage can be derived from the conventional leakage calculations. It is sometimes assumed that the primary slot reactance represents the entire primary leakage reactance (ref. 55). Taking this assumption, the leakage between the coil pairs is due only to the spatial positioning of the two coils in the slots. Thus similar methods to those used for calculating primary slot leakage may be applied. The

method will be described with regards to a square bottomed, straight sided slot (fig. 6.6), and the numbers for the actual slot geometry (fig. 6.7) will also be given.

The motor was wound with two stator windings, one inside the other. It had concentric coils, with 6 slots per pole per phase. Thus phases do not share slots. Each slot only contains the two halves of one phase, as shown in figures 6.6 and 6.7. The insulation is assumed to be of negligible thickness. The flux is assumed to cross the slot in straight lines. The bunched groups of conductors are taken to be continuous conducting regions, with the number of turns proportional to area. The lower conducting region, A, is assumed to be carrying a current of 1 Amp, evenly distributed.

It can be seen from the dotted example flux pattern in figure 6.6, that the mutual coupling and leakage between phase halves is related to the slot leakage.

Regions A and B share all the flux paths in common except those crossing parts of A and B. Thus the leakage between A and B may be found by calculating the difference between the inductance of A, due to the flux in areas A and B, and the mutual coupling inductance, A to B, by the flux in B only. To calculate the total leakage, the winding details need to be taken into account, and the slot leakages summed. However, this is standard procedure

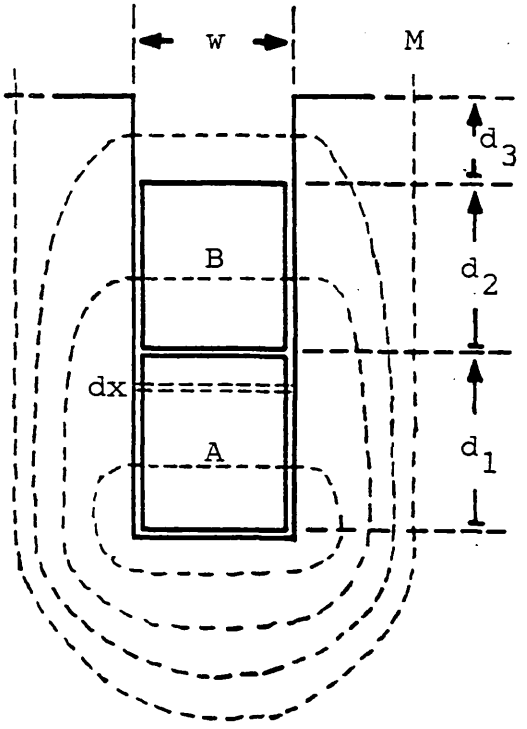

FIGURE 6.6 SQUARE BOTTOMED, STRAIGHT SIDED SLOT

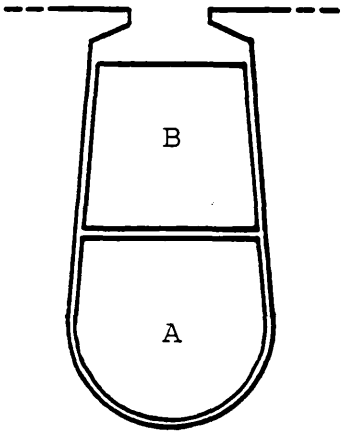

FIGURE 6.7 STATOR SLOT OF THE EXPERIMENTAL COIL PAIR MOTOR

for the calculation of primary slot leakage and therefore it will be sufficient to determine a ratio of leakage between phase halves to primary leakage. Here, the measured value of primary leakage (Sect. 5.6) will be reduced by the calculated ratio and compared to the measured value of leakage between phase halves.

The calculations are performed in terms of mmf, flux and permeance. The slot is considered in a number of parts, depending on slot geometry and the type of region under consideration. There are three types of region to be dealt with:

a) where the flux crosses the slot opening and encloses all the conductors in the slot.
b) where the flux crosses the body of the slot, enclosing all the conductors in current carrying region A, but only a part of those in region B.
c) where the flux crosses the lower part of the body of the slot enclosing only a part of the conductors in the current carrying region A.

Consider the incremental flux path dx (fig. 6.6). Within A the width of the slot is a function of x and the permeance is the integral with resect to x. However the mmf is proportional to the number of turns enclosed, which is also a function of x. The inductance is proportional to the number of turns linked, therefore the same function of x again. Thus the self inductance due to the flux crossing A is given by:

$$\int \frac{N^2(x)}{w(x)}\,dx \qquad 6.7$$

This is complicated for the round bottomed slot (fig. 6.7). For the square slot (fig. 6.6), $N(x) = \frac{x}{d_1}$ and the width is constant. The integral becomes,

$$\int_{x=0}^{d_1} \left(\frac{x}{d_1}\right)^2 \frac{dx}{w} = \frac{1}{3}\frac{d_1}{w} \qquad 6.8$$

Within region B the mmf is constant. Thus the contribution to the mutual inductance A to B, due to the flux in B, is given by,

$$\int \frac{N(x).dx}{w(x)} \qquad 6.9$$

For the straight sided slot this becomes,

$$\int_{x=0}^{d_2} \frac{x}{d_2}\frac{dx}{w} = \frac{1}{2}\frac{d_2}{w} \qquad 6.1\text{Ø}$$

At the unfilled part of the slot, only the permeance need be integrated. For the straight sided slot the result is

$$\int_{x=0}^{d_3} \frac{dx}{w} = \frac{d_3}{w} \qquad 6.11$$

Thus the total inductance of A is proportional to

$$\frac{1}{3}\frac{d_1}{w} + \frac{d_2}{w} + \frac{d_3}{w} + M \qquad 6.12$$

where M is a term representing the air gap permeance. The mutual coupling inductance A to B,is proportional to

$$\frac{1}{2}\frac{d_2}{w} + \frac{d_3}{w} + M \qquad 6.13$$

Thus the leakage from A to B is given by equations 6.12 minus 6.13

$$\frac{1}{3}\frac{d_1}{w} + \frac{1}{2}\frac{d_2}{w} \qquad 6.14$$

For the total primary inductance A and B are both conducting, therefore the primary leakage is given by

$$\frac{1}{3}\frac{d_1}{w} + \frac{1}{3}\frac{d_2}{w} + \frac{d_3}{w} \qquad 6.15$$

In the square sided slot example $d_1 = d_2$, and $d_3 = \frac{1}{2} d_1$ Substituting these values, the leakage A to B is proportional to

$$\frac{5}{6}\frac{d_1}{w}$$

In the same way the primary slot leakage is proportional to

$$\frac{7}{6}\frac{d_1}{w}$$

Thus the ratio of leakage from A to B to primary slot leakage is Ø.7 to 1.

If the process is repeated for coil B conducting, it will be found that there is no leakage from B to A. All the flux linking B links A also. This suggests that the assumption made in Section 5.5 that the two coils have the same self inductance is incorrect. The leakage was divided equally between the two phase halves. However it will be seen that this assumption makes very little real difference to the situation.

Taking the actual slot geometry into account, and using the graphs given by Puchstein (ref. 56), the same method gives a ratio of Ø.862 to 1.23. This too is Ø.7 to 1.

The measured value of primary leakage was .Ø1 H. Thus the leakage from A to B is Ø.ØØ7 H. The assumption of equally divided leakage gave a measured value of Ø.ØØ3 H. Dividing the calculated value equally gives Ø.ØØ35 H. The agreement is very close.

The worst case fault condition will be when the leakage inductances between the phase halves with the fault are at a minimum. This depends on the saturation of the iron. The

calculations for the primary leakage inductance are the most straight forward when the iron is unsaturated.

The value of Lss-Mss for the bifilar motor was never measured. There is no recognised method for calculating the coupling between bifilar wound coils. The fault simulation test is probably the most reliable way of measuring it, as the usual tests do not yield satisfactory results, the coupling being so great and the resistance being relatively high. Measuring from the curve in figure 6.4, the time constant is 1Ø microseconds, which gives a value of leakage between phase halves of approximately 4Ø microHenries.

6.4 FAULT CALCULATIONS

The work on leakage reactance estimation (Sect. 6.3) has shown that the leakage between phase halves is mainly on one side, rather than equally divided, as was assumed in Section 6.1. It is of interest to find how much variation in current this causes, and whether it affects the initial rate of rise of fault current. It should be noted that some of the leakage is due to the end windings, and will be equally divided.

The equations for the currents in the case of the first fault, with respect to figure 6.2 were,

$$L \frac{d}{dt} I_1 + M \frac{d}{dt} I_2 + R I_1 = V \qquad (6.1)$$

$$M \frac{d}{dt} I_1 + L \frac{d}{dt} I_1 + R I_2 = \emptyset \qquad (6.2)$$

These are solved for the primary current, when the fault is on the upper coil and when it is on the lower coil. The actual values will be used to avoid lengthy algebra. The time constants remain the same whatever excitation is applied.

Using; L1=Ø.458, M=L2=Ø.452, R=3.78, the two solutions (note differing self inductances) are,

$$I_1 = V (\ 0.264 - 0.131 \ e^{(-1264t)} - 0.133 \ e^{(-4.17t)} \ )$$

$$I_2 = V (\ 0.264 - 0.133 \ e^{(-1264t)} - 0.131 \ e^{(-4.17t)} \ )$$

The differences in the fractions of the exponentials are very small. The fraction expected from equally divided leakage (Sect. 6.1) is Ø.132. The fast time constant expected earlier was $\frac{(L-M)}{R}$ = Ø.794 mS. Here it is 1/1264, which is Ø.791 mS. These differences are negligible.

The equations for the second fault similarly exhibit little variation on those suggested in Section 6.1. The multiple of the exponential with the slow time constant, which appears, is in the fourth significant figure compared to that of the exponential with the fast time constant and may be neglected. Thus the division of the leakage has little effect on the fault currents and the assumption made in Section 5.6 is reasonable.

As the over-current detection should respond rapidly, compared to the rate of rise of fault current, it is only ever the quickly decaying exponential term that is of interest. Thus even a simple transformer equivalent circuit, neglecting the magnetising branch, is sufficient for design purposes.

So far the rotor has been neglected. If a step in voltage is applied to one phase half, the other being open circuit, the system is once again a transformer, but with the rotor as the secondary. The equation for the primary

current, taking values from Section 5.6,is as follows:

$$I = V\ (0.264 - 0.2\ e^{(-120.9t)} - 0.064\ e^{(-2.15t)}\ )$$

The fast time constant is 8.27 mS. Thus the rotor circuit only marginally increases the fault current for the first fault. In the case of the second type of fault, the mmfs caused by the currents in the phase with the fault cancel almost completely with respect to the rotor. Generally, then, the second type of fault is the more extreme.

The calculated curves for both fault conditions are given in figure 6.8. Comparing the calculated di/dt for the second fault with the experimental (fig. 6.5), it appears that the actual current rises more quickly than expected. The calculated rate of rise of fault current at 1ØØ V is Ø.Ø34 A/μS compared to Ø.Ø76 A/μS. The discrepancy is mainly because the values of both the primary leakage and the leakage between phase halves found in Section 5.5 were at slight saturation. This was necessary then for the values to be correct at full load torque. It is also difficult to separate the stator and rotor leakages for an induction motor. As the motor has closed slots and relatively deep bars on the rotor, dividing the leakage found in the locked rotor test equally between stator and rotor is not very accurate. Other effects, such as eddy currents in the laminations and end winding leakage, were also neglected.

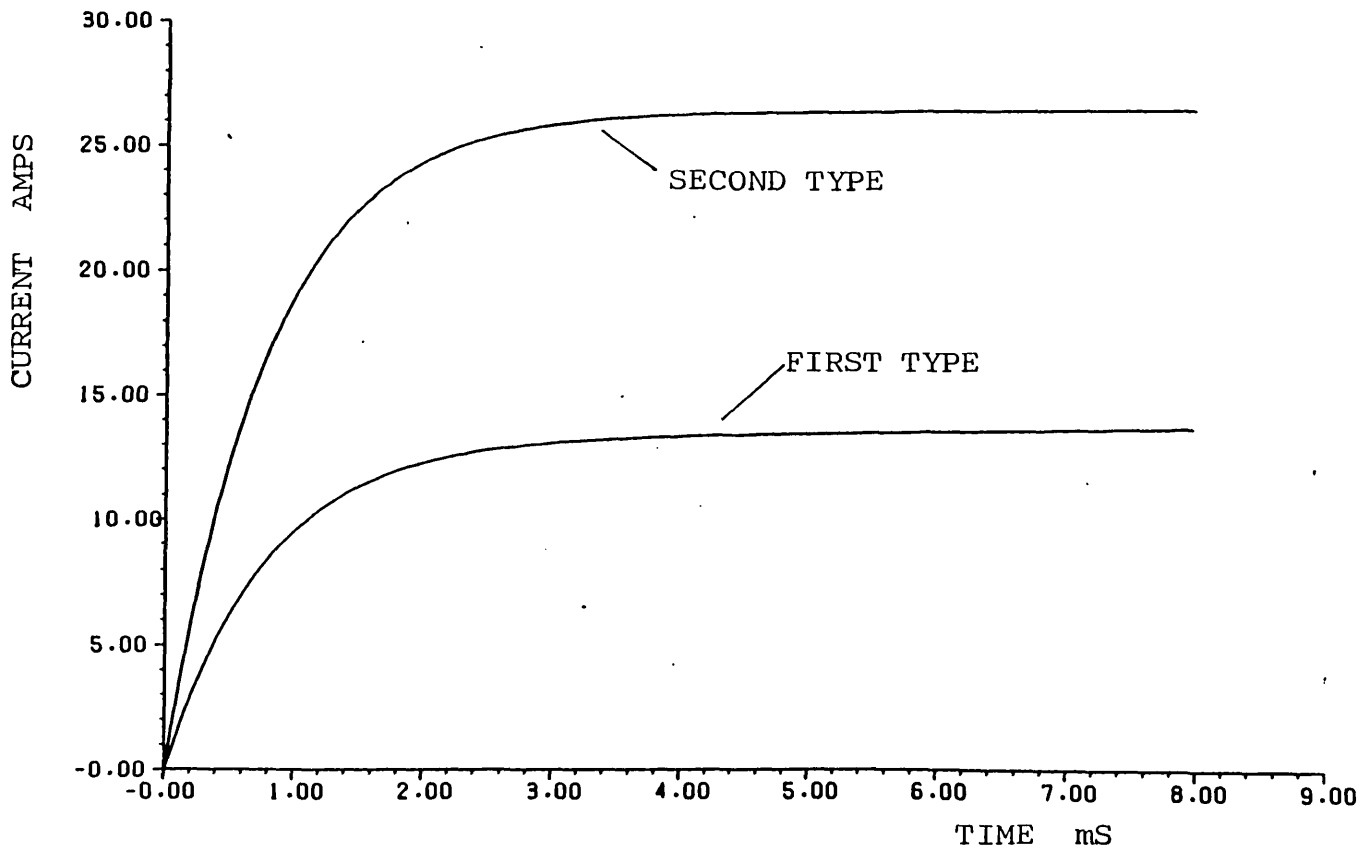

FIGURE 6.8 CALCULATED FAULT CURRENTS

However, with detailed calculation of primary slot leakage and with use of the slot geometry to give a reduction factor, it is likely that better agreement may be achieved. In any event there will be some margin of safety in the design of the over-current detection circuitry. When the motor is running, parts of the magnetic circuit will be saturated and the rate of rise of fault current will be altered.

From the tests it is apparant that the fault condition will not greatly affect the existing levels of saturation. The ampere-turns of the two phase halves will largely cancel (only for the first part of the fault in the first case) and the fault should be cleared quickly (depending on the circuitry).

6.5 CONCLUSIONS AND METHODS OF PROTECTION

The most significant conclusion is that the coil pair motor has an advantage over the bifilar motor from the point of view of limiting the rate of rise of fault currents to a controllable level. This is also important in reducing the snubber capacitor charging currents.

The fault simulation and calculations have only considered a fault with zero initial conditions. If the motor is running and a fault occurs, it may be that parts of the motor are to some extent saturated and consequently, in the coil pair motor, the leakage inductances between the phase halves are modified. This will change the initial rate of rise of fault current. Calculations for the leakage inductances should include consideration of saturation.

Given the slow rate of rise of the fault current, two methods of fault protection are possible. In transistor and MOSFET circuits a linear operation detection circuit can be incorporated into the drive circuit. These can operate and turn off the transistor in, commonly, less than a microsecond. They make use of the increasing saturation voltage with increasing current (ref. 58). In GTO and thyristor circuits, the high overload capacity of these devices may be used to good effect. Simple dc rail current monitoring (using LEM modules for example) could be used to detect a fault, before the peak commutation

level is reached, and all the devices may be turned off.

Fuses would be a last resort for safety purposes and would not be expected to blow under forseeable fault conditions.

Whenever a fault is detected and the protection circuits have operated, it is recommended that the inverter is turned off automatically until it is manually reset. Then it will become clear whether the fault was momentary and has cleared, or still remains. It may be worth-while to have a system of automatic reseting, particularly if the system is computer controlled, and the faults may be logged.

The method proposed for determining the leakage inductance between phase halves, and therefore the rate of rise of fault current, is expected to be quite useful for making an estimation of the protection circuitry required for a given motor and inverter.

7.Ø RATINGS AND SCALING

7.1 INTRODUCTION

Many motors, and induction motors in particular, are considered as standard items, which can be purchased off the shelf. There is a large number of manufacturers and to ensure that motors are equivalent to one another a rating system has evolved.

"The purpose of the motor rating, therefore, is to define accurately its useful range of performance, in a way most intelligible to the user" P.L.Alger (ref. 1,p499).

Great advances have been made in the rating of induction machines over the past eighty years, as is illustrated by table 7.1. This has been due to ever improving materials and progress in design methods.

Years	KW. rating
1898-19Ø3	5.5
19Ø3-19Ø5	7.5
19Ø5-1914	11.Ø
1914-1924	15.Ø
1924-1929	19.Ø
1929-194Ø	22.5
194Ø-1956	3Ø.Ø
1956-1961	37.5
1961-1966	45.Ø
1966-	75.Ø

Trend in output power for a 4 pole NEMA 4Ø4 motor

Table 7.1

As soon as inverters are mentioned, the concept of rating is lost, because there is no standard as yet. Ideally, for any variable speed drive, a full knowledge of the maximum duty cycle required is of utmost importance, if the drive is to be well utilized and reliable. Commonly induction motors are sold with a standard continuous rating and specified overload capacity. Immediately, there is some conflict, especially as inverter drives are often marketed as an addition to existing equipment.

To try and retain some idea of a rating "intelligible to the user", it was decided that the maximum continuous output power of the inverter drive operating at 50Hz would be considered as its rating. It is assumed that the inverter rating will exceed the motor rating, as inverters are usually required to supply peak loads, which exceed the continuous rating. The inverter will have a low thermal capacity. The dynamic rating or the motor, not included here, is discussed in Section 4.3.

In Section 5.8 it became clear that the unipolar inverter is disadvantaged because of the effective doubling of the stator resistance. This causes increased loss on the stator side and the motor is no longer rated as it was. It was also found that the peculiarities in the current waveforms have little effect on the losses.

Therefore it was necessary to test the motor under inverter feed to obtain its new rating. It is also of

interest to find out how much this differs from the rating for ac feed with one winding only. Such a comparison in the computed results in Section 5.8 suggested that the difference in efficiency and therefore rating is slight. It also remains to be decided how the novel inverter drive will scale, taking into account that the parameters of induction motors change with size.

7.2 RATING TESTS.

The difficulty with any rating test is in measuring the temperatures of the various parts. It is usual to measure the stator temperature by means of the rise in the winding resistance. This is because it is usually the insulation of the wire that is the most important limiting factor in the stator temperature. This is taken as the standard method. The rated temperature allows for hot spots with another 5 degrees centigrade (ref. 1), if measurement is by this method. Thus an 80 degree rise is allowable for a class B motor, which is a 33% increase in copper resistance.

It so happens that the motors used had class F insulation, as this will greatly prolong the life of the winding, if used at class B temperatures. It is not usual to exceed class B, because of the increase in copper resistance, causing even lower efficiency and problems of differential expansion. The change from class A to class B was largely responsible for the leap in ratings in the 1960's (cf. table 7.1).

There is less concern with the rotor temperature. It is very robust and the only problems, in terms of construction, are the thermal expansion and the lubrication. However the rise in rotor temperature, particularly with aluminium rotor bars, considerably alters the motor's characteristic torque-speed curve and

the losses, as a percentage of output power, are increased. This can lead to thermal run-away. In such a situation the stator will be affected also, because the stator current will increase, sometimes dramatically. The reverse is also true, that an increase in stator resistance affects the rotor. The airgap flux is reduced, and consequently the torque-speed curve is pulled down, at the square of this percentage difference in flux, and the slip will increase, as will the rotor loss if the load is the same.

The problem is that temperature effects lag because of the heat capacity of the different parts. Thus extreme care has to be taken to find the maximum rating. The input and output powers must be measured regularly and the load adjusted as necessary. The case temperature is also worth measuring. The manufacturer's figure for the permissible loss for the frame size was used as the basis for the tests, although it was exceeded as the ambient was 25 degrees approximately, and not the 40 degrees the standard permits. The results would have to be scaled a little for higher ambients, because of the change in the torque-speed curve with temperature. The results for the various motor supplies and windings are given in table 7.2

a) Both windings; ac feed

b) One winding; ac feed

c) Unipolar Inverter feed

	SPEED rpm	TORQUE Nm.	INPUT Watts	OUTPUT Watts	EFF %	TEMP RISE deg.C
a)	28Ø8	12.67	465Ø	3726	8Ø.1	68
b)	2858	9.35	369Ø	278Ø	75.3	81
c)	2857	8.24	351Ø*	2481	73.2#	78

* includes inverter losses

\# estimated efficiency taking the same loss as row b

Table 7.2 Comparison of ratings.

The maximum stator temperature rise is not achieved for the full winding ac test (a). This is because the output is rotor limited. Attempting to increase the output power caused the motor to slow and the output power decreases again, with the efficiency worsening. If left it would soon overheat. The rating test on the bifilar motor, which was entirely standard gave 4143W output, 75 deg.C. rise, with 5Ø8ØW input power. The losses are fairly consistent, but the efficiencies are different. The coil pair motor probably had slightly more turns than the original design. In the single winding ac test (b), the motor was definitely stator limited. It was not quite so liable to thermal run-away as might be expected, the losses being shared more satisfactorily than in the previous case. Lastly, the inverter rating (c) is quite a bit less than

the single winding ac rating. However it must be noted that a small change in efficiency causes a large change in rating.

In Section 5.8 the efficiency, at this speed was predicted to be about Ø.3% less due to harmonics plus Ø.2% less for the circulating currents. It should be noted that the snubbers, not modelled earlier charge up via the windings (cf. Sect. 3.4). The damping of the winding resistance on the resonant nature of the circuit is low, so that the charging current may be considered as sinusoidal for half a cycle. The peak may be found from the rail voltage and the impedance, neglecting the resistance. The energy dissipated is found from the current squared times the resistance, and multiplying this by the repetition rate gives the average power. The total is 25W, which is another Ø.9% of 278ØW. The iron loss was also neglected in Section 5.8. Estimation of the experimental motor efficiency (see table 7.2) puts it at 2.1 percent less. The combination of these effects largely accounts for the loss in the rating for the inverter compared to the single winding ac case. The experimental errors are much greater than the difference remaining, although these errors tend to cancel in making the comparison.

7.3 THE PER-PHASE EQUIVALENT CIRCUIT

The major loss in rating is due to the doubled stator resistance. It is therefore of interest to estimate a continuous rating for this increased resistance, and also to inspect how sensitive the rating is to changing stator resistance.

To this end a per-phase equivalent circuit model for the fundamental flux and current was used (fig. 7.1). The frequencies higher than the fundamental in the voltage waveforms were assumed to have little effect as seen above. Therefore a pure ac voltage was applied. A new rating implies a new operating point, thus an equation for losses must be solved to find the value of slip at which the losses are the same, assuming the cooling by the fan is the same. Using this value of slip the output power, hence the new rating, may be found.

It is necessary to decide which losses will remain unchanged and which will vary with slip. The eddy current and hysteresis losses were assumed to remain constant, although they were included as a resistor in parallel with X_m and not across the terminals. Thus they were not entirely constant but give a worst case situation. The friction and windage are not included in the tests (cf. Sect. 4.1) and were not included here. This leaves the stator and rotor copper losses. Since the motor is only cooled by the stator, it is unclear whether both

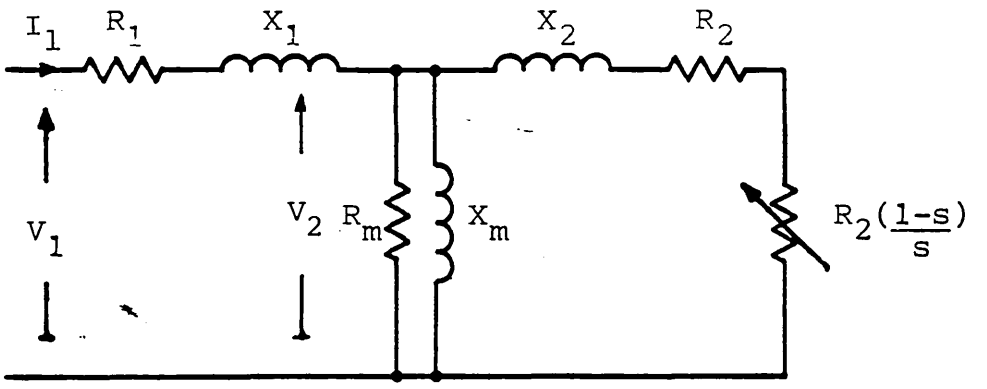

FIGURE 7.1 PER PHASE EQUIVALENT CIRCUIT FOR THE INDUCTION MOTOR

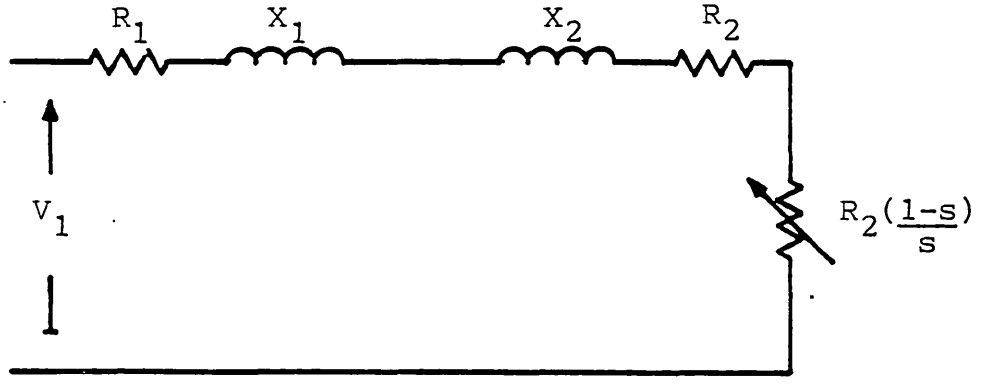

FIGURE 7.2 SIMPLIFIED EQUIVALENT CIRCUIT

should be solved for or just the stator losses. This decision depends on the thermal impedances of the machine and on which loss is the limiting one.

Taking the constant loss case, increasing the stator resistance essentially moves the loss to the stator. Reducing it moves the loss to the rotor. This can be understood from the simplified eqivalent circuit in figure 7.2. Increasing R1 means that the current drawn must be reduced to retain the same total loss. If the relationship,

$$\left|(R_1+R_2) + (X_1+X_2)\right| << R_2 \left(\frac{1-s}{s}\right)$$

is assumed the resistance R_2 (1-s)/s, which absorbs power equal to the mechanical output, must increase to significantly reduce the current , and the slip s will decrease. This identity also means that the voltage across this resistance will remain approximately the same. Thus the power dissipated in it, which represents the mechanical output, will be reduced. R_2, representing the rotor loss, remains constant and the power it dissipates is reduced.

Therefore, with these conditions, the regulation of the airgap flux, due to R_1, cannot cause an increase in rotor loss, however much the torque-speed curve is altered, as the parameter R_2 is in series with R_1.

Taking best and worst cases the equations for the copper loss were solved for both constant sum of stator and rotor losses and constant stator losses only.

The equation for the total copper loss is as follows:-

$$\text{Copper Loss} = \frac{V_2^2 R_2}{\frac{R_2}{s}^2 + X_2^2} + \frac{V_1^2 R_1}{\left| R_1 + X_1 + ZED \right|^2}$$

where ZED is the rotor impedance in parallel with X_m and R_m The V_2 term is dropped and the stator loss only is solved for in the latter case.

The method of solution was the bisection algorithim, as the function for the losses is continuous. Two values of slip, hence $\frac{R_2}{s}$,which bound the solution ,are estimated. The average of these two values is put into the equation and depending on whether the losses are too small or too great this bisection value of $\frac{R_2}{s}$ replaces the respective boundary, and the solution is bounded more accurately. The process is repeated until the boundaries are sufficiently close, or the exact solution is found. It is a very simple method, and could go unstable , so a limit on the number of iterations was set.

The value of rotor copper loss used was derived from the output power and slip of the first ac test using the

equation;

$$\text{Rotor Loss} = \text{Slip} \cdot \text{Output Power}$$

The stator copper loss was found from the input current and measured resistance. The remaining losses were calculated and the value of the resistance in parallel with X_m, which gives the same losses, was found.

To see the sensitivity of the rated power against increasing stator resistance, a range of values for R1 was used. They covered 1 Ohm to 6 Ohms , which is approximately 1 Ohm either side of the measured values. This was done for both cases and the resulting graphs are shown superimposed on the test results in Figure 7.3 .

The point corresponding to the full winding test lies very close to the intersection, which is expected, as it is the point from which the extrapolation proceeds. The point corresponding to the single winding ac test lies very definately on the upper curve. This means that it is the sum of copper losses that is important in considering the rating of the unipolar inverter in this case. However, it must be noted that the motor was originally rotor temperature limited. The rotor losses for both cases are shown in figure 7.4

The point corresponding to the inverter rating happens to lie on the lower curve, which is that for constant stator losses. That it does so is a coincidence, in fact the additional derating is due to the operation of the

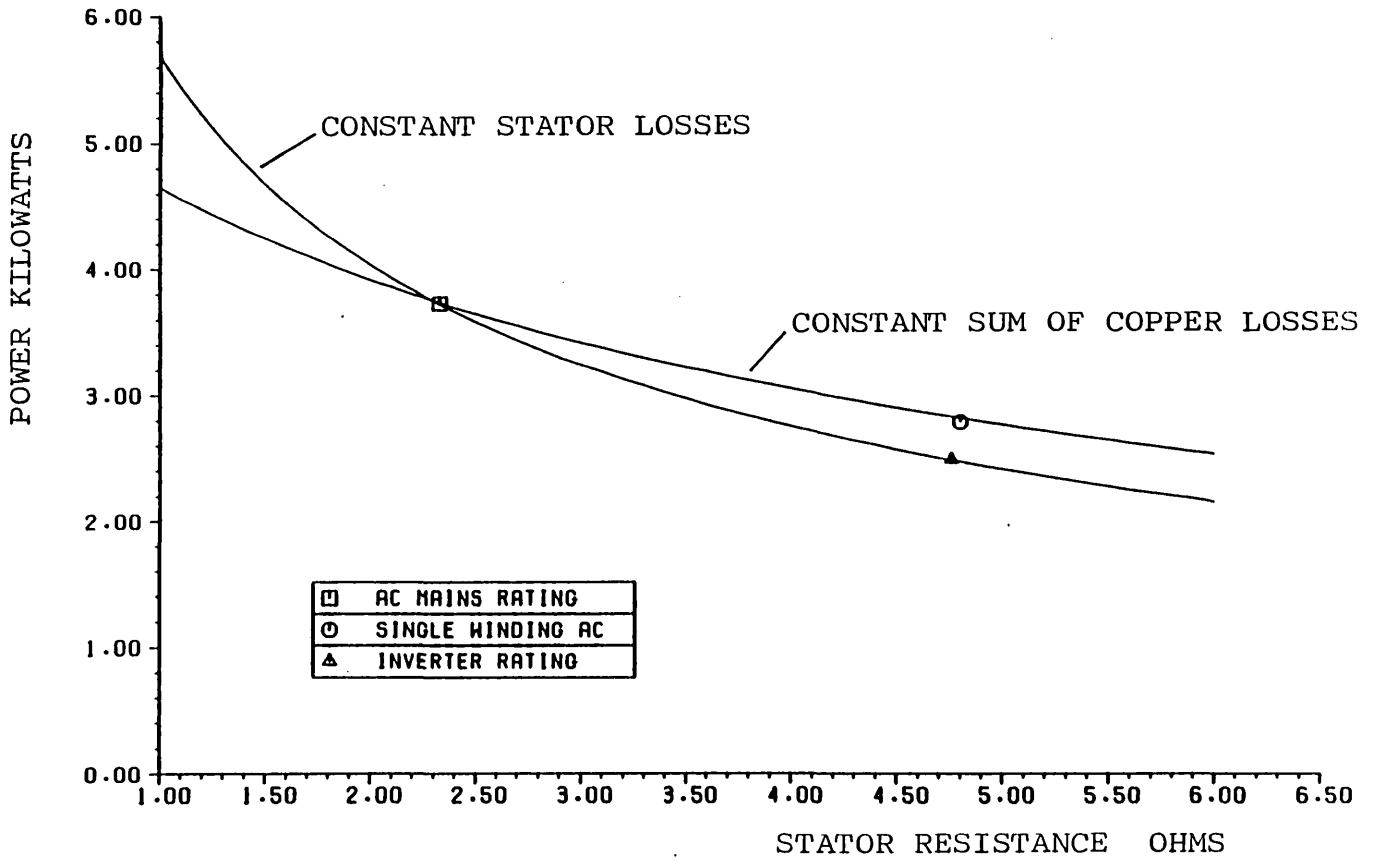

FIGURE 7.3 RATED CONTINUOUS OUTPUT POWER EXTRAPOLATION (BOTH CASES)

AND MEASURED VALUES

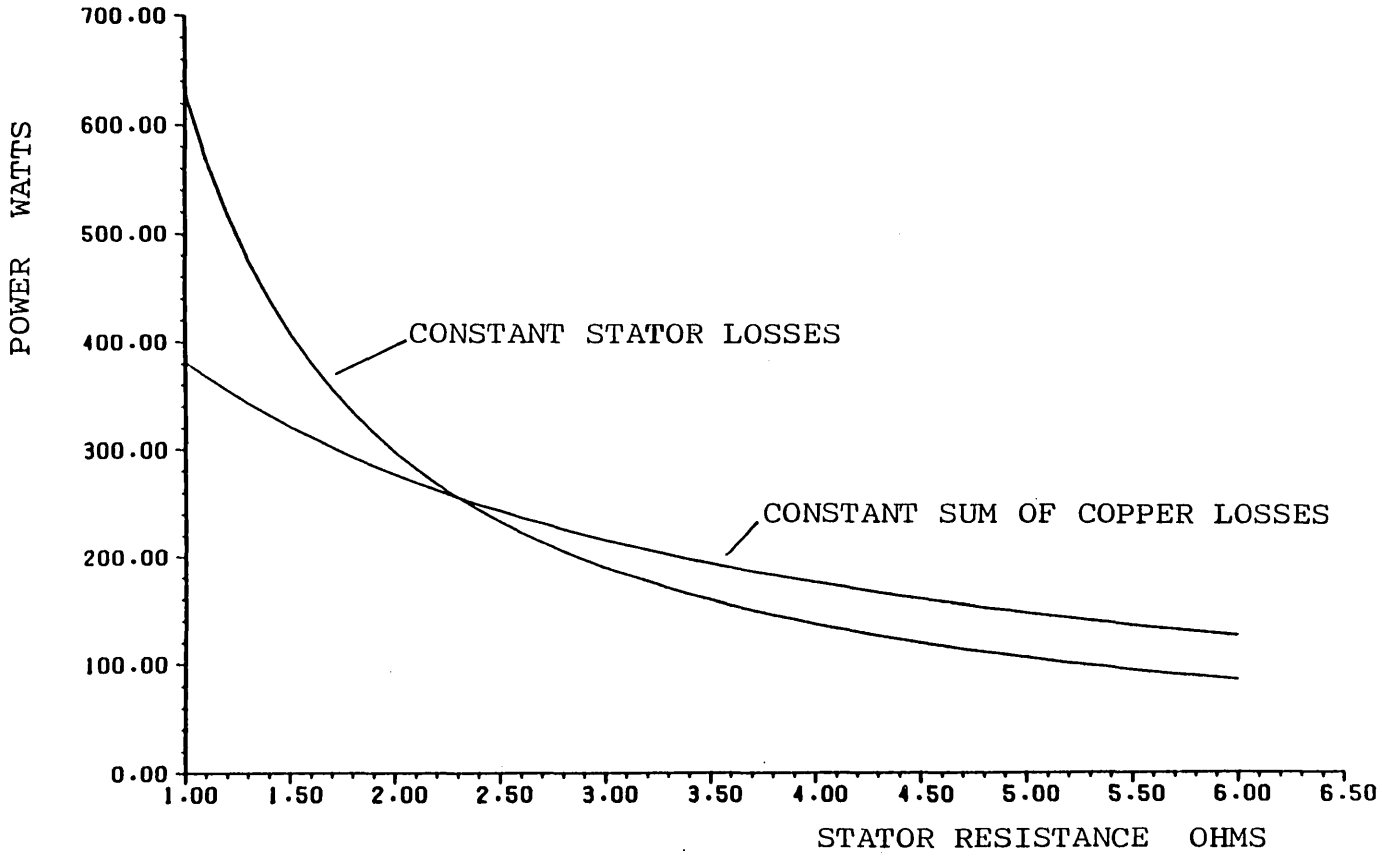

FIGURE 7.4 ROTOR LOSSES VERSUS STATOR RESISTANCE (BOTH CASES)

inverter, in particular the snubber charging currents, higher iron losses and harmonic voltage waveforms, all of which can be reduced.

7.4 DISCUSSION OF THE THEORETICAL APPROACH

The curve representing constant stator loss in figure 7.3 is rather meaningless at values of stator resistance less than that at the intersection. It is implying that more losses in total can be dissipated than are at the original rating as the rotor loss is greater. Even if a machine is severely stator limited, the frame, with its fins, cowl and fan can only dissipate a fixed amount of losses for a given temperature rise. If a motor is stator limited, at least the losses are where they are to be removed. If a motor is rotor limited, the rotor to stator thermal impedence has to be taken into acount. Then the motor may not be able to dissipate as much total loss, although the output may still rise a little with reducing stator resistance.

Considering the constant total copper loss curve, the motor shows a higher output before the intersection. That means a higher rotor loss, which may not be possible on account of the thermal impedence from rotor to stator. Thus this curve is also doubtful at lower values of resistance than that of the original design. More detailed knowledge of the thermal circuit is required.

After the intersection both curves have reducing rotor losses (see fig. 7.4). The constant total loss curve is more likely to give the rating , because the losses are more easily dissipated from the stator side. The constant

stator loss curve will therefore be an under estimate.

The discussion of the test motor will not necessarily be valid for other motors. The parameters of standard motors are not dimensionless, nor do they remain independent of the number of poles. Thus the inverter waveforms may affect the rating of a particular motor more significantly. There are also special purpose motors available and larger induction machines are not always specified to be totally enclosed.

What has become clear is that transferring some of the losses to the stator is safe. However, each motor must be taken for its own merits, and any possible problems of over rating will be shown up from similar calculations to those performed here.

The rated load torque on the inverter is 8.2 Nm. This may be achieved across the speed range (cf. fig. 4.1). As the efficiency remains high, the losses are not increased above the level that the motor can dissipate at 282Ø rpm. However it may be necessary for the motor to have separate fan cooling.

The safest way to approach the rating of any motor (suitably rewound or reconnected) applied to the unipolar inverter is to take the stator loss alone as constant. To help choose a motor this calculation can be done approximately using the equations;

$$I_1^2 R_1 = I_1'^2 R_1'$$

$$\text{OUTPUT POWER (per phase)} = V_1 I_1 \cos(\phi)\eta$$

As the stator resistance doubles in the arrangement discussed

$$I_1' = \frac{I_1}{\sqrt{2}}$$

and taking the power factor and efficiency as constant, the new rated output is the original output divided by $\sqrt{2}$. Having chosen a motor more detailed calculations can be done.

Using this criterion for the rating it seems that the unipolar inverter drive is independant of scale. The derating necessary for the motor on such an inverter is not extreme. Whilst this estimate of rating should allow for the losses due to the harmonic content of the waveforms, as seen in Section 7.3, these inverter losses account for a varying proportion of the losses depending on the machine parameters. This is a problem common to all inverters and requires investigation. For the unipolar inverter the possibility of high switching frequencies with filtering may alleviate the problem.

The conclusion is that the motor for a given application will occupy more volume than a conventional machine. This is not serious as the increase in volume , using the criterion for the rating and taking manufacturer's data (ref. 59), is generally just one frame size. This may be seen from table 7.3.

Rated Output	Frame Size	
kW	ac feed	Inverter (unipolar)
Ø.25	D63	D71
Ø.37	D71	D71
Ø.55	D71	D8Ø
Ø.75	D8Ø	D8Ø
1.1	D8Ø	D9ØL
1.5	D9ØS	D9ØL
2.2	D9ØL	D1ØØL
3.Ø	D1ØØL	D112M
4.Ø	D112M	D132S
5.5	D132S	D132S
7.5	D132S	D16ØM
11.Ø	D16ØM	D16ØM
15.Ø	D16ØM	D18ØM
18.5	D16ØL	D2ØØL
22.Ø	D18ØM	D2ØØL
3Ø.Ø	D2ØØL	D225M
37.Ø	D2ØØL	D25ØS
45.Ø	D225M	D25ØM
55.Ø	D25ØS	-
75.Ø	D25ØM	-

Table 7.3 Comparison of frame sizes

In some cases that means a longer motor of the same diameter. This is only a small retrograde step in the progress of induction machine ratings (cf. table 7.1). The efficiency is only slightly worse and this is probably often better than running a constant speed machine at low torque as discussed in Section 1.

8.Ø CONCLUDING REMARKS

8.1 AUTHOR'S CONTRIBUTION

This thesis makes a contribution to the state of the technology of inverters as a whole, unipolar inverter drives specifically and in computer simulation of cage induction motors and inverters. A complete unipolar drive of a useful rating is described. It is independent of the motor parameters and therefore may be applied to any size of motor.

Previous unipolar induction motor drives have used bifilar wound motors, whereas in this work a coil pair motor was used. Two separate and complete 3 phase windings are inserted into the stator one on top of the other, thus increasing the leakage between them. The transistor base drives used exhibit some novelty compared to those presented elsewhere and this led to work covered in reference 22.

The explanation of the continuous operation of the unipolar inverter drive was confirmed by the computer simulations. The computer model itself is unusual in that observable quantities are used as much as possible. Only the rotor is reduced to its minimal form of two quadrature coils, which is reasonable as it is a cage rotor.

The contribution here is in the method of removing the

rotating terms from the inductance matrix for the machine. The matrix would otherwise have to be inverted at each time step, which is very costly in computer time. Thus the computer time required for this method becomes of the same order as that necessary for the stationary reference frame DQ axis technique. It is easily adaptable to any supply conditions as the stator phase coils in the model correspond directly to those of the motor. Therefore it is possible to use computer models of the power electronics in series with the machine model. This was the approach taken to model the inverter. It was found that it could be represented by known voltage waveforms and diodes in series with each stator coil. The model used for the diode was a resistor in the reverse direction and a short circuit in the forward direction.

Methods for measuring the stator parameters are also discussed. The inductance bridge test was updated with the use of a computer to perform integrations of the waveforms recorded. The complete method for determining the parameters for the model is given. The choice of model for the diodes is also discussed, with regards to the time step length used and the computer run time.

Once it was established that the computer model was of sufficient accuracy, it was used for conducting idealized experiments. The unipolar inverter drive was compared to conventional inverter drives and to direct ac mains feed. An alternative inverter switching strategy was also

implemented in both the experimental drive and the computer simulation.

Having explored the characteristics of the unipolar inverter drive, it was necessary to establish the nature of the faults that may occur and whether they may be withstood. It was the form of the faults that made the coil pair motor attractive. Faults were practically simulated using an otherwise unexcited motor. The rate of rise of fault current is determined by the leakage between the phase halves. A method is given for obtaining this leakage, for the coil pair motor, from the slot geometry. Then calculations are performed to predict the characteristics of the fault currents. This is necessary for the design of other unipolar inverter drives.

The rating of the unipolar induction motor drive is discussed and tests were conducted. A per-phase model was used to investigate the rating of an induction motor with various stator resistances. A simple rule was defined to determine approximately the rating of any induction motor, when reconnected and fed from a unipolar inverter.

8.2 CONCLUSIONS

The most important conclusion is that the inverter fed unipolar induction motor drive is a viable alternative to the popular chopper fed or phase controlled rectifier fed dc motor drive. It offers high reliability and low maintenance. The totally enclosed fan cooled induction motor is more immune to environmental effects than the dc motor. The high switching frequency that is possible with the unipolar inverter drive means that the acoustic noise produced may be very low, which is important in air conditioning systems.

It has been found that there are no ill effects caused by the unipolar feed of induction motors. The currents that appear to circulate during certain periods are not very large and contribute little to the losses. The winding of the stator with one complete winding inside another does not cause unbalanced magnetic pull as each coil is symmetrical across the diameter of the motor. The computer analysis has shown that the torque waveform produced is almost identical to that of a conventional inverter drive. Using a high switching frequency the torque produced may be very smooth, which is important in certain applications.

The efficiency of the motor is reduced by a few percent across the speed range. The computer simulation has shown that this is mainly due to the effective doubling of the

stator resistance. This also results in the breakdown torque being reduced, and it reduces more at motor frequencies below 3Ø Hz. In conventional inverters this reduction is usually only significant at less than 1Ø Hz. However, in both inverter drives the breakdown torque may be increased by voltage boosting. In the case of the unipolar inverter drive this boosting must be proportional to the current, to avoid oversaturating the machine on low load. As with all inverter fed induction motors, if they are to be used continuously at low speed and high torque, separate fan cooling may be necessary to maintain the airflow over the motor.

The small change in efficiency lead to a large change in rated output. Tests and analysis have shown that increasing the stator resistance, and therefore the stator losses, has no adverse thermal effect on the motor, as long as the total losses do not exceed those at the original rated value. This was proved to be so for any size of standard motor. However, the new rating will depend on the thermal properties of each machine. There are also losses due to harmonics with any inverter feed and some small additional losses, due to the snubbers, in the unipolar inverter, which must be taken into account. However, it can be taken as a simple worst case rule that the stator loss must remain constant, therefore the output must be reduced to Ø.7Ø7 of its nameplate rating. Using manufacture's data, this means that generally a single frame size larger than that for ac mains feed is necessary

for the same output power. This is not expected to be a problem unless space is crucial.

Simulated fault tests showed that the unipolar inverter performs predictably under fault conditions. The most extreme fault was found to be when both phase halves are supporting the rail voltage. The phase half currents cancel so far as the rotor is concerned, which simplifies the analysis, and the equations governing the fault.

The maximum rate of rise of fault current is very low in the coil pair motor, as it is determined by the leakage between the motor phase halves. This is a situation like that of the chopper drive for dc motors, where the motor is in series with the switches. The high controllability of the faults means that, with over-current detection, the switching devices may be very closely rated, and work reliably. The inductance that would have to be inserted in each conventional inverter leg for equivalent performance is 3.5mH. Each would be rated at the full load current and would be of significant volume and cost.

The inverter-motor model used in the analysis of the drive has significant advantages over models presented by others. The motor flux is used as the state variable, since physically it cannot change instantaneously. The method of transformations used to eliminate motional terms from the inductance matrix allows the solution to be formed in observable variables, rather than transformed

variables. The resistances used to model the diodes under reverse voltage were adequate and allowed a reasonable step length to be used. The combination of the step length and the transformation technique gave permissible run times. The diode model may be improved by increasing the resistance that it has under reverse voltage. However this requires a shorter step length and leads to increased computer time. This model would also be suitable for the simulation of phase controlled motors and cycloconverters.

The methods used for determining the parameters of the motors were found to be practical and consistent. Removing the bars from a rotor by etching allows the stator parameters to be measured accurately. Taking values around the rated levels of current and saturation gives a set of matched values.

The unipolar inverter drive model was successfully used to perform idealised experiments. It was by these means that the performance of the drive was assessed and compared to the conventional inverter drive, modelled in a similar way. It was also found that the loss in efficiency due to the inverter waveforms themselves (using the conventional inverter drive model) was very small. This was contrary to the results given in other work, and is due to the fact that a 2 pole motor was used. The parameters of induction motors are both pole number and size dependant.

The higher switching frequency that is viable with the

unipolar inverter drive would enable a relatively harmonic free voltage waveform to be produced. As this would cause lower losses it was hoped that it would compensate for the loss in performance due to the doubled stator resistance. However this was not the case with the 2 pole motor. Using motors with greater pole numbers it may be expected to make a more noticeable improvement.

8.3 RECOMMENDATIONS FOR FURTHER WORK

This thesis has been concerned mainly with the operating principles and the performance of the unipolar inverter drive when under totally open loop control. However, it has been seen that voltage boosting proportional to the current would be attractive. Another possibility is to use a single search coil in the motor airgap to determine the time-averaged level of flux and to adjust the voltage to suit. In certain applications the efficiency may also be improved by voltage control.

During the time that the work contained in this thesis was done, a 20 kHz switching frequency PWM chip set became available commercially (ref. 60). It would be of interest to incorporate this into the unipolar inverter drive and to develop suitable filters. The filters required with 20 kHz modulation will be quite compact as the cut-off frequency of the filter may be much higher than the motor frequency. It is the cut-off frequency that largely determines the size of the elements used. As snubbers are easily incorporated into the unipolar inverter, snubber energy recovery (ref. 22) should be included, particularly for 20 kHz PWM, where the switching losses will be much higher, as they are proportional to the switching frequency. Current control PWM may offer a solution for low harmonics and minimum switching frequency and should be applied experimentally to the unipolar inverter.

Manufacturers are now considering making motors specific to inverters. An important requirement for any such motor is that it has low stator resistance, to avoid the drop in breakdown torque at low frequencies. Lower stator resistance will also improve the efficiency of the unipolar motor. It may be possible with the unipolar motor to arrive at a compromise with the winding, to achieve a lower effective stator resistance and yet retain sufficient leakage between the phase halves for limiting the rate of rise of fault current.

A field solving program would be of use in calculating the leakage between the coil pairs from the machine geometry. It could be expected to be of more accuracy than the method presented here. Accurate knowledge of this leakage would allow the margins in the switching device ratings to be reduced further.

For the same reason, attention should be paid to fast over-current detection techniques for transistors, and to apply them, if possible, to GTO thyristors.

Finally, both conventional and unipolar inverter drive ratings and efficiencies, with various PWM strategies and motors of different sizes and pole numbers, should be investigated. In doing so trends may appear that would influence the development of PWM strategies.

REFERENCES

1 P.L.ALGER "Induction machines".
Gordon and Breach, 2nd. edn. published 1970

2 H.WARD LEONARD "Volts versus ohms".
A.I.E.E. TRANS.,Vol.13,1896,pp.337-399

3 B.L.JONES and J.E.BROWN "Electric variable speed drives".
I.E.E. PROC.,Vol.131,Pt.A,No.7,Sept 1984,pp.516-558

4 WILLIAMS, LAITHWAITE and EASTHAM "Development and design of spherical induction motors".
I.E.E. PROC.,Vol.106,Pt.A,No.106,1959,pp.471-484

5 B.C.C.TV. "The mysterious Mr Tesla".
Horizon,first shown 20th.Dec. 1982

6 E.W.HUGET "Squirrel cage induction motor-performance versus efficiency".
I.E.E.E. TRANS.,Vol.IA-19,No.5,Sept 1983,pp.818-823

7 D.A.BALL "Motors and motor drives. The new challenge".
Drives and Controls,Aug/Sept 1982,pp.19-21,32-34

8 E.R.LAITHWAITE and L.L.FRERIS "Electric energy: its generation, transmission and use".
McGraw-Hill, published 1980

9 LAWRENSON,STEPHENSON,BLENKINSOP,CORDA and FULTON
"Variable-speed swithed reluctance motors".
I.E.E. PROC.,Vol.127,Pt.B,No.4 July 1980,pp.253-265

10 RAY, DAVIS, STEPHENSON, LAWRENSON, BLAKE and FULTON
"Industrial switched reluctance drives-concepts and performance".
I.E.E. Conference publication No.234, May 1984,pp.

11 M.STOHR "Die typenleistung kollectorloser stromrichter motoren bei der einfachen sechsphasenschaltung".
Archiv Fur Electrotechnik,Berlin, 1938,pp.691-720

12 UK PATENTS OFFICE:

967506	"Direct current motor"	1964
1048682	"Electrical control systems"	1966
1068843	"Synchronous motors"	1967
1136482	"Variable frequency oscillators"	1968
1167320	"An arrangement for controlling the speed of an electric induction motor"	1969
1245318	"Induction motor speed control arrangement"	1971
1353759	"Controlling of asynchronous motors"	1974
1385205	"Polyphase electric motor system with dc motor characteristics"	1975
1387534	"Brushless variable speed drive for ac synchronous motor"	1975

13 I.J.WILLIAMS "Induction motors for inverter drives".
Drives,Motors,Controls Conference Oct 1983,pp.81-88

14 R.S.RAMSHAW "Power electronics-thyristor controlled power for electric motors".
Chapman and Hall, London, published 1973

15 S.B.DEWAN and A.STRAUGHEN "Power semiconductor circuits".
John Wiley, published, 1975

16 J.B.FORSYTHE and S.B.DEWAN "Output current regulation with pwm inverter-induction motor drives".
I.E.E.E. TRANS.,Vol.IA-11,No.5,Sept/Oct 1975,pp.517-525

17 E.E.WARD "Inverter suitable for operation over a range of frequency".
PROC.I.E.E. Vol.111,No.8,August 1964,pp.1423-1434

18 Mullard "Thyristors and triacs".
Technical handbook, Book 1, part 4b, pub. 1984

19 Toshiba "Power transistors"
Data book, published 1983

2Ø P.D.EVANS and B.M.SAIED "Fault-current control in power conditioning units using power transistors".
PROC.I.E.E.,Vol.128,Pt.B,No.6,November 1981,pp.335-337

21 A.BRAJDER "Experiences in protecting power transistors against current overloads by means of U.be monitoring". Power Conversion International Conference October 1984 pp.3Ø4-311

22 B.W.WILLIAMS and P.R.PALMER "Drive and snubber techniques for GTOs and power transistors-particularly for inverter bridges". I.E.E.Conference on power electronics and variable speed drives 1984 (publication No.234).

23 F.W.FUCHS and A.MUELLER-HELLMANN "Control methods for reducing the inductance in the DC link of current source inverters". I.E.E.E. TRANS.,Vol.IA-19,No.5, Sept/Oct 1983,pp.699-7Ø7

24 B.W.WILLIAMS and P.R.PALMER "A novel unipolar inverter for a squirrel cage induction motor drive". I.E.E. PROC.B paper submitted.

25 P.G.HOLMES and N.A.ELSONBATY "Cycloconverter-excited divided winding doubly-fed machine as a wind power converter". PROC.I.E.E.,Vol.131,Pt.B,No.2, March 1984,pp.61-69

26 B.W.WILLIAMS "High reliability 3-phase variable frequency inverter". PROC.I.E.E.,Vol.129,Pt.B,No.6,Nov.1982,pp.353-354

27 "Hi-Line power darlingtons"
General Electric Semicondutors 1981

28 B.G.STARR and J.C.F.van LOON "LSI circuit for AC motor speed control".
Mullard Technical Pulication M82-ØØ15 published Feb.1982

29 M.G.SAY "The performance and design of alternating current machines".
Pitman Paperbacks published 1968

3Ø FITZGERALD,KINGSLEY and KUSKO "Electric machinery".
McGraw-Hill, 3rd.edn. published 1971

31 M.LOCKWOOD "Simulation of inverter/induction-machine systems including discontinuous phase currents".
Electrical Power Applications,1978,Vol1,No.4,plØ5-114

32 T.A.LIPO and F.G.TURNBULL "Analysis and comparison of two types of square-wave inverter drives".
I.E.E.E Transactions.,1975,IA 11,pl37-147.

33 D.A.B.AL-NIMMA and S.WILLIAMS "Modelling a variable-frequency induction motor drive".
I.E.E. Electrical Power Appl'ns,1979,Vol2,No.4,pl32-134

34 G.KRON "Equivalent circuits of electric machinery"
Wiley and sons, published 1951.

35 O'KELLY and SIMMONS "Introduction to general electrical machines theory".
McGraw-Hill published 1968.

36 B.ADKINS and R.G.HARLEY "General theory of alternating current machines".
Chapman and Hall published 1975.

37 S.R.BOWES and R.R.CLEMENTS "Digital computer simulation of variable-speed PWM inverter-machine drives".
I.E.E.PROC.,Vol.13Ø,Pt.B,No.3,May 1983,pp.149-16Ø

38 S.R.BOWES and J.CLARE "Steady-state performance of PWM inverter drives".
I.E.E.,PROC.,Vol.13Ø,Pt.B,No.4,July 1983,pp.229-244

39 S.RAHMAN and W.SHEPERD "Thyristor and diode controlled variable voltage drives for 3-phase induction motors"
I.E.E.PROC.,Vol.124,Pt.B,No.9,Sept.1977,pp.784-79Ø

4Ø H.F.JORDAN "Digital computer analysis of induction machines in dynamic systems" .
I.E.E.E. TRANS.,Vol.PAS-86,No.6,June 1967,pp.722-728

41 P.C.KRAUSE and C.H.THOMAS "Simulation of symmetrical induction machinery".
I.E.E.E. TRANS.,Vol.PAS-84,No.11,Nov.1965,pp.1Ø38-1Ø53

42 S.WILLIAMSON and R.G.CANN "Current waveforms for inverter fed induction motor drives-their prediction and measurement" International Machines Conference, Lausanne, 1984,pp.798-801

43 A.K.DE SARKAR and G.J.BERG "Digital simulation of three phase induction motors" and discussion.
I.E.E.E. TRANS.,Vol.PAS-89,No.6,July 1970,pp.1031-1037

44 G.NATH and G.J.BERG "Transient analysis of three phase SCR controlled induction motors".
I.E.E.E. TRANS.,Vol.IA-17,No.2,March 1981,pp.133-142

45 S.D.T.ROBERTSON "A digital model for three-phase induction machines".
I.E.E.E. TRANS.,Vol.PAS-88,No.11,Nov.1969,pp.1624-1634

46 BURDEN,FAIRES and REYNOLDS "Numerical analysis".
Prindle,Weber and Schmidt, 2nd.ed. published 1981

47 FO2AGF-Eigenvalues and Eigenvectors
NAGFLIB:987/623:Mk11:Nov.1983
National Algorithims Group, Oxford

48 J.E.GILLIAM "Understanding and using the Philips AC. motor speed control IC.HEF 4752".
Mullard Application Laboratory Report MP08201.

49 C.V.JONES "Unified theory of electrical machines"
Butterworths, published 1967

5Ø R.M.GREEN and J.T.BOYS "Inverter AC-drive efficiency"
I.E.E.PROC.,Vol.129,Pt.B,No.2,MARCH 1982,pp.75-81

51 R.G.CANN "Calculation of the efficiency of PWM inverter fed induction motor drives".
Thesis for Ph.D. University of London 1983

52 E.R.LAITHWAITE "Induction machines for special purposes".
Newnes, published 1966

53 F.G.G.BUCK "Losses and parasitic torques in electric motors subjected to PWM waveforms".
I.E.E.E. TRANS.,Vol.IA-15,No.1,January 1979,pp.47-53

54 UEDA, SONDA, INOUE, UMEZU "Unstable oscillating mode in PWM variable speed drive of induction motors and its stabalisation".
I.E.E.E. I.A.S. 1982,pp.686-691

55 H.C.J.DE JONG "AC motor design with conventional and converter supplies".
Clarendon Press, published 1976

56 A.F.PUCHSTEIN "Calculation of slot constants"
A.I.E.E. TRANS.,Vol.66,1947,pp.1315-1323

57 B.J.CHALMERS and R.DODGSON "Saturated leakage reactances of cage induction motors". I.E.E. PROC.,Vol.116,No.8,August 1969,1395-1404

58 J.M.PETERS (ed.) "The power transistor in its environment" Thomson C.S.F. published 1981

59 G.E.C. Small Machines product data "Cage induction motors" publications C10AS1G and C10AS3A

60 D.A.GRANT and J.A.HOULDSWORTH "PWM AC motor drive employing ultrasonic carrier". I.E.E.Conference publication 234, May 1984,pp.237-240

APPENDIX A: MOTOR PARAMETERS

SINGLE PHASE EQUIVALENT CIRCUIT

R_1 = 4.7 Ohms

R_2 = 1.8 Ohms

(2.14 Ohms at rated temperature)

X_1 = 3.0 Ohms reactive

X_2 = 3.0 Ohms reactive

X_m = 198.0 Ohms reactive

R_m = 380.0 Ohms

V_1 = 234.0 volts per phase (rating tests)

MUTUALLY COUPLED COILS MODEL

R_{ss} = 4.7 Ohms

R_{rr} = 2.7 Ohms

L_{ss} = 0.455 H

L_{sm} = 0.186 H

L_{rr} = 0.962 H

M_{ss} = 0.452 H

M_{sr_a} = 0.631 H

M_{sr_b} = 0.6305 H

(M_{sr} is 0.631 H for the 5 coil model)

A.C. MOTOR CONTROL CIRCUIT

The HEF4752V is a circuit for a.c. motor speed control utilizing LOCMOS technology. The circuit synthesizes three 120° out of phase signals, of which the average voltage varies sinusoidally with time in the frequency range 0 to 200 Hz. The method employed is based upon the pulse width modulation principle, in order to achieve a sufficient accuracy of the output voltages over the whole frequency range. A pure digital waveform generation is used.

All outputs are of the push-pull type. Inputs and outputs are protected against electrostatic effects in a wide variety of device-handling situations. However, to be totally safe, it is desirable to take handling precautions into account.

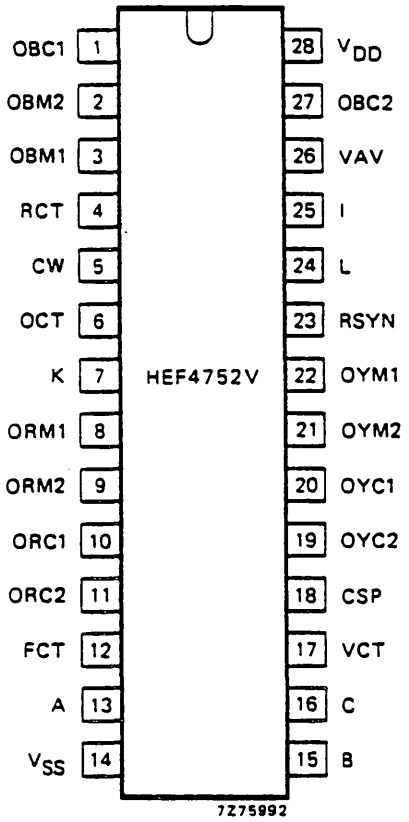

Fig. 1 Pinning diagram.

PINNING

Inputs; group I		Inputs; group II	
24 = L	data	12 = FCT	frequency clock
25 = I	data	17 = VCT	voltage clock
7 = K	data	4 = RCT	reference clock
5 = CW	data	6 = OCT	output delay clock
13 = A	data		
15 = B	data		
16 = C	data		

Outputs; group I

23 = RSYN	R-phase synchronization
26 = VAV	average voltage
18 = CSP	current sampling pulses

Outputs; group II

8 = ORM1	R-phase main
9 = ORM2	R-phase main
10 = ORC1	R-phase commutation
11 = ORC2	R-phase commutation
22 = OYM1	Y-phase main
21 = OYM2	Y-phase main
20 = OYC1	Y-phase commutation
19 = OYC2	Y-phase commutation
3 = OBM1	B-phase main
2 = OBM2	B-phase main
1 = OBC1	B-phase commutation
27 = OBC2	B-phase commutation

SUPPLY VOLTAGE

	rating	recommended operating
HEF4752V	−0,5 to 18	4,5 to 12,5 V

HEF4752VP : 28-lead DIL; plastic (SOT-117).
HEF4752VD: 28-lead DIL; ceramic (cerdip) (SOT-135A).
HEF4752VT : 28-lead mini-pack; plastic (SO-28; SOT-136A).

FAMILY DATA see Family Specifications

CLOCK INPUTS

There are three main clock inputs which are used to control the output wveforms.

Frequency Control Clock FCT

The clock input fct controls the inverter output frequency Fout, and therefore the motor speed. The clock frequency Ffct is related to Fout by the following equation:

$$Ffct = 336Ø \times Fout$$

Voltage Control Clock VCT

To maintain constant motor flux, the voltage-time product Vt must be kept constant. The IC automatically satisfies this requirement by making the output voltage directly proportional to the output frequency. The level of the average inverter output voltage, at a given output frequency, is controlled by the vct clock input, changes in output voltage being achieved by varying the modulation depth of the carrier. Increasing Fvct reduces the modulation depth, and hence the output voltage, while decreasing Fvct has the opposite effect.

The maximum undistorted sinusoidal output voltage, which is obtainable in a given system, is determined by the voltage of the dc link, Vlink; the maximum rms value of the fundamental component is given by Ø.624xVlink. This voltage occurs at 1ØØ% modulation of the carrier; that is, when some adjacent pulses are just about to merge. The output frequency at which this condition can apply in a given system is determined by the Vt product of the motor. The frequency at 1ØØ% modulation, Fout(m), can be determined by relating the maximum rms inverter output voltage to the motor ratings as follows:

$$Fout(m) = \frac{Fnx\ Ø.624\ Vlink}{Vn}$$

where Fn is the motor rated frequency and Vn the motor rated rms voltage.

Once Fout(m) has been established, a value of Fvct can be determined which will set the Vt product corrrectly throughout the frequency range of the motor to be controlled. This nominal value of Fvct is denoted by Fvct(nom), and is related to Fout(m) by:

$$Fvct(nom) = 672Ø \times Fout(m)$$

With Fvct fixed at Fvct(nom), the output voltage will be a linear function of the output frequency up to Fout(m). Any required variation in this linear relationship is obtained by changing Fvct. For example, to double the

output voltage at low frequencies, as a possible compensation for IR losses, Fvct is made equal to Ø.5 Fvct(nom).

The frequency ratio Ffct/Fvct is important in system design. At 1ØØ% modulation it will have a value given by:

$$\frac{Ffct}{Fvct(nom)} = \frac{336Ø \times Fout(m)}{672Ø \times Fout(m)} = Ø.5$$

Below Ø.5 the modulation is sinusoidal, while above Ø.5 the phase waveform approaches a squarewave, giving a quasi-squarewave line-to-line voltage. At approximately 2.5, the full squarewave is obtained. Above 3.Ø, the waveform becomes unstable as the internal synchronising cicuits cannot function correctly, and 3.Ø is therefore the recommended limit.

Reference Clock RCT

RCT is a fixed clock which is used to set the maximum inverter switching frequency, Fs(max). The clock frequency, Frct, is related to Fs(max) by the following equation:

$$Frct = 28Ø \times Fs(max)$$

The absolute minimum value of the inverter switching frequency, Fs(min), is set by the IC at Ø.6 Fs(max).

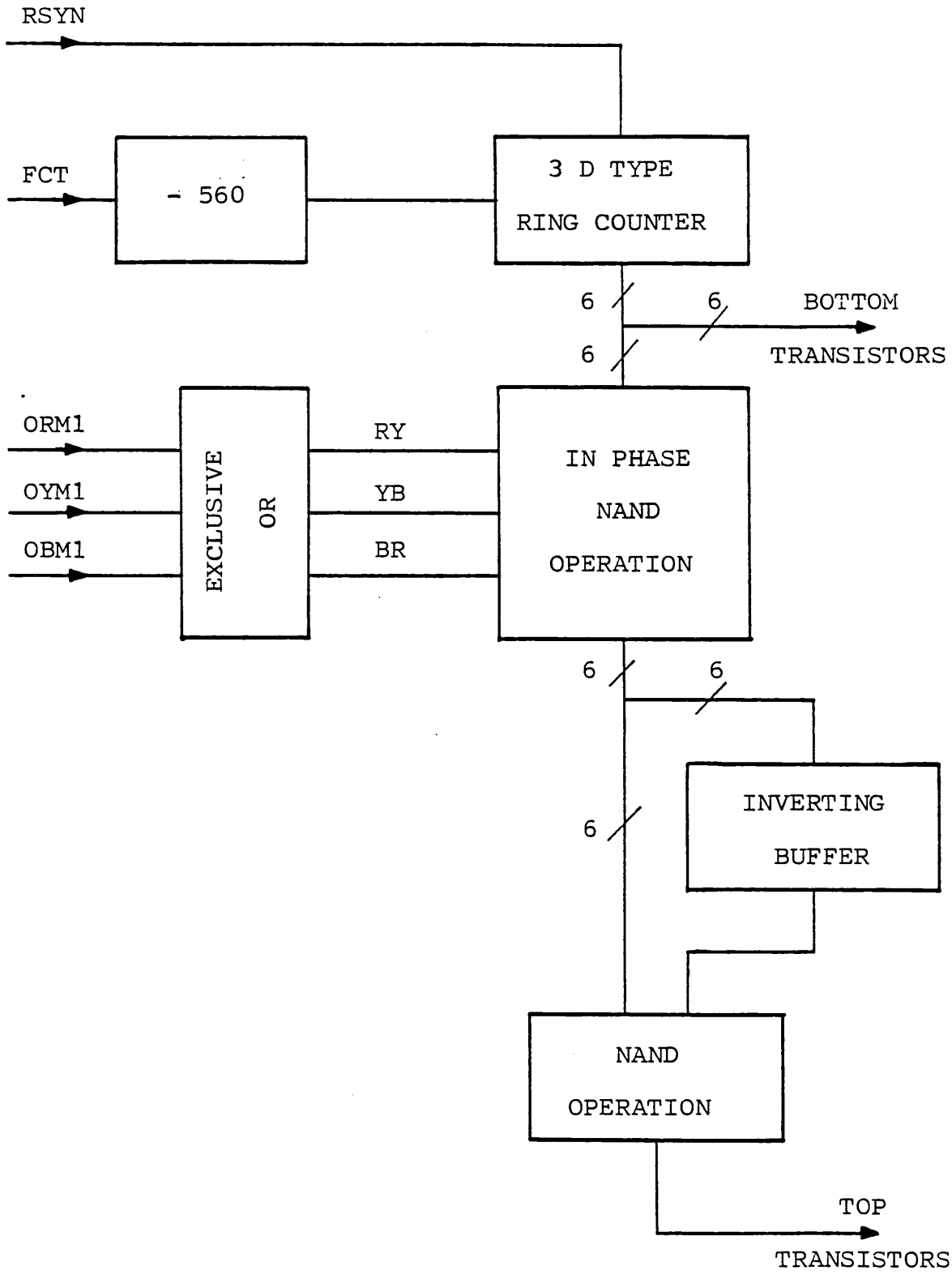

SCHEMATIC CIRCUIT FOR OBTAINING THE MODULATION SIGNALS USED.

APPENDIX C: SAMPLE PROGRAM MOTOR-INVERTER MODEL

```
00100 PROGRAM MOT8I(INPUT,OUTPUT,GRAPH,TAPE23=GRAPH)
00101C
00110C*****************************************************************
00120C      A PROGRAM TO MODEL THE MOTOR UNDER INVERTER SUPPLY
00130C       THE COILS ARE CONSIDERED SEPERATLY. CONSTRAINTS
00140C           ARE APPLIED BY CURRENT ON THE TOPOLOGY
00141C
00142C                COPYRIGHT P.R.PALMER 1985
00143C            NOT TO BE USED WITHOUT PERMISSION
00150C*****************************************************************
00151C
00152C                                    Y(8) IS THE STATE VARIABLE (FLUX)
00160 DIMENSION Y(8)
00161C
00170 COMMON/INDUCT/SSL,SML,SSM,RRL,SRMA,SRMB
00180 COMMON/CURRENT/CURR(8),E(8)
00190 COMMON/RES/ R(8),RR(8)
00200 COMMON/ANGLE/THETA
00210 COMMON/ELEC/NTOT,NC,FCV,IW(21,2)
00220 COMMON/OMEGA/OMEGA,VMAX,OMEGAS,VRAIL
00230 COMMON/LOGIC/IDEC
00240 LOGICAL IDEC
00241C
00242C                                    MOTOR DATA
00243C
00250 DATA SSL,SML,SSM,RRL,SRMA,SRMB/.455,-.186,.452,.962,-0.631,-0.6305/
00260 DATA R/4.7000,4.700,4.700,4.700,4.700,4.700,2.700,2.700/
00270 DATA ERTIA,H,T/0.00001,0.00000195313,0.0/
00280 DATA OMEGA,VMAX,OMEGAS,VRAIL/314.0,340.0,301.6,385.0/
00281C
00282C                                    INVERTER DATA
00283C
00290 DATA NTOT,NC,FCV/21,0,336000.0/
00300 DATA IW/2,4,7,9,10,10,9,8,6,3,0,-3,-6,-8,-9,-10,-10,-9,-7,-4,-2,
00310+        -3,-6,-8,-9,-10,-10,-9,-7,-4,-2,2,4,7,9,10,10,9,8,6,3,0/
00311C
00312C                                    SET VARIABLES TO ZERO
00313C
00320 DATA PINTOT,TTOT,RLOSS,TOUT/0.0,0.0,0.0,0.0/
00330 DO 100 I=1,8
00340 CURR(I)=0.0
00350 Y(I)=0.0
00360    100 CONTINUE
00370 NT=40
00371C                                    (H) IS THE TIME STEP
00380 H=.4/(NT*17600.0)
00381C                                    (N) SETS THE NUMBER OF COILS
00390 N=8
00400 IDEC=.TRUE.
00410C
00420C                                    TIME STEPPING BEGINS
00430C
00440 DO 1000 I=1,17600
00450 IF(MOD(I,100).EQ.1)  WRITE(*,*) (I-1)/100
00460    DO 1000 K=1,NT
00461C
00462C                                    STEP PERFORMS THE INTEGRATION
00463C
00470            CALL STEP(H,T,Y,N)
00480            T=T+H
00490C
00500C                                    WRITING OUT DURING THE LAST CYCLE
00502C
00510 IF(I.LE.16720) GOTO 1000
00520 IF(K.GT.1) GOTO 500
00521C
00530 WRITE(23,10000) T,CURR(1)
00540 WRITE(21,10000)T,E(1)/38.5
00550 WRITE(22,10000)T,CURR(4)
00560 WRITE(20,10000) T,TOUT
00570    500 CONTINUE
```

```
00571C
00572C                                  POWER IN (PINTOT), TORQUE (TTOT),
00573C                                  COPPER LOSS (RLOSS) ACCUMULATED IN LAST CYCLE
00574C
00580 DO 600 L=1,6
00590 PINTOT=PINTOT+CURR(L)*E(L)
00600     600 CONTINUE
00610 TOUT=TORQ(THETA,CURR,SRMA,SRMB)
00620 TTOT=TTOT+TOUT
00630 RLOSS=RLOSS+CULOSS(CURR,R,THETA)
00631C
00640     1000 CONTINUE
00650C
00660C                                  AVERAGE POWER IN (PIN), TORQUE (TAV),
00670C                                  COPPER LOSS (CULAV) ARE CALCULATED BY
00680C                                  DIVIDING THE ACCUMULATED VALUES BY THE
00681C                                  NUMBER OF SAMPLES (NT*880)
00682C
00690 TAV=TTOT/(NT*880)
00700 PIN=PINTOT/(NT*880)
00710 CULAV=RLOSS/(NT*880)
00720 POUT=TAV*OMEGAS
00721C
00722C                                  OUTPUT OF THE AVERAGES
00723C
00730 SPEED=OMEGAS/(2.0*4.0*ATAN(1.0))*60.0
00740 WRITE(*,20000)
00750 WRITE(*,10000)SPEED,TAV,CULAV,PIN,POUT
00760 WRITE(3,10000) SPEED,TAV
00770      10000 FORMAT(1X,7G14.7)
00780    20000 FORMAT(4X,"SPEED          TAV          CULOSSAV       PIN         POUT")
00781C
00790 STOP
00800 END
00801C
00810C*************************************************************************
00820C           CALCULATION OF THE FLUX DIFFERENTIAL
00830C
00840                    SUBROUTINE DIFF(Y,F,T)
00841C*************************************************************************
00842C
00844C                                  (F) DIFFERENTIAL OF THE FLUX, (Y) FLUX
00845C                                  (T) TIME
00846C                                  CALLS; MATFORM FOR THE INDUCTANCE MATRIX
00847C                                         ESET FOR THE APPLIED VOLTAGE
00848C                                         CURRENT FOR THE NEW CURRENTS
00850 LOGICAL IDEC
00860 DIMENSION Y(8),F(8),A(8,8)
00870 COMMON/INERTIA/ ERTIA
00880 COMMON/CURRENT/ CURR(8),E(8)
00890 COMMON/RES/ R(8),RR(8)
00900C
00910 CALL MATFORM(T,A,8)
00920 CALL ESET(E,T)
00930 CALL CURRENT(A,8,CURR,Y,T)
00931C
00940 DO 100 L=1,3
00950 IF(CURR(L).LE.0.0) GOTO 10
00960 RR(L)=R(L)
00970 GOTO 20
00980     10   RR(L)=20000.0
00990     20   IF(CURR(L+3).GE.0.0) GOTO 30
01000          RR(L+3)=R(L+3)
01010          GOTO 100
01020     30   RR(L+3)=20000.0
01030     100 CONTINUE
01040 RR(7)=R(7)
01050 RR(8)=R(8)
01051C
01060 DO 200 K=1,8
01070 F(K)=E(K)-CURR(K)*RR(K)
01080     200 CONTINUE
01090C
01100 RETURN
01110 END
01111C
```

```
01120C*****************************************************************
01130C               VOLTAGE APPLIED BY INVERTER
01140C
01150                      SUBROUTINE ESET(E,T)
01151C*****************************************************************
01152C
01153C                                  (E) APPLIED VOLTAGE, (T) TIME
01154C
01160 DIMENSION E(8),K(3),S(3)
01170 COMMON/OMEGA/OMEGA,VMAX,OMEGAS,VRAIL
01180 COMMON/ELEC/NTOT,NC,FCV,IW(21,2)
01190 TM=1.0/(50.0*NTOT)
01200 OMEGA=2.0*4.0*ATAN(1.0)*50.0
01210 PI=4.0*ATAN(1.0)
01220 B=-PI/6.0+OMEGA*0.000240
01221C
01222C                                  THE VOLTAGES ARE WORKED OUT USING THE
01223C                                  MODULATION NUMBERS (IW) AND THE VOLTAGE
01224C                                  CLOCK FREQUENCY (FCV). (NTOT) IS THE
01225C                                  NUMBER OF STEPS PER CYCLE. (S) IS THE LEG
01226C                                  OUTPUT VOLTAGE
01227C
01230 TSET=(NC+1)*TM
01240 IF(T.GE.TSET) NC=NC+1
01250 DO 100 I=1,3
01260 K(I)=1+MOD(NC+(I-1)*7,NTOT)
01270 T1=NC*TM+TM/4.0+IW(K(I),1)*8.0/FCV
01280 T2=NC*TM+3.0*TM/4.0+IW(K(I),2)*8.0/FCV
01290 IF(T.GT.T1) GOTO 5
01300 GOTO 20
01310     5 IF(T.GT.T2) GOTO 20
01320 EX=0.0
01330 GOTO 30
01340      20 EX=VRAIL
01350      30 S(I)=EX
01360      100 CONTINUE
01361C
01370 E(1)=E(4)=S(1)-S(2)
01380 E(2)=E(5)=S(2)-S(3)
01390 E(3)=E(6)=S(3)-S(1)
01400 E(7)=0.0
01410 E(8)=0.0
01411C
01412C                                  ALTERATION FOR THE SIMPLIFIED WAVEFORMS
01413C
01420 GOTO 200
01430 DO 200 I=1,3
01440 E(I)=340.0*SIN(OMEGA*T+B+(I-1)*2.*PI/3.0)
01450 E(I+3)=E(I)
01460 IF(SIN(OMEGA*T+B+(I-1)*2.*PI/3.).GT.0.0)   GOTO 150
01470 E(I)= -VRAIL
01480 GOTO 200
01490     150 E(I+3)=VRAIL
01500     200 CONTINUE
01510 RETURN
01520 END
01521C
01530C*****************************************************************
01540C            HEUN'S METHOD (2ND ORDER RUNGE-KUTTA)
01550C
01560                   SUBROUTINE STEP(H,T,Y,N)
01561C*****************************************************************
01562C
01563C                                  (H) STEP LENGTH, (T) TIME, (Y) FLUX
01564C                                  CALLS DIFF FOR THE DIFFERENTIAL
01565C
01570 DIMENSION Y(8),F(8),Y23(8)
01580 CALL DIFF(Y,F,T)
01590 DO 100 I=1,N
01591C                                  (Y23) IS THE INTERMEDIATE VALUE OF FLUX
01600 Y23(I)=0.0
01610 Y23(I)=Y(I)+2.0/3.0*H*F(I)
01620 Y(I)=Y(I)+H/4.0*F(I)
01630     100 CONTINUE
01631C
01640 CALL DIFF(Y23,F,T+2.0/3.0*H)
01641C
01650 DO 200 I=1,N
01660 Y(I)=Y(I)+3.0/4.0*H*F(I)
01670     200 CONTINUE
01680 RETURN
01690 END
01691C
```

```
01700C*****************************************************************
01710C              CREATING AND INVERTING THE L MATRIX
01720C                   ON THE FIRST PASS ONLY
01730C
01740                    SUBROUTINE MATFORM(T,A,N)
01741C*****************************************************************
01742C
01743C                                   (A) INDUCTANCE MATRIX, (T) TIME
01744C
01750 DIMENSION A(N,N)
01760 COMMON/OMEGA/OMEGA,VMAX,OMEGAS,VRAIL
01770 COMMON/INDUCT/ SSL,SML,SSM,RRL,SRMA,SRMB
01780 COMMON/RES/REST(8)
01790 COMMON/LOGIC/IDEC
01800 LOGICAL IDEC
01801C                                   TESTS FOR EXISTING MATRIX
01810 IF(.NOT.IDEC) RETURN
01811C
01820 THETA=-OMEGAS*T
01830C
01831C                                   CREATES THE INDUCTANCE MATRIX
01840 DO 100 I=1,6
01850 A(I,I)=SSL
01860       100 CONTINUE
01870 PI=4.0*ATAN(1.0)
01880 A(1,7)=SRMA*COS(THETA)
01890 A(4,7)=SRMB*COS(THETA)
01900 A(2,7)=SRMA*COS(THETA-2.0*PI/3.0)
01910 A(5,7)=SRMB*COS(THETA-2.0*PI/3.0)
01920 A(3,7)=SRMA*COS(THETA+2.0*PI/3.0)
01930 A(6,7)=SRMB*COS(THETA+2.0*PI/3.0)
01940 A(1,8)=SRMA*COS(THETA+PI/2.0)
01950  A(4,8)=SRMB*COS(THETA+PI/2.0)
01960 A(2,8)=SRMA*COS(THETA-PI/6.0)
01970 A(5,8)=SRMB*COS(THETA-PI/6.0)
01980 A(3,8)=SRMA*COS(THETA+7.0*PI/6.0)
01990 A(6,8)=SRMB*COS(THETA+7.0*PI/6.0)
02000 DO 150 I=7,8
02010 DO 150 J=1,6
02020 A(I,J)=A(J,I)
02030       150 CONTINUE
02040 DO 200 I=1,5
02050 A(I,1+I)=SML
02060 A(1+I,I)=SML
02070       200 CONTINUE
02080 DO 300 I=1,4
02090 A(I,2+I)=SML
02100 A(2+I,I)=SML
02110       300 CONTINUE
02120 DO 400 I=1,3
02130 A(I,3+I)=SSM
02140 A(3+I,I)=SSM
02150       400 CONTINUE
02160 DO 500 I=1,2
02170 A(I,4+I)=SML
02180 A(4+I,I)=SML
02190       500 CONTINUE
02200 A(1,6)=A(6,1)=SML
02210 A(7,7)=A(8,8)=RRL
02220 A(7,8)=A(8,7)=0.0
02221C                                   MATRIX (A) IS COMPLETED
02222C
02230 WRITE(8,30000) ((A(I,J),J=1,N),I=1,N)
02231C
02232C                                   MATRIX INVERSION (GAUSS-JORDAN)
02233C
02240 DO 15 I=1,N
02250 P=1.0/A(1,I)
02260 DO 11 J=2,N
02270       11 A(J-1,I)=A(J,I)*P
02280 A(N,I)=P
02290 DO 15 L=1,N
02300 IF(L.EQ.I) GOTO 15
02310 R=A(1,L)
02320 DO 13 J=2,N
02330       13 A(J-1,L)=A(J,L)-A(J-1,I)*R
02340 A(N,L)=-A(N,I)*R
02350       15 CONTINUE
02360 WRITE(*,20000)
02370 IDEC=.FALSE.
02371C
```

```
02372C                                  RESISTANCE (REST) UPON INDUCTANCE (A)
02373C                                  IS WRITTEN TO TAPE 4, FOR EIGENVALUES
02374C
02380 WRITE(4,*)((A(I,J)*REST(J),J=1,8),I=1,8)
02390  20000 FORMAT(/////"INVERSE OK"/////)
02400  30000 FORMAT(1X,7(G9.3,1H,),G9.3)
02410C
02420 RETURN
02430 END
02431C
02440C*****************************************************************
02450C                  CALCULATION OF CURRENTS
02460C          USING FORWARD AND BACKWARD TRANSFORMATION
02470C
02480               SUBROUTINE CURRENT(A,N,CURR,Y,T)
02481C*****************************************************************
02482C
02483C                                  (A) INDUCTANCE MATRIX, (CURR) CURRENT
02484C                                  (Y) FLUX, (T) TIME
02485C
02490 DIMENSION A(N,N),CURR(N),Y(N)
02500 COMMON/OMEGA/OMEGA,VMAX,OMEGAS,VRAIL
02510 COMMON/ANGLE/THETA
02520 THETA=-OMEGAS*T
02521C
02522C                                  ROTOR FLUXES ARE RELABLED
02530 ZD=Y(7)
02540 ZQ=Y(8)
02550 C=COS(THETA)
02560 S=SIN(THETA)
02561C
02562C                                  ROTOR FLUXES ARE TRANSFORMED AND REPLACED
02570 Y(7)=ZD*C-ZQ*S
02580 Y(8)=ZD*S+ZQ*C
02581C
02582C                                  THE TRANSFORMED CURRENT IS FOUND FROM
02583C                                  (A) AND THE TRANSFORMED FLUX
02590 DO 100 K=1,N
02600 CURR(K)=0.0
02610 DO 100 L=1,N
02620     100 CURR(K)=CURR(K)+A(K,L)*Y(L)
02621C
02622C                                  THE ROTOR CURRENTS ARE RELABLED
02630 CD=CURR(7)
02640 CQ=CURR(8)
02641C
02642C                                  ROTOR CURRENTS ARE TRANS FORMED BACK
02643C
02650 CURR(7)=CD*C+CQ*S
02660 CURR(8)=-CD*S+CQ*C
02661C
02662C                                  ORIGINAL ROTOR FLUXES ARE REPLACED
02670 Y(7)=ZD
02680 Y(8)=ZQ
02690 RETURN
02700 END
02701C
```

```
02710C*****************************************************************
02720C         TOTAL COPPER LOSS PER SAMPLE IS CALCULATED
02730C
02740                  FUNCTION CULOSS(CURR,R,THETA)
02741C*****************************************************************
02742C
02743C                                    CULOSS IS THE TOTAL COPPER LOSS PER SAMPLE
02744C                                    (CURR) CURRENT, (R) RESISTANCE
02745C                                    (THETA) ANGLE OF ROTOR TO STATOR
02750 DIMENSION CURR(8),R(8),C(8)
02760 CULOSS=0.0
02770 DO 100 I=1,8
02780 C(I)=R(I)*CURR(I)**2.0
02790 CULOSS=CULOSS+C(I)
02800       100 CONTINUE
02810 RETURN
02820 END
02821C
02830C*****************************************************************
02840C            TORQUE IS CALCULATED FROM MUTUAL COUPLING
02850C
02860                  FUNCTION TORQ(THETA,CURR,SRMA,SRMB)
02861C*****************************************************************
02862C
02863C                                   TORQ IS  THE INSTANTANEOUS TORQUE
02864C                                   (THETA) ANGLE OF ROTOR TO STATOR
02865C                                   (CURR) CURRENT, (SRMA), (SRMB) MUTUAL
02866C                                   INDUCTANCES STATOR TO ROTOR
02870 DIMENSION CURR(8),CUR(3)
02880 PI=4.*ATAN(1.0)
02881C
02882C                                   ASSUMES (SRMA)=(SRMB) AND TAKES AVERAGE
02883C
02890 DO 100 I=1,3
02900 CUR(I)=CURR(I)+CURR(I+3)
02910      100 CONTINUE
02920 T17=CUR(1)*SIN(THETA)
02930 T27=CUR(2)*SIN(THETA-2.0*PI/3.0)
02940 T37=CUR(3)*SIN(THETA+2.*PI/3.)
02950 T18=CUR(1)*SIN(THETA+PI/2.0)
02960 T28=CUR(2)*SIN(THETA-PI/6.0)
02970 T38=CUR(3)*SIN(THETA+7.0*PI/6.0)
02980 TORQ=(SRMA+SRMB)*0.5*(CURR(7)*(T17+T27+T37)+CURR(8)*(T18+T28+T38))
02990 RETURN
03000 END
```